SELF-TRAPPING OF ELECTRONS AND POSITRONS IN DENSE HELIUM GAS: A SIMPLE VARIATIONAL MODEL

A THESIS

Presented to

The Faculty of the Division of Graduate Studies

By

Charles Lee Cleveland

In Partial Fulfillment

of the Requirements for the Degree

Doctor of Philosophy in the

School of Physics

Georgia Institute of Technology

August, 1978

SELF-TRAPPING OF ELECTRONS AND POSITRONS

IN DENSE HELIUM GAS: A SIMPLE VARIATIONAL MODEL

Approved:

H. A. Gersch, Chairman

C. H. Braden

R. F. Fox

Date approved by Chairman 15 AUG 1978

ACKNOWLEDGMENTS

I am sincerely grateful to all who have contributed to the completion of this thesis. I wish to thank Dr. Ronald F. Fox and Dr. Charles H. Braden, who served on my Reading Committee and offered helpful suggestions on the manuscript. I also wish to thank Ricky L. Moore, with whom I enjoyed a fruitful collaboration in the early stages of this research, as well as Eric J. Kuster, with whom I shared many long, fertile conversations.

Thanks also go to Mrs. Jackie Van Hook, who expertly and quickly typed the final manuscript.

In particular, however, I most heartily appreciate the guidance and inspiration which I have received from my thesis advisor, Dr. Harold A. Gersch. The influence which he has had on this thesis, and on my development as a physicist, is impossible to overestimate. Any future success which I may enjoy will be, in part, his success as well; I am happy to be able to acknowledge the debt which I owe him.

Finally, I must express the deep gratitude which I feel toward my family, whose support gave purpose to my efforts. Wisdom is more important than knowledge, and what little wisdom that I have I owe to both my parents, who will always be an inspiration to me. My stepmother and stepsister, who have freely accepted me as son and brother, have also been of great comfort to me. Lastly, I must thank my uncle and aunt, Adrian and Ollie Mae Bradford, whose aid, both emotional and financial, has eased many of the difficulties which I have encountered while carrying out this research.

TABLE OF CONTENTS

TABLE OF CONTENTS (Continued)

LIST OF ILLUSTRATIONS

SUMMARY

This thesis explores the self-trapping of electrons and positrons in dense helium gas through the minimization of a free-energy functional.

In Chapter I, we first introduce the electron self-trapping problem through a historical review of the literature and point out the contributions that this thesis makes in this area. We then treat the positron self-trapping problem in the same manner.

In Chapter II, we consider electron self-trapping in an ideal gas. First we use an old variational model which presumes that the density profile around the self-trapped particle is a square well, and that the particle's wave function is that appropriate to a particle trapped in an infinitely deep potential well of the same radius. We find that this model only poorly predicts the conditions under which the transition between free-particle and self-trapped states occurs. We then devise a new variational model, using the exact ground-state solution to Schrödinger's equation for the finite square well, and find that the quantitative accuracy of the prediction is greatly improved.

In Chapter III, we consider the treatment of helium as a non-ideal gas. We decide to treat the bulk properties of helium through an approximate lattice-gas equation of state. We also obtain an expression for the surface energy of the density fluctuation produced by the self-trapped particle. In preliminary form, this expression

involves the gradient of the density near the self-trapped particle. Through the use of an approximate force-balance relation, this expression is simplified to a form that is amenable to our new variational model.

In Chapter IV, we consider the self-trapping of an electron in helium, using the characterizations of helium as a non-ideal gas which were found in the previous chapter. The repulsive part of the helium-helium interaction is included first, then the attractive part, which has much less effect, and finally the surface energy, which has almost no effect at all. We find that at high densities, the self-trapped stated ceases to be energetically favorable, so that in a mobility experiment the mobility should increase when the electron returns to free-particle behavior as the density is increased. This is a novel prediction which remains to be experimentally tested.

In Chapter V, we apply our new variational model to positron self-trapping. Here the surface energy is seen to play an important role, despite the claims of some other workers. The final predictions which we make concerning the conditions under which the transition from free-particle behavior to self-trapped behavior occurs is compared with both experiment and with the available theoretical predictions of other workers. Our agreement with experiment is at least as good as any previously obtained, while the calculations necessary to obtain these predictions are much simpler than the previous calculations that have been performed.

In Chapter VI, our conclusions are summarized and some suggestions are made for further work.

CHAPTER I

INTRODUCTION

In this Introduction, we shall try to prepare the reader for the main text of this thesis by considering in turn the self-trapping of an electron in helium, and then the self-trapping of a positron. In the first case, we start with the description of a mobility experiment for positive and negative charge carriers in helium and of the problems posed by the anomalous behavior of the negative carriers. Early attempts to explain the results of these experiments are reviewed, leading up to the "bubble model" of an electron in helium. Some subsequent theoretical and experimental developments are then reviewed, with the hope of bringing the reader reasonably well up to date on the literature, after which the contributions that this thesis hopes to make are briefly noted.

Turning to the positron, a positron annihilation experiment is described. Two theories of the sudden increase in annihilation rate which may occur at some temperatures as the density of the helium is increased are briefly examined, followed by a preview of the contributions to be offered here.

The Electron in Helium

L. Meyer and F. Reif [1958] performed an experiment to measure the mobility of helium ions in the following way. The cavity between two large, flat electrodes was filled with liquid helium, so that by

applying a potential across these electrodes a reasonably uniform electric field could be created in the liquid. Alpha particles, emitted from Po^{210} plated on one of the electrodes, strongly ionized the helium in its vicinity. Depending on the direction of the electric field in the cavity, either positive or negative chanrges could be pulled through the helium toward the other electrode. Between the electrodes described so far were two pairs of closely spaced grids, and between each pair an AC electric field was induced, creating two gates through which the charge carriers had to pass on their way to the second electrode. Only when the average transit time of the charge carriers between the pairs of grids was a multiple of the period of the applied AC field could a maximum current reach the second electrode.

This arrangement allowed the average transit time of the charge carriers to be accurately measured. Given this time, the distance between the pairs of grids, the applied electric field, and the fact that only singly ionized carriers could be expected, the mobilities could be easily calculated.(1)

The results showed a dramatic drop in the mobilities of both positive and negative carriers as the temperature was lowered, well beyond what could be expected on the basis of the kinetic theory of gases: the charge carriers were simply not behaving like particles of

(1) Electron mobility has also been measured in gaseous and liquid neon (Loveland, et al., [1972]), liquid nitrogen (reported by Hernandez [1973]), gaseous hydrogen (Harrison [1971a], Harrison and Springett [1971b]), liquid argon (Halpern, et al., [1966], Schnyders, et al., [1966], Janke, et al., [1970]) and liquid krypton (Schnyders, et al., [1966]). Gases other than helium will be discussed in Chapter VI.

atomic mass diffusing through the helium with an average drift velocity imposed by the external electric field. These experiments also showed the negative carrier to have a mobility of about two-thirds of that of a positive carrier under the same conditions.

K. R. Atkins [1959] attempted to explain these low mobilities by supposing that the attractive polarization forces between a charged particle and the fluid around it could, if the temperature of the fluid was low enough, induce a high density cluster of fluid atoms around the charge carrier. The charge carrier's mass would be effectively increased by the mass of all the fluid atoms it would have to drag around with it, as well as by the "hydrodynamic" mass arising from fluid drag forces, and its mobility would be correspondingly lower.

While this theory acocunts for a reduced mobility of charge carriers under the conditions of the experiments it tries to explain, it also implies that there should be little difference between the mobilities of positive and negative helium ions, regardless of their nature, since the effective mass of both carriers almost entirely arises from the high density clusters of fluid atoms surrounding them, and the density and size of the cluster essentially depend only on the electric charge on the carrier. The same argument also holds if the negative carrier is presumed to be a singly ionized atom of an impurity in the helium, such as O_2^-, as had been proposed. Following these lines of reasoning, C. G. Kuper [1961], among others including Atkins himself, was forced to the conclusion that the negative charge carrier must be a "free" electron, and not a charge bound to an atom.

If this hypothesis is accepted, however, an explanation must be found for the electron's extraordinarily low mobility.

Atkins [1963] put forth a theory emphasizing the role of the attractive polarization forces. He imagined that the electron moves almost freely in the regions between the widely spaced atoms, but that because of polarization forces, the density of the liquid tends to be higher in the vicinity of the electron than elsewhere, just as is the case for positive ions. The difference between the electron and a positive ion rests, for Atkins, solely on the fact that the electron's kinetic energy increases rapidly when it is confined to a small volume, while the ion's does not. Thus the density increase around the electron is spread over a wider volume, and never becomes nearly as high as it would close to a positive ion. Atkins is able to show that the effective mass of such a complex of helium atoms around an electron must be greater that the effective mass of the complex around an ion, so that the mobility must be correspondingly lower.

Somewhat earlier, another theory had been put forward by G. Careri, et al. [1959], who had carried out some of the mobility experiments. Careri proposed that the repulsive core of the interaction between electrons and helium caused the helium density in the electron's vicinity to decrease, creating a "bubble". Around the bubble, he envisioned a barrier of dense helium created by the longer-ranged attractive polarization forces.

The choice between these two alternatives was settled, at least for Kuper [1961, 1963], by the conviction that the electron-helium interaction had a repulsive core that dominated the relatively weak

long-range polarization forces: a conviction later given experimental support (Sommer [1964]). Such a core gives the electron in Atkins' picture a high zero-point kinetic energy, making the bubble model more plausible, and winning it general acceptance. Kuper went on to estimate the size of the bubble by requiring that the pressure exerted outward by the electron on the liquid be equal to the pressure exerted by the atoms on the electron. This approach is equivalent, as Kuper points out, to minimizing the total energy of the system, which is the method used by most later researchers. He estimates the bubble radius in liquid helium to be about 12 A, and the effective mass to be about 100 helium masses, which is about the same as the effective mass of a positive ion under the same conditions. From one point of view, subsequent workers have only refined this model of the self-trapped state.

From a different perspective, I. M. Lifshitz [1965], in a paper with emphasis largely on the solid state, treated the problem of the energy spectrum of a quantum mechanical particle interacting repulsively with impurity atoms in a crystal. He supposed that the particle could create a void in its vicinity from which impurity atoms are excluded: an analogy to the situation for the electron in helium just described[1]. He went on to calculate the energy spectrum of the

---

[1] To a fair number of workers in the area of self-trapping in gases, this description of self-trapping is known as the Lifshitz' model, in spite of Careri and Kuper's precedence.

system by a simple argument. For a particle trapped entirely inside a spherical square potential well, the wavelength, and thus the excess kinetic energy, of the particle is simply related to the well radius: $KE \sim 1/\lambda^2 \sim 1/R_o^2$. On the other hand, the relative probability, ν, that a spherical void will occur in an ideal gas is simply related to the volume, V, of the void by elementary statistical mechanics: $\nu \sim e^{S/k} \sim e^{-\rho V}$, where S is the entropy cost of creating the void and ρ is the impurity density. Thus the probability of finding a particle with an excess kinetic energy, KE, goes like $\exp(-KE^{-3/2})$, in contrast to the case of a free particle, for which it goes like $KE^{1/2}$. This result quickly points out that the "thermodynamics" of such a "self-trapped" state is drastically different from that of a free or nearly free particle.

Less than a year after Lifshitz' paper, an experiment of considerable impact was reported by Levine and Snaders [1966]. In this experiment, designed to measure electron mobilities in low temperature helium gas, a cavity between two electrodes was again filled with helium. Here, however, the negative electrode was a photocathode, stimulated into emitting electrons by a xenon flash tube. Once again, time of flight between the two electrodes gave the average drift velocity of the electrons. The striking feature of the results of these experiments was a drastic drop in electron mobility when the pressure was increased to a certain point while the temperature was held constant. For example, at a temperature of 4.19 K, between the pressures of six-tenths and seven-tenths of the saturated vapor pressure, the mobility dropped by two orders of magnitude. At low densities

the mobilities were in agreement with the kinetic theory of gases, while at the highest densities observed (near the normal boiling point), the mobilities were lower than the kinetic theory result by four orders of magnitude.

On the theoretical side, Levine and Sanders made the most careful treatment of the electron self-trapped state so far.[1] Although they still assumed that a complete void in the helium is created around the electron, they improved the electron wave function by allowing it to overlap the walls of the square potential well in which it finds itself. They also represent helium-helium interactions through the second virial coefficient. At a specified temperature and density, the only variable in their model is the well radius. Minimizing the free energy of the system with respect to variations in this quantity then gave them the best choice of well radius for the model chosen. To calculate the mobility of an electron under specified conditions, they used a weighted average of the mobilities of a free electron and of a self-trapped electron under those conditions. The weight factor is the relative probability of the occurrence of each type of state. The mobilities are calculated from a interpolation formula which reduces to the kinetic theory mobility at low densities and, at high densities, to the hydrodynamic mobility of a hard sphere whose radius was taken as the classical turning radius of a helium atom

---

[1] From this point on, all bubble models of self-trapping of electrons discussed here use a Fermi pseudopotential for the interaction between the electron and the fluid atoms surrounding it.

approaching the self-trapped electron. This turning radius was about 16A at 4.3 K and saturated vapor pressure. Their results for electron mobility agree well with their experiment in the hydrodynamic and kinetic theory limits, but poorly in between. In particular, the drop in calculated mobility to hydrodynamic values occurs virtually instantaneously as the density is increased. This mobility "edge" also is predicted to occur at too high a density, reflecting the approximate nature of their model.

This failure at intermediate densities is characteristic of the bubble model. At such densities, the electron bubble is not very stable and the free particle is not very stable either. As the density is increased, the electron, at first free, falls with increasing frequency into pockets where the density of helium is locally reduced, from which it subsequently escapes or from which it is ejected by the occurrence of a density fluctuation increasing the density of the helium near it. The higher the density, the longer the elctron remains in the pocket, until finally it finds itself too stably situated there to be evicted. In the transition region fluctuations, ignored in the theory of stable equilibria used so far, play the central role.

A theory based on this idea was presented by Eggarter [1972] and in more preliminary form by Eggarter and Cohen [1970], within the context of percolation theory. Two adjustable parameters arise, and when their values are adjusted optimally, this theory gives the best overall agreement with Levine and Sanders experimental mobilities that has been obtained to this day, at least to our knowledge. Unfortunately

for one primarily interested in the nature of the stable self-trapped state, where fluctuations are again unimportant, this theory is too complex to permit a clear physical picture of the system.

Another "stochastic" approach that could well be mentioned here is that of Friedberg and Luttinger [1975] and Luttinger [1976]. This approach is more akin to Lifshitz' than any others reported here, in that its central interest is the energy spectrum of electrons in a disordered system. The "scattering centers", which are helium atoms in our application, are taken to form a stochastic potential for the electron. That is, every possible arrangement of fixed scattering centers provides a potential in which the elctron can move, and thus determines a "partition function" for the electron. Averaging this partition function for the electron over all possible arrnagements of scattering centers gives an effective partition function for the electron, from which the density of electronic energy levels, that is, the energy spectrum in Lifshitz' language, may be determined. In the limit of very low energies, they find that the leading term is precisely the one advanced by Lifshitz on the simple physical grounds mentioned earlier, and find first correction terms as well. Again, however, to one interested in the general nature of the self-trapped state, this theory does not provide enough clear answers. Let us leave, with some appreciation, these stochastic approaches and return to the main line of development leading to this thesis.

The next substantial theoretical contribution in the vein of Levine and Sanders' work was made by Hernandez [1973], who, interestingly, has made contributions to both Eggarter's work (Eggarter

[1972]) and to Luttinger's (Hernandez [1977]). In his 1973 paper, he replaced the square well density profile by one which changed gradually, which did not require the density at its center to vanish, and for which exact solutions to Schrödinger's equation were known.[1] He extremized the energy of the system with respect to variations in the "depth" and "radius" of the density well in his model, correcting for the effects of atom-atom interactions through the second virial coefficient. Since his theory essentially ignores the fluctuations which are so important in the transition region between free states and self-trapped states, as Levine and Sanders' did, it suffers the same "instantaneous" drop in mobility when the self-trapped state becomes physically realizable. However, the densities at which this drop occurs fit the mobility data much more closely than in Levine and Sanders' theory, as might be expected. Hernandez also applied this theory to electron self-trapping in neon, hydrogen, and nitrogen, and reported reasonably good agreement with available experimental data.

Later (Hernandez [1975]), he extended this theory by representing the electronic state by a sum of harmonic oscillator eigenstates, truncating the series when it apparently introduced no error to do so. The corresponding density profile of the fluid was easy to calculate, since the fluid was presumed to be an ideal gas. The energy of the system was then minimized by varying the coefficients of the harmonic oscillator states in the series for the electron wave

---

[1] In fact, it is problem four of Section 23 of the well-known text of Landau and Lifshitz on non-relativistic quantum theory. See bibliography.

function. No one has produced a better estimate of the conditions for the onset of the self-trapped state than the one this theory gives. Hernandez also explored in this paper the behavior of the system energy as a function of both the "depth" of the well and of its "radius", and noted the existence of an energy barrier which the electron must overcome in order to make the transition from a free state to a self-trapped state. While it is not perfectly clear on the basis of this paper that using harmonic oscillator basis states in the way he did will truly locate the minimum of the system's energy, it is made very plausible. Unfortunately, all Hernandez' calculations, except for a perturbation method that fails badly at very low temperatures and at high densities, require complex numerical work which would be nice to avoid, if possible.

Finally, we turn to the work previously conducted here on this problem (Cleveland, Gersch, and Moore [1977], Moore, Cleveland, and Gersch [1978a]). Minimizing the free energy of an electron with arbitrary wave function, interacting with an ideal gas with arbitrary density profile, we found that the coupled equations for the density profile and wave function usually employed by other researchers could be replaced by the problem of solving a non-linear Schrödinger equation. We found it practical to directly solve this equation numerically, after noting that a scaling transformation permitted all of the variables characterizing experimental conditions, such as density and temperature, to be replaced by a single scaled energy.[1] This

[1] This scaling transformation will be performed in the next Chapter.

transformation meant that it was not necessary to solve the equation at every individual value of density and temperature of interest. Each solution found for a value of the scaled energy corresponded to many interconnected values of the density and temperature, when the scaling procedure was reversed.

The scaling procedure is the most attractive method of this approach. As we shall see in the next chapter, the scaling alone permits us to determine the functional form of the conditions that the density and temperature must satisfy at the onset of the self-trapped state.

Aside from exploring the analytic properites of these solutions, and considering, self-consistently, the importance of fluctuations to our results, we also presented a simple variational model in which the electron is entirely trapped inside a square well (that is, the wave function does not overlap the edges of the well) but for which the density inside the square well was not required to be zero. This simple model contains all the qualitative features of the exact solution and is physically transparent, but gives poor quantitative results. It will be discussed at some length in the next chapter.

It is worth mentioning here that some other experiments have been proposed to investigate the self-trapped state. Northby and Sanders [1967] have experimentally investigated the photoejection of electrons from bubble states in liquid helium, and have obtained good agreement with their experiments by presuming that the density profile of the helium is a square well devoid of helium atoms, and that the wave function is the exact solution of Schrödinger's equation for that

well, just as Levine and Sanders [1966] did. Fowler and Dexter [1968] suggested that infrared radiation might induce transitions between the ground electronic state and an excited state, and that the radiation produced by the subsequent decay of the electron back to a lower energy state could provide detailed information about the self-trapped electron's energy levels. They provide the results of their own calculations, carried out on several large computers, using Levine and Sanders' model. One of us (R. Moore [1978b]) has also considered the effect of infrared radiation on a self-trapped electron and has calculated oscillator strengths for the transitions and linewidths. He has also investigated, through the second virial coefficient, the effect of helium-helium interactions on the exact numerical solutions mentioned earlier, and found them unimportant.

The contributions this thesis will make to the theory of electron self-trapping in helium are the following. We shall present a simple variational model, which works about as well quantitatively as the best of the other models that have been proposed, but which does not require difficult numerical calculations. In addition, helium-helium interactions will be taken into account through an approximate equation of state, rather than by just the second virial coeffieient, and the effects of surface tension will be considered. The most interesting result is the novel prediction of a second mobility edge at sufficiently high densities.

The Positron in Helium

Let us again begin with an experiment. Canter, et al., [1975a]

measured the annihilation rate of slow positrons in low temperature helium gas. They placed a hollow aluminum needle containing Na^{22} along the axis of a cylindrical cell that was to be filled with helium. When a positron is emitted from Na^{22}, a 1.28 MeV gamma ray is emitted simultaneously. Observation of this gamma ray provided the benchmark from which the positron lifetimes were measured. Subsequent annihilation of the positron yields two or three gamma rays, each of 0.51 MeV or less. Observation of this second emission of gamma rays determined the lifetime of the positron.

Unfortunately, the annihilation event can arise from a variety of processes, and random coincidences will inevitably be picked up as real events. Background coincidences were apparently constant, so their contribution could be simply subtracted out. Contributions from positrons annihilating in the source, or in the walls of the cell, and contributions arising from the annihilation of para-positronium typically occurred within five nanoseconds of the emission event, so that by ignoring this time interval, their contribution could be left out. Ortho-positronium is very long-lived compared to the other species of positrons in the helium,[1] so that by waiting until it was the only component left, the experiments could determine its exponential decay rate. Then assuming that this decay rate is adequately constant, they could estimate the ortho-positronium contribution over the time interval

---

[1] In fact positronium forms a bubble in helium, just as the electron does. The suggestion by Ferrell [1957] that bubble formation could explain the long lifetime of ortho-positronium in liquid helium was the first appearance of a bubble model for self-trapping.

of interest. Subtracting this out, they were left with an annihilation rate for the only component presumably left: the slow, thermalized positron. Their results are striking.[1]

At a temperature of 5.0 K, the annihilation rate increased from about 10^8 annihilations/sec to five times that value when the density of the helium was increased from about 2×10^{21} atoms/cm^3 to 2.7×10^{21} atoms/cm^3. Further increases in the density, at least up to about 16×10^{21} atoms/cm^3 where their measurements stopped, had no further effect on the annihilation rate, which had reached a magnitude expected only in liquid helium. This is to be contrasted with the belief, well upheld at higher tempearatures, that the annihilation rate should increase linearly with the density. When the density was fixed, say at 3.5×10^{21} atoms/cm^3, a sudden drop in annihilation rate was observed when the temperature was increased past about 6.7 K. Making the behavior of the positron even more remarkable, later researchers (Hautojärvi, et al., [1977]) found that if the density was increased still further at a fixed temperature, the annihilation rate would abruptly begin to increase linearly with the density, again following the simple theory successful at higher temperatures.

Everyone seems to have interpreted these experiments in terms of helium atoms clustering around the positron, for which the atoms feel an attractive interaction. The rapid changes in annihilation rate presumably arise from the formation or breaking up of such a

---

[1] Positron annihilation rate experiments have also been carried out for He^3 (Manninen and Hautojärvi, et al., [1978]), neon and argon (Canter and Roellig [1975b]).

cluster and occur when the cluster makes a transition between being energetically favorable and being energetically unfavorable.

Canter, et al., attempted to explain the experimental results through the clustering of atoms around the positron, for example, in a way very akin to Atkins' theory of the mobility of positive ions. Considering the positron to provide a static electric field, they picked a trial wave function and calculated the density of helium atoms aroudn the positron by requiring that the attractive force produced on a volume element of helium polarized by the positron's electric field must be balanced by the repulsive force from the pressure gradient acting on that element. Then freezing the helium density and polarization, they find the amount of work necessary to move a positive charge from infinity to an arbitrary point, giving them a potential energy function, $V(r)$, for the positron. They found that this potential always turned out to be too weak to support a bound state, and concluded that cluster formation could not occur unless other processes, such as multiple scattering or possibly chemical bonding between the positron and a few helium atoms, were involved.

As Manninen and Hautojärvi [1978] pointed out, this argument is flawed. The mistake occurred when the helium polarization was frozen in, before calculating the work necessary to move the positron into the helium cluster. Instead, the helium polarization almost instantaneously follows the position of the positron and thus always exerts an attractive force on it throughout the slow, quasi-static process envisioned in the calculation of the potential. If the polarization

is fixed, on the other hand, the positron, as it is moved in, will find itself approaching atoms which have been polarized in the wrong direction and are actually exerting a repulsive force on it. Thus the potential energy for the positron in Canter's calculation is not nearly as negative as it should be, and it is no surprise that this potential is too weak to support a bound state.

In this same paper, Manninen and Hautojärvi [1978] presented their own theory of the self-trapped positron state, which will be discussed in more detail in Chapter III and V. In essence, they minimized the Gibbs' free energy of a system consisting of a gas, described with a Van der Waals' equation of state, and a quantum mechanical positron which interacts with the atoms of the gas via a Fermi pseudopotential interaction $V(r) = g\,\delta^3(r)$. After they neglected surface tension, this gave them two coupled equations in the positron wave function and the gas density which they solved by a supposedly exact, unspecified, numerical method. They apply this method to positrons in He^3, He^4, neon, and argon, but He^3 and He^4 occupied most of their attention, since the experimental results were clearest there. For each of these two gases, they found that their predictions of the highest temperature, regardless of density, at which a self-trapped state can appear was accurate when compared with experiment, but that their values for the minimum and maximum densities at which these states can appear were much too low at all temperatures. They offered no explanation.

Another theory of positrons in He^4, that of Stott and Zaremba [1977], had more success. This paper will also be discussed later in

more detail in Chapters III and V. Stott and Zaremba also applied the equations connecting the density and positron wave function which arise from the minimization of the Gibbs' free energy of the system. They, however, described the helium with an empirical equation of state, derived and included a surface energy term that also involves the empirical equation of state, calculated the strength of the positron-helium interaction by adapting a positron pseudopotential[1] method that was developed by Kubica and Stott [1969] to treat positrons in metals, and used a Gaussian-like wave function for the positron. They self-consistently solved the equations connecting the density and positron wave function for various choices of the single fitting parameter in their wave function, and sought out the value of this fitting parameter that minimized the system energy. Their results agree well with the experiments on He^4, except that for most of the densities at which they calculate the maximum temperature at which self-trapped states appear, their maximum temperature is too high by around ten percent.

These results are a substantial improvement over Hautojärvi's. The only complaint to be made is that the computation is so complex, the factors which have been carefully accounted for are so many, that it is difficult to penetrate the physics lodged in the calculation. Are all these improvements over Hautojärvi's work essential? Cannot a simpler calculation be done which will yield reasonably good agreement with experiment and yet still retain enough physical transparency

[1] Not to be confused with the Fermi pseudopotential.

to illuminate the basic processes at work in positron self-trapping in helium? We shall see.

The contributions this thesis hopes to make to the theory of positron self-trapping in helium are the following. We shall present a simple variational model, actually the same one we will have used for the electron case, for which computations are relatively simple compared with the ones previously carried out for this problem, and which seems to work about as well as Stott's model. We will characterize the helium by an approximate equation of state as simple as Van der Waals', but quantitatively superior to it. We will demonstrate that it is the surface energy term which Stott includes which is the essential one, and that it cannot be neglected as Manninen and Hautojärvi claim. And finally, we shall show that there is a way to include this crucial surface term that not only simplifies subsequent calculations, but is physically enlightening as well.

CHAPTER II

THE ELECTRON IN AN IDEAL GAS AND THE NEW VARIATIONAL MODEL

Let us begin by constructing a free energy functional for a system consisting of an electron[1] interacting with a classical, ideal gas consisting of N particles in a volume V. It is convenient to use the free energy change which occurs when the interaction between the electron and the ideal gas is turned on. This free energy change will have several parts: the change in the kinetic energy of the electron, the change in the electron-ideal-gas interaction energy, and the change in the free energy of the gas.

First, let us find the kinetic energy change. When the electron becomes localized, its kinetic energy is increased because it is confined to a much smaller volume than before. This kinetic energy of localization is

$$\Delta KE = -\frac{\hbar^2}{2m}\int d^3r\, \chi(r)\, \nabla^2\chi(r) = \frac{\hbar^2}{2m}\int d^3r\, |\nabla\chi(r)|^2 \qquad (1)$$

where $\chi(r)$ is the electron's wave function in the self-trapped state,[2]

---

[1] We imagine that the electron density is so low that interactions between electrons can be ignored. Thus it is sufficient to consider only a single electron.

[2] In general, the electron state is a mixture of the wave function for the ground state of the system and the wave functions are the various excited states of the system. However, these excited states turn out to be much less likely than the ground state, as our computer studies show, so that it is safe to use a wave function.

presumed real for convenience.

Next we find the electron-gas interaction energy. In a mean field approximation, where the effects of fluctuations are neglected, the interaction energy is

$$V = \int d^3r \int d^3R \chi^2(r) u(r-R) \rho(R) \qquad (2)$$

where $\rho(R)$ is the local gas density at the point R, and where $u(r-R)$ is the interaction between an electron situated at r and an atom situated at R.

In general, the interaction between an electron and an atom has two parts, a short-range repulsive core and a long-range attractive tail. The repulsive core arises from the Fermi exclusion principle. The electrons in an atom are already situated in their lowest energy states, and cannot tolerate a low energy intruder in their midst without greatly increasing their own energy. The excess electron is effectively excluded from the volume of the atom. The attractive tail arises from the polarization forces which the charged electron induces when near an atom. Helium is the gas of principle interest here, and because of helium's great stability, the polarizability is quite low and the repulsive forces are much stronger. The range of the forces then turns out to be only a few Angstroms, so that the picture we consequently form is one of the electron interacting with a predominately repulsive interaction, whose range is short compared with the electron's wavelength in the self-trapped state ($\gtrsim$ 20 Å). Under these circumstances, we may neglect the range of the interaction entirely, and use a Fermi pseudopotential

$$u(r-R) = g\delta^3(r-R) \tag{3}$$

where g is the interaction strength, related to the s-wave scattering length, a, by

$$g = \frac{2\pi\hbar^2 a}{m} \tag{4}$$

If we choose to do so, we may correct this interaction strength to account crudely for the effects of multiple scattering to high gas densities by using a Wigner-Seitz correction (Eggarter [197]]). The interaction energy now becomes

$$V = g\int d^3r\rho(r)\,\chi^2(r) \tag{5}$$

Since the interaction is repulsive, g is positive.

Finally, we find the free energy change of the ideal gas, which is on account of the deviation of its density from a uniform value, $\rho = N/V$. Since, by assumption, the atoms do not interact with each other, the change in local density produces a change only in the configurational entropy, so

$$\Delta F_{gas} = - T\Delta S_{gas} \tag{6}$$

This entropy change is found by dividing the volume V into K cells, each of volume $\tau = V/K$. The entropy is then

$$\Delta S_{gas} = - Nk \sum_{j=1}^{K} P_j \ell n P_j \tag{7}$$

where P_j is the probability for one atom to be in the jth cell. With no electron present, $P_j = \tau/V$; inserting this expression in Equation (7) gives the entropy of the gas in the absence of the electron. With an electron present, we write $P_j = (\rho_j/\rho)\,\tau/V$, where $\rho = N/V$, and ρ_j is interpreted as the density of atoms in the jth cell. The desired entropy change is the difference between the entropies with and without the electron.

$$\Delta S_{gas} = - k \sum_{j=1}^{K} \rho_j \tau \, \ell n(\rho_j/\rho) \tag{8}$$

Going to the continuum limit, τ becomes d^3r and ρ_j becomes $\rho(r)$, resulting in the expression

$$\Delta S_{gas} = - k \int d^3r \, \rho(r) \, \ell n(\rho(r)/\rho) \tag{9}$$

Combining Equations (1), (5), (6), and (9), we find the total free energy change of the system:

$$\Delta F = \frac{\hbar^2}{2m} \int d^3r |\nabla\chi(r)|^2 + g \int d^3r \rho(r) \chi^2(r) + kT \int d^3r \rho(r) \, \ell n(\rho(r)/\rho) \tag{10}$$

If the electron remains in a free particle state after the interaction is turned on, $\Delta F = \rho g$, so whenever $\Delta F/\rho g < 1$, the self-trapped state is energetically preferred.

In Equation (10) we can see how the transition to the self-trapped state can occur. The interaction term tries to reduce the

density in the vicinity of the electron, but this decreases the entropy of the gas. While the temperature is high, the free energy cost of this entropy decrease is too great for the formation of the self-trapped state to be economical. When the temperature is decreased, however, the entropy decrease becomes less and less important. When the relative importance of the entropy becomes small enough, the system will be able to lower its free energy by forming a self-trapped state.

Minimizing the ΔF of Equation (10) with respect to variations in $\rho(r)$, subject to the constraint $\int d^3r\rho(r) = N$, yields

$$\rho(r) = \frac{Ne^{-\beta g\chi^2(r)}}{\int d^3Re^{-\beta g\chi^2(R)}} \tag{11}$$

It is useful to note that the denominator of Equation (11) differs from V only by a very small term. Thus we can write

$$\rho(r) = \rho e^{-\beta g\chi^2(r)}\left[1 + \frac{1}{V}\int d^3Re^{-\beta g\chi^2(R)}\right] \tag{12}$$

where the second term vanishes in the thermodynamic limit.

On the other hand, minimizing the ΔF of Equation (10) with respect to variations in $\chi(r)$, subject to the constraint $\int d^3r\chi(r) = 1$, yields

$$-\frac{\hbar^2}{2m}\nabla^2\chi(r) + g\rho(r)\chi(r) = E\chi(r) \tag{13}$$

Equation (13) and Equation (12) with the second term neglected are typical of the coupled equations which other researchers have attempted to solve in various ways. Alternatively, however, substitution of Equation (12) with its second term neglected into Equation (13) gives a non-linear Schrödinger equation, which an be solved instead.

$$-\frac{\hbar^2}{2m}\nabla^2\chi(r) + \rho g e^{-\beta g\chi^2(r)}\chi(r) = E\chi(r) \qquad (14)$$

A different procedure gives the same non-linear equation but produces a useful form for ΔF in the process. Substituting Equation (12) into Equation (10) and remembering that the second term in Equation (12) is small gives

$$\Delta F = \frac{\hbar^2}{2m}\int d^3r|\nabla\chi|^2 + \frac{\rho}{\beta}\int d^3r(1 - e^{-\beta g\chi^2(r)}) \qquad (15)$$

Further extremization of this ΔF with respect to variations in $\chi(r)$, subject to the normalization constraint, again produces Equation (14).

Before returning to Equation (10) in order to apply a simple variational model to it, let us apply a scaling transformation[1] to some of these equations. This transformation will permit us to deduce the functional form of the equation determining the experimental conditions at which self-trapped states first begin to appear. We replace the distance r with a dimensionless length

---

[1] This transformation was first suggested by Eric J. Kuster in a conversation.

$$s = r\sqrt{2m\rho g/\hbar^2} \tag{16}$$

and χ with a dimensionless wavefunction ϕ

$$\phi = \sqrt{\beta g}\ \chi \tag{17}$$

The wave function $\phi(s)$ is not normalized to unity. Instead the normalization of $\chi(r)$ requires

$$\int d^3s\phi(s) = K\rho^{3/2}/T \tag{18}$$

where

$$K = k^{-1}g^{5/2}(2m/\hbar^2)^{3/2} \tag{19}$$

Application of this transformation to ΔF, written in the form of Equation (14), produces

$$\frac{\Delta F}{\rho g} = \int d^3s\ [|\nabla\phi(s)|^2 + 1 - e^{-\phi^2(s)}]/\int d^3s\ \phi^2(s) \tag{20}$$

while its application to the Schrödinger equation yields

$$-\nabla^2\phi + e^{-\phi^2}\phi = \varepsilon\phi \tag{21}$$

where $\varepsilon = E/\rho g$.

In principle, Equation (21) may be solved for various values of ε, and this is not especially difficult to do numerically if spherically symmetric solutions are assumed to be the only physically relevant ones. Given a solution of this equation for some value of ε,

we may perform the normalization integral of Equation (18), to find the value of $K\rho^{3/2}/T$ to which this solution beongs. Note that particular values of ρ and T are not associated with each value of ε, but only the value of $K\rho^{3/2}/T$. Thus all combinations of ρ and T which given the same value of $K\rho^{3/2}/T$, correspond to the same solution of Equation (21), and through Equation (20), to the same value of $\Delta F/\rho g$.

Thus if a self-trapped state can occur at a density ρ^* and a temperature T^*, then a self-trapped state can occur at every density, ρ, and temperature, T, such that

$$\frac{K\rho^{3/2}}{T} = \frac{K\rho^{*3/2}}{T^*} \tag{22}$$

which determines the form of the equation determining the experimental conditions at which the self-trapped states first begin to occur.

As reported in the Introduction, we have obtained the actual solution of Equation (21) by numerical techniques (Moore, et al,. [1978a]). Such methods, however, are not on the path this thesis will follow. Let us turn to the simple variational model reported in (Moore, et al., [1978a]), as an introduction to the new variational model to be subsequently presented.

Let us suppose that the density profile near the electron is like a square well:

$$\rho(r) = \begin{cases} \rho_i & r < R_o \\ \rho_o & r > R_o \end{cases} \tag{23}$$

where $\rho_i < \rho_o$. This density profile creates for the electron a square potential well:

$$V(r) = \begin{cases} \rho_i g & r < R_o \\ \rho_o g & r > R_o \end{cases} \tag{24}$$

If the temperature is low enough, this well will be so deep that the electron will be almost entirely trapped inside it and have a wave function of the form

$$\chi(r) = \frac{1}{\sqrt{2\pi R_o}} \frac{\sin(\pi r/R_o)}{r} \tag{25}$$

This model uses this wave function at all temperatures, on the grounds of its simplicity.

Using these forms for $\rho(r)$ and $\chi(r)$, Equation (10) becomes

$$\Delta F = \frac{\hbar^2}{2m}\left[\frac{\pi}{R_o}\right]^2 + \rho_i g + \frac{v_o}{\beta}\rho_i \ln(\rho_i/\rho) + \frac{V-v_o}{\beta}\rho_o \ln(\rho_o/\rho) \tag{26}$$

where $v_o = 4\pi R_o^3/3$ is the volume of the well.

Now ρ_i and ρ_o are connected through the condition

$$\rho_i v_o + \rho_o(V-v_o) = \rho V = N \tag{27}$$

If we use this expression to find ρ_o in terms of ρ_i and substitute it into Equation (26), keeping only terms that will not vanish in the

thermodynamic limit, we find

$$\frac{\Delta F}{\rho g} = \frac{\hbar^2}{2m\rho g}\left(\frac{\pi}{R_o}\right)^2 + \frac{\rho_i}{\rho} + \frac{kTv_o}{g}\left[\frac{\rho_i}{\rho}\ln\left(\frac{\rho_i}{\rho}\right) + 1 - \frac{\rho_i}{\rho}\right] \tag{28}$$

Then making the substitutions

$$y = \frac{\rho_i}{\rho} \tag{29}$$

and

$$s = \frac{R_o}{\pi}\sqrt{2m\rho g/\hbar^2} \tag{30}$$

we have

$$\frac{\Delta F}{\rho g} = \frac{1}{s^2} + y + GTs^3[y \ln y + 1 - y] \tag{31}$$

where

$$G = \frac{4\pi^4 k\hbar^3}{3(2m\rho)^{3/2} g^{5/2}} \tag{32}$$

If we are to have an extremum of the free energy, we must have

$$\frac{\partial(\Delta F/\rho g)}{\partial y} = 1 + TGs^3 \ln y = 0 \tag{33}$$

or

$$y = \exp(-1/TGs^3) \tag{34}$$

Substituting Equation (34) back into Equation (31) and making the convenient substitutions

$$D = (TG)^{2/3} \qquad \text{and} \qquad x^3 = TGs^3 \tag{35}$$

we find

$$\frac{\Delta F}{\rho g} = \frac{D}{x^2} + x^3 \left[1 - e^{-1/x^3}\right] \tag{36}$$

Graphs of this $\Delta F/\rho g$ versus x^{-1} are shown in Figure 1 for several values of D. The point on each curve at $x^{-1} = 0$ corresponds to the non-localized state, for which $\rho(r)$ has the uniform value ρ everywhere. We see from this figure that if D is small enough -- less than about 0.4 -- a local minimum can occur in $\Delta F/\rho g$ for $x^{-1} \neq 0$. If the value of $\Delta F/\rho g$ at this local minimum is less than one, we say that the self-trapped state is absolutely stable or simply "stable", since its free energy is less than the free energy of the free particle state. If the value of $\Delta F/\rho g$ is greater than one at the local minimum, we say that the self-trapped state is metastable, which is the case for the $D = 0.4$ curve in Figure 1.

A more accurate assessment of the values which extremize $\Delta F/\rho g$ can be obtained by setting the derivative of Equation (36) with respect to x equal to zero. This results in

$$\frac{3}{2}\chi_0^5 \left[1 - \left(1 + \frac{1}{\chi_0^3}\right) \exp\left(-\frac{1}{\chi_0^3}\right)\right] = D \tag{37}$$

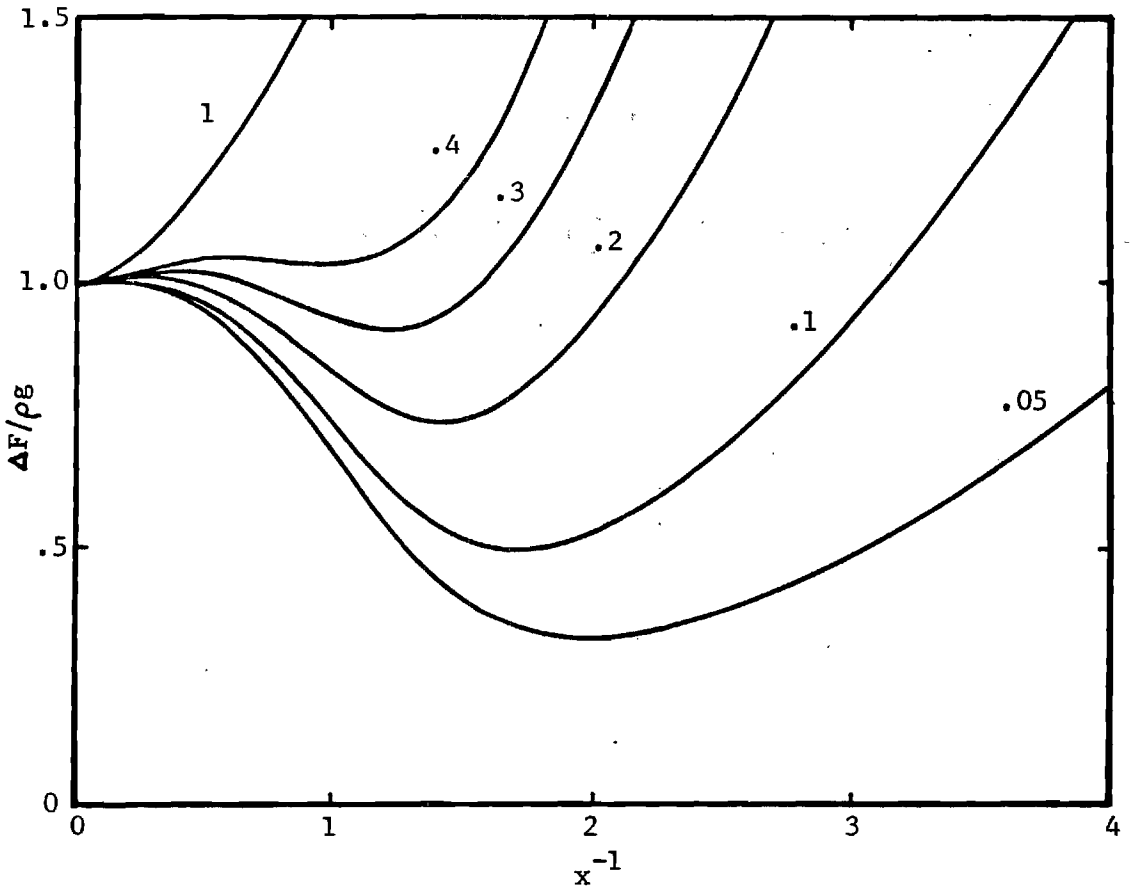

Figure 1. Scaled Free Energy Versus the Reciprocal of the Scaled Bubble Radius for Several Values of D (Old Variational Model).

Here x_0 is the extremum value of x. A graph of the left hand side of Equation (37) as a function of x_0 is given in Figure 2. Clearly no solutions exist for D > .430, which restricts the values of $T^{2/3}/\rho$ for which self-trapping can occur. When D < .430, there are two solutions to Equation (37) for each value of D , one of which corresponds to a local minimum of $\Delta F/\rho g$, and one of which corresponds to a local maximum, such as the extrema easily visible in Figure 1 for D = .3 or .4. For this simple model, the curvature of $\Delta F/\rho g$ as a function of x can be examined just by taking the second derivative of Equation (36) with respect to x. In this way, we find that of the two solutions for x_0, the smaller always corresponds to a local minimum of $\Delta F/\rho g$ and to either a stable or a metastable state, while the larger corresponds to a local maximum of $\Delta F/\rho g$ and to a state that we simply call unstable. This unstable state represents a free energy barrier separating free and self-trapped states.

Whether or not the local minimum in $\Delta F/\rho g$ is a stable or a metastable state is also determined by the numerical value of D. If D < .370, $\Delta F/\rho g$ at the local minimum is less than one, and the self-trapped state is stable. If D > .370, the self-trapped state is metastable. In summary, if D > .430 there is no self-trapped state, if .430 > D > .370 there is a metastable self-trapped state, and if .370 > D, the self-trapped state is stable. The equation D = .430 specifies a line in the (ρ,T)-plane that marks the threshold at which self-trapped states first become possible. This line we call the metastable limit line. The equation D = .370 marks the threshold

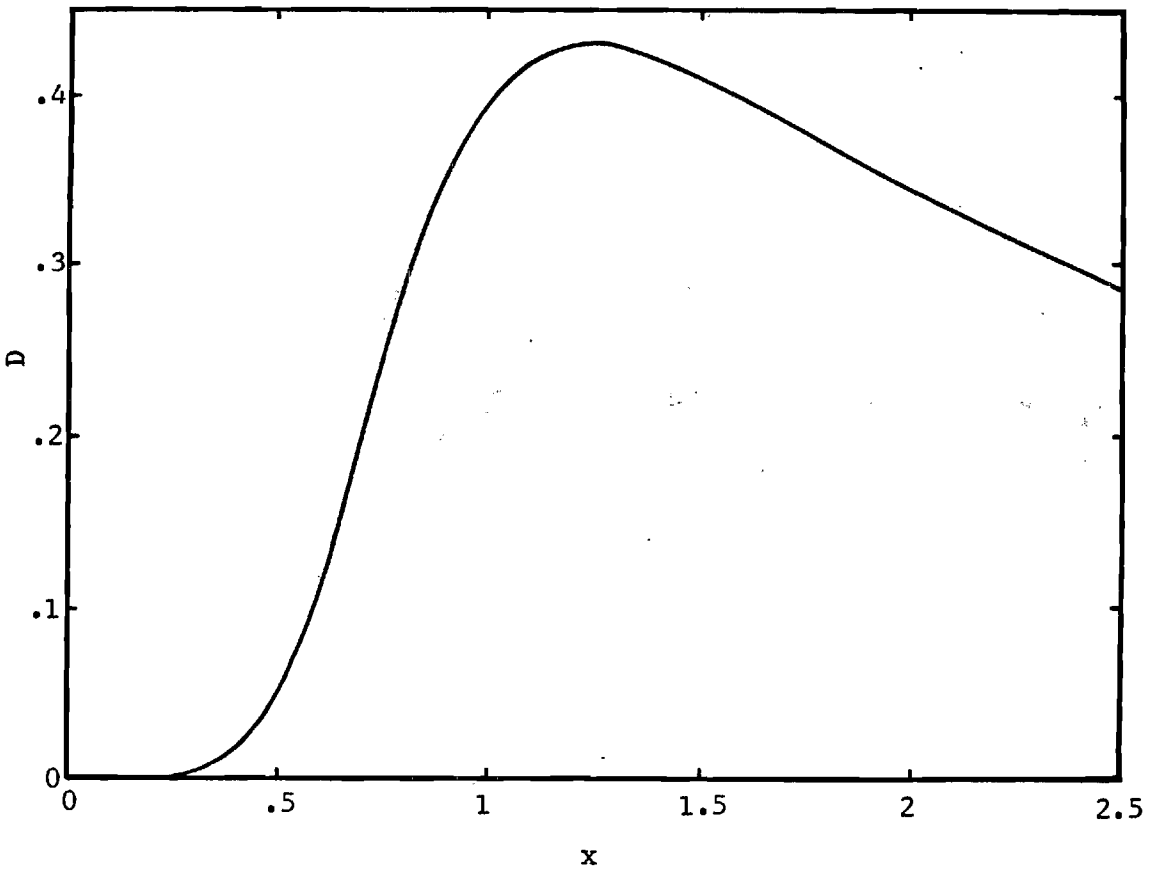

Figure 2. D Versus the Extremum Value of the Scaled Bubble Radius (Old Variational Model).

between metastable and stable states. We call the corresponding line in the (ρ,T)-plane the stable limit line.

All these results turn out to be qualitatively accurate when compared with the exact numerical solutions of Equations (16) through (21). Quantitatively, though, the results are bad. The exact numerical solution gives, for the metastable limit line, $D = 1.058$, instead of $D = .430$, corresponding to a 50 percent error for this variational model. For the stable limit line, the numerical solution gives a value of .926 for D, instead of .370, corresponding to a 60 percent error.

At least one fault in the model is the assumption that the wave function does not overlap the walls of its potential well, but always remains the wave function for a well of infinite depth. On the limit lines, the potential well turns out not to be deep enough to support this assumption. Put another way, the free energy change has been poorly minimized with respect to variations in the wave function, given the choice for $\rho(r)$.

An obvious improvement to attempt, if it does not too greatly complicate the problem, is to use the exact ground-state wave function for a particle trapped in a spherical square well of finite depth. This is the choice taken for the new variational model.

Let us take the potential well to be unchanged:

$$V(r) = \begin{cases} \rho_i g & r < R_o \\ \rho_o g & r > R_o \end{cases} \tag{38}$$

The corresponding ground-state wave function is of the form $\chi(r) = \psi(r)/r$, where

$$\psi = \begin{cases} A \sin (kr) \\ \\ Be^{-k'r} \end{cases} \tag{39}$$

Here A and B are constants and $\psi(r)$ satisfies the Schrödinger equation

$$-\frac{\hbar^2}{2m}\frac{\partial^2}{\partial r^2}\psi + V(r)\psi = E\psi \tag{40}$$

The requirement that $\psi(r)$ and its derivative be continuous at $r = R_o$ gives the condition

$$k \cot kR_o = -k' \tag{41}$$

A further connection between k and k' comes from the Schrödinger equation. If Equations (38) and (39) are substituted into Equation (40) one finds, for $r < R_o$, that

$$\frac{\hbar^2 k^2}{2m} + \rho_i g = E \tag{42}$$

and, for $r > R_o$, that

$$-\frac{\hbar^2 k'^2}{2m} + \rho_o g = E \tag{43}$$

so that we must have

$$\frac{\hbar^2 k^2}{2m} + \rho_i g = -\frac{\hbar^2 k'^2}{2m} + \rho_o g \tag{44}$$

Equations (41) and (44) may be combined to give

$$\tan kR_o = \sqrt{\frac{\hbar^2 k^2}{2m(\rho_o - \rho_i)g - \hbar^2 k^2}} \tag{45}$$

and since for the ground state $\pi/2 < kR_o < \pi$, we may write this as

$$\sin kR_o = \frac{\hbar k}{\sqrt{2m(\rho_o - \rho_i)g}} \tag{46}$$

or letting $z = kR_o$, as

$$\frac{\sin(z)}{z} = \frac{1}{\pi}\sqrt{\frac{\frac{\hbar^2}{2m}\left(\frac{\pi}{R_o}\right)^2}{(\rho_o - \rho_i)g}} \tag{47}$$

Thus z measures the extent to which the state is bound. The numerator in the square root in Equation (47) is just the kinetic energy the particle would have if it were in an infinitely deep well of the same radius. The larger this numerator is, the less tightly the particle will be bound. The denominator inside the square root is just the depth of the potential well. For an infinitely deep well, $\sin(z)/z$ must be zero, corresponding to $z = \pi$ and to a wave function with no overlap at the well's edges. The smallest value z can have for a bound ground state is $\pi/2$, corresponding to $\sin(z)/z = 2/\pi$, and

to the kinetic energy for the infinitely deep well being four times the depth of the actual well.

The energy of the electron in its well can be taken from Equation (42). Thus the new expression for ΔF, replacing Equation (28) is

$$\frac{\Delta F}{\rho g} = \frac{\hbar^2}{2m\rho g}\left(\frac{z}{R_o}\right)^2 + \frac{\rho_i}{\rho} + \frac{kTv_o}{g}\left[\frac{\rho_i}{\rho}\,\ell n\left(\frac{\rho_i}{\rho}\right) + 1 - \frac{\rho_i}{\rho}\right] \qquad (48)$$

If again, we express ρ_o in terms of ρ_i as we did before and make the substitutions of Equations (29) and (30, we find Equation (33) is replaced with

$$\frac{\Delta F}{\rho g} = \frac{z^2}{\pi^2 s^2} + y + GTs^3\,(y\,\ell n\,y + 1 - y) \qquad (49)$$

where, from Equation (47), z depends on s and y as

$$\frac{\sin(z)}{z} = \frac{1}{\pi s\sqrt{1+y}} \qquad (50)$$

We will now extremize $\Delta F/\rho g$ with respect to variations in s and y, as we did before, but we must be careful to remember that z is also a function of these variables. If we let $b(z) = \sin(z)/z$, we find

$$\frac{\partial z}{\partial s} = \frac{\partial z}{\partial b}\frac{\partial b}{\partial s} = -\frac{1}{s}\frac{b(z)}{b'(z)} \qquad (51)$$

$$\frac{\partial z}{\partial y} = \frac{1}{2(1-y)}\frac{b(z)}{b'(z)} \qquad (52)$$

where b'(z) is the derivative of b(z) with respect to z. We then find from $\partial(\Delta F/\rho g)/\partial s = 0$ that

$$-2z(z + b/b')/\pi^2 s^3 + 3GTs^2(y\ \ell ny + 1 - y) = 0 \qquad (53)$$

and from $\partial(\Delta F/\rho g)/\partial y = 0$ that

$$z\frac{b^3}{b'} + 1 + GTs^3\ \ell n\ y = 0 \qquad (54)$$

In spite of the apparent complexity of these equations, the stable limit line is easy to find. If in Equation (49), $\Delta F/\rho g$ is set equal to one and multiplied by $\pi^2 s^2$, the equation may be written as

$$z^2 + \pi^2 GTs^5(y\ \ell ny + 1 - y) = \pi^2 s^2(1-y) = \frac{1}{b^2(z)} \qquad (55)$$

whereas Equation (53) may be written as

$$-2z\left[z + \frac{b}{b'}\right]/3 + \pi^2 GTs^5(y\ \ell ny + 1-y) = 0 \qquad (56)$$

Eliminating the common term between these two equations yields

$$-1 + 5\ \sin^2(z)/3 + 2\ \sin^3(z)/3(z\ \cos\ z - \sin\ z) = 0 \qquad (57)$$

which has the solution z = 2.121558. Thus, along the stable limit line, z is constant. Dividing the last term of Equation (53) by the last term of Equation (54) gives

$$s^2(y\ \ell n\ y + 1 - y)/\ell ny = \frac{-2z\left[z + \frac{b}{b'}\right]/3\pi^2}{1 + z\frac{b^3}{b'}} \qquad (58)$$

and then eliminating s through Equation (50) and using the known value of z on the stable limit line gives

$$\frac{y \ln y + 1 - y}{(1-y) \ln y} = -.40000 \qquad (59)$$

which has the solution y = .2923121. Along the stable limit line, y is constant, too. And from Equation (50) so is s: its value is .9420634.

Solving Equation (54) for GT and substituting in the values now known for s, y, and z, we find the equation of the stable limit line.

$$GT = .6658550 \qquad \text{or} \qquad D = (GT)^{2/3} = .76252 \qquad (60)$$

This value of D is to be compared with the exact numerical result of D = .926. The percentage error in D is 17.6 percent as opposed to the 60 percent error from the old model. This new level of error compares well with the results obtained by other workers using variational models, such as that of Hernandez [1973], although the calculations here require much less effort.

The stable limit line is taken to mark the onset of the self-trapped state in this thesis, so it is gratifying that this line is so easy to find. To finish the comparison between the two models discussed in this chapter, however, we should also provide a general method of solution, provide a graph like Figure 2 for the new model, and compare the metastable limit line of the new model with that of the old.

Let us again divide Equation (53) by Equation (54) and use Equation (50), as we did in obtaining Equation (59), but this time we will not substitute for z its value on the stable limit line. We find

$$\frac{y \ln y + 1 - y}{(1-y) \ln y} = \frac{-2z\left[z + \frac{b}{b'}\right]\frac{b^2}{3}}{1 + z\frac{b^3}{b'}} \qquad (61)$$

And if one is added to both sides, we have

$$\frac{1}{\ln y} + \frac{1}{1-y} = 1 - \frac{2z\left[z + \frac{b}{b'}\right]\frac{b^2}{3}}{1 + z\frac{b^3}{b'}} \qquad (62)$$

For any z, we compute the right hand side, and then seek a solution of the resulting equation that lies between zero and one, since ρ_i will necessarily be less than ρ. The left hand side of Equation (62) drops smoothly from one to one-half as y increases from zero to one (despite appearances) and these solutions are not hard to find. As y goes to one, s goes to infinity, and the state becomes non-localized. The value of z corresponding to this non-localized state is 1.928350, there are no solutions to Equation (62) for any values of z less than this. When z = 2.021426 metastable self-trapped states first become possible. This metastable limit line corresponds to D = .871. The exact value of D from our numerical solution is 1.058, as mentioned earlier, giving the new variational model an error of 17.7 percent in D, as opposed to a 59 percent error from the old variational model.

A graph of D versus x, instead of versus s, is shown as the solid curve in Figure 3. The dashed curve in Figure 3 is a reproduction of Figure 2 for the old model, and is included to aid comparison between the models. The crosses on each curve mark the stable limit lines.

It is hoped that we have shown that it is possible to allow the wave function to overlap the edges of the well, without unduly increasing the difficulty of the calculations. Admittedly, these calculations are more difficult than those in the old model. Even so, they remain much simpler than those in any other methods known to us which give comparable accuracy.

We shall soon see that the computations remain manageable even if atom-atom interactions are included. First, however, we need to decide how we shall incorporate the effects of those interactions into the model. We shall do this in the next chapter.

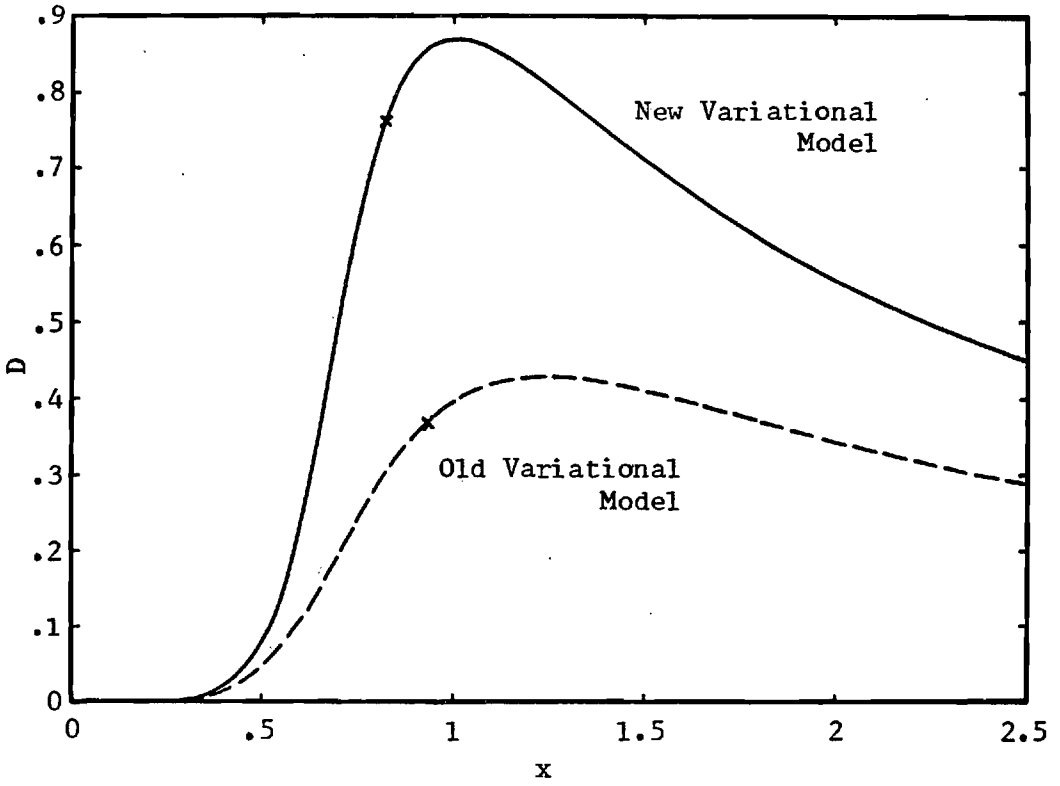

Figure 3. D Versus the Extremum Value of the Scaled Bubble Radius for the New and the Old Variational Models.

The crosses mark the stable limit line.

CHAPTER III

THE CHARACTERIZATION OF HELIUM AS A NON-IDEAL GAS

In this chapter, we shall decide how to describe, first, the bulk properties of helium, and then the surface properties.

The question of how to treat the bulk properties of helium comes down to choosing an equation of state for the gas. One choice is to use an empirical equation of state, which is of unquestionable quantitative accuracy. The choice of this thesis, however, is to use an approximate equation of state, such as Van der Waals'. We feel that this approach provides clearer physical insight into the processes which affect the experimental results that we want to understand. Parameters in the approximate equation of state may be varied to gauge the importance of different aspects of the helium-helium interactions to the phenomena under study, in a way which is not practical with an empirical equation of state.

Two features, at a minimum, can be expected in any approximate equation of state which can successfully characterize helium at high densities and low temperatures: the attractive forces between helium atmos should be represented in the equation at least well enough to permit a phase transition from the gaseous to the liquid state, and the repulsive short-range forces between the atoms should be reflected by the presence in the equation of a maximum density, or a "jamming density", beyond which it is practically impossible to compress the fluid.

One well-known equation of state which meets these criteria is the Van der Waals equation.[1]

$$P + \frac{a}{v^2}(v - b) = kT \qquad (1)$$

Here P is the pressure of the system and v is the volume per particle. In this equation, b is the smallest volume per particle which the system can attain, and is the reciprocal of the jamming density, ρ^*, while a, whose presence reduces the pressure of the gas, represents the attractive forces between the particles or atoms.

If we wish to apply this equation of state within our methods, we need to find the free energy to which it corresponds. If we remember that $P = -(F/V)_{N,T}$ where V is the volume of the whole system, then we may find F by integration (of course, here the constant of integration will be an arbitrary function of N and T). We obtain

$$F = \frac{3}{2}NkT + kTV[\rho \ln \rho - \rho \ln(1 - \rho b)] - V\rho^2 a \qquad (2)$$

where ρ is the density of the gas and we have used the fact that the free energy of our system must go over to the free energy of an ideal gas as $V \to \infty$ while N and T remain fixed.

We must still determine the constants a and b. The two most widespread methods are to choose these parameters so that the Van der Waals equation predicts the experimental critical temperature, T_c,[2]

[1] Manninen and Hautojärvi [1978] use the Van der Waals equation of state when treating positron self-trapping in helium.

[2] For helium, $T_c = 5.21k$

and either the experimental critical pressure, P_c,[1] or the experimental critical density, ρ_c.[2] We may find the connection between a and b and the critical data analytically: this provides another exercise in the minimization of free energies.

Suppose that we replace the uniform gas of density ρ in Equation (2) by a gas which has a density ρ_1 in subvolume V_1 and ρ_2 in subvolume V_2 (we assume that $V_1 \ll V_2 = V - V_1$, without loss of any relevant generality). The change in free energy which occurs when we make this replacement is

$$\begin{aligned}\Delta F = {} & kTV_1[\rho_1 \ln \rho_1 - \rho_1 \ln(1 - \rho_1 b)] - V_1 \rho_1^2 a \\ & + kTV_2[\rho_2 \ln \rho_2 - \rho_2 \ln(1 - \rho_2 b)] - V_2 \rho_2^2 a \\ & - kTV[\rho \ln \rho - \rho \ln(1 - \rho b)] - V \rho^2 a \end{aligned} \tag{3}$$

If we let $y_1 = \rho_1/\rho$, $y_2 = \rho_2/\rho$, and $y^* = 1/\rho b$, we find

$$\begin{aligned}\Delta F = {} & kTV_1\rho \left[y_1 \ln y_1 - y_1 \ln \left(\frac{y^* - y_1}{y^* - 1} \right) \right] - V_1(\rho_1^2 - \rho^2)a \\ & + kTV_2\rho \left[y_2 \ln y_2 - y_2 \ln \left(\frac{y^* - y_2}{y^* - 1} \right) \right] - V_2(\rho_2^2 - \rho^2)a \end{aligned} \tag{4}$$

But since $V_1 \ll V_2 = V - V_1$ and $\rho_1 V_1 + \rho_2 V_2 = \rho V$, we have

---

[1] For helium, $P_c = 2.26$ atm.

[2] For helium, $\rho_c = 10.43 \times 10^{21}$ atoms/cm^3

$$y_2 = 1 + (1 - y_1)V_1/V \tag{5}$$

and noting that $V_1/V << 1$, we may write

$$\Delta F = kTV_1\rho\left[y_1 \ln y_1 - y_1 \ln\left(\frac{y^*-y_1}{y^*-1}\right)\right] - \frac{y^*(y_1-1)}{y^*-1}$$

$$- V_1\rho^2(y_1-1)\, a \tag{6}$$

If the two differing densities are to coexist in equilibrium, then the partial derivatives of ΔF with respect to y_1 and V_1 must vanish. The condition $\partial(\Delta F)/\partial V_1 = 0$ gives

$$kT\left[y_1 \ln y_1 - y_1 \ln\left(\frac{y^*-1}{y^*-1}\right) - \frac{y^*(y^*-y_1)}{y^*-1}\right] - \rho(y_1-1)^2 a \tag{7}$$

while the condition $\partial(\Delta F)/\partial y_1 = 0$ gives

$$\frac{2\rho a(y_1-1)}{kT} = \ln\left[\frac{y_1(y^*-1)}{y^*-y_1}\right] + \frac{y^*}{y^*-y_1} - \frac{y^*}{y^*-1} \tag{8}$$

We may use Equation (8) to find the connection between a and b and the critical data. Near the critical point, $\rho_1 \approx \rho_2 \approx \rho$, we we may write

$$y_1 = 1 + \Delta y \tag{9}$$

where Δy is small. Substituting Equation (9) into Equation (8) and keeping only term up to the first order in Δy yields

$$\frac{2a}{kT}\Delta y = \Delta y\left(\frac{y^*}{y^*-1}\right)^2 \tag{10}$$

so

$$T = \frac{2a\rho}{k}(1 - \rho b)^2 \tag{11}$$

Now the critical temperature is the highest temperature, regardless of average density, ρ, at which two phases can coexist, so that we must have $\partial T/\partial \rho = 0$ at the critical point. This condition gives

$$(1 - \rho_c b)(1 - 3\rho_c b) = 0 \tag{12}$$

The solution $\rho_c = 1/b$ is no good here, since if the density of one of the phases is near the jamming density, $\rho^* = 1/b$, the density of the phase that can coexist with it is very small and these conditions do not correspond to the critical point. Therefore, at the critical point, we must have

$$\rho_c = \frac{1}{3b} \tag{13}$$

Substituting Equation (13) back into Equation (14) gives the critical temperature

$$T_c = \frac{8a}{27kb} \tag{14}$$

If we wish to fit the Van der Waals equation to the critical density and temperature, Equations (13) and (14) give

$$b = \frac{1}{3\rho_c} \tag{15}$$

and

$$a = 9kT_c/8\rho_c \tag{16}$$

If we wish to fit the Van der Waals equation to the critical pressure and temperature, Equations (1) and (14) give

$$b = kT_c/8P_c \tag{17}$$

and

$$a = \frac{3}{4} kT_c^{\ 2}/P_c \tag{18}$$

Actually, Equations (7) and (8), once a and b are determined, give the values of the two densities which can coexist at any temperature below the critical temperature, without employing Maxwell's construction. If T is eliminated between these equations, we obtain an equation that only involves y_1 and y^*. Once the average density, ρ, is specified, $y^* = 1/\rho b$ is known, and the roots of this equation may be sought. One of these roots is $y_1 = 1$, corresponding to the fact that one of the phases has been taken to occupy almost all of the volume V of the system, so that the average system density, ρ, is essentially the density of this phase. The other root, which is not difficult to find, corresponds ($\rho_1 = \rho y$) to the density of the phase which can coexist with a phase of density ρ at some temperature. Placing this solution back into Equation (11) determines the temperature at which these densities can coexist.

We have done this for Van der Waals' equation of state fit to both critical density and fit to critical pressure. The resulting "coexistence curves" are shown in Figure 4, along with the experimental coexistence curve. Note that both fits fail at low temperatures by predicting that the condensed phase has a density quite a bit higher that the experimental value. In other words, the Van der Waals equation predicts a jamming density that is too high: too high for the fit to critical pressure ($\rho^* = 25.4 \times 10^{21}$ atoms/cm^3), and much too high for the fit to critical density ($\rho^* = 30.7 \times 10^{21}$ atoms/cm^3). This is nothing new, for the failure of a Van der Waals equation of state for helium is well-known, and Manninen and Hautojarvi [1978] apologize for using it in their theory of positron self-trapping in helium.[1] There is another equation of state with only two parameters, however, which is as easy to work with as Van der Waals', but which fits the experimental coexistence curve much better. It is the topic of the next subsection.

The Lattice Gas

In the lattice model, a system is subdivided into many small cells, of volume τ, so that there are $K = V/\tau$ cells in all. This is just what was done in the previous chapter to find the entropy of a non-uniform ideal gas, but there the cell size was arbitrary, while here the cell size is physically important. A cell in the lattice model cannot be more than singly occupied, that is, there is either

[1] They use the critical pressure, critical temperature fit.

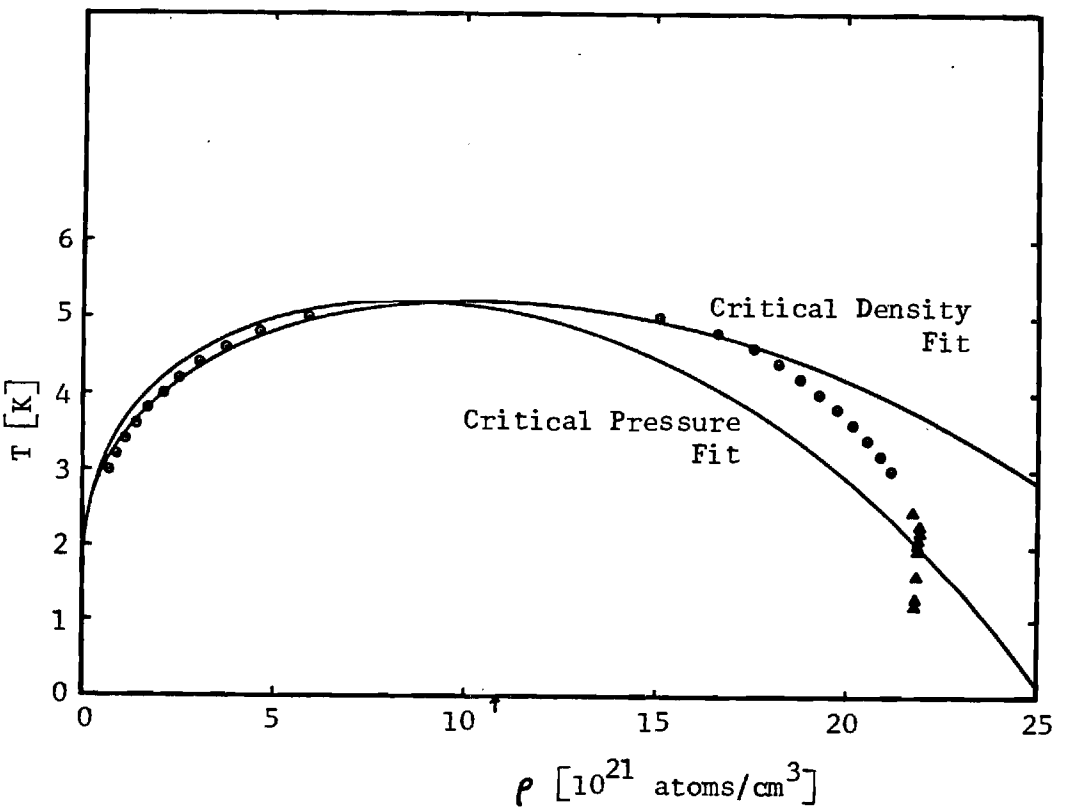

Figure 4. Van Der Waals Coexistence Curves.

The circles are experimental points from (National Bureau of Standards [1962]).

The triangles are experimental points from (Keesom [1942]).

The small arrow on the horizontal axis marks the experimental critical density.

one atom in a cell, or none in it. In the case of helium gas, this means that the cells must be so small that the repulsive forces between helium atoms prevent two from occupying the same cell. On the other hand, the cells cannot be too small: because fractional occupancy is not considered, each cell must be at least large enough to hold an entire helium atom.

The lattice model also makes an assumption about the attractive interactions between the atoms: if two atoms are in adjacent cells, then because of the attractive interaction between them, they share a potential energy of $-u_o$, but if the atoms are not in adjacent cells, there is no interaction between them at all. The lattice model reduces the interactions between the atoms to extremely basic terms.

Taking this model, we shall find the entropy of a non-uniform system, just as we did in the last chapter for the ideal gas. We shall also find an expression for the interaction energy of this non-uniform system. Together these give the lattice gas free energy, just as the entropy of a non-uniform ideal gas gave its free energy.

We start with a definition of the entropy that is equivalent to Equation (7) of the previous chapter, but more convenient here:

$$S = k \ln \Omega \tag{19}$$

where Ω is the number of equally probable states of the system. A state of the system is taken to be a distinguishable arrangement of N indistinguishable particles among the K cells. The number of such arrangements is the number of ways N distinguishable particles can be put into K cells, divided by N factorial.

$$\Omega = \frac{K!}{(K-N)!N!} \tag{20}$$

Of course, all these arrangements are not equally likely: an arrangement in which many atoms have nearest neighbors is energetically preferred and more probable than an arrangement in which few atoms have nearest neighbors. However, in this lattice model, such atom-atom correlations are ignored in what is known as the Bragg-Williams approximation (Bragg and Williams [1934]).

Substituting Equation (20) into Equation (19) and using Stirling's approximation, we find

$$S = - kK \ln\left[\frac{K}{K-N}\right] + kN\ln\left[\frac{K-N}{K}\right] \tag{21}$$

Since $K = V/\tau$ and $N = \rho V$, and we may take the jamming density $\rho^* = 1/\tau$, this may be written as

$$S = k\rho V \ln\left[\left[\frac{\rho^* - \rho}{\rho}\right] - \frac{\rho^*}{\rho} \ln\left[\frac{\rho^* - \rho}{\rho^*}\right]\right] \tag{22}$$

for the uniform lattice gas.

If the lattice gas is not uniform we generalize Equation (22) by writing

$$S = k\int d^3r \left[\rho(r) \ln\left[\frac{\rho^* - \rho(r)}{\rho(r)}\right] - \rho^* \ln\left[\frac{\rho^* - \rho(r)}{\rho^*}\right]\right] \tag{23}$$

If we subtract Equation (22) from Equation (23) we obtain the change in the entropy cuased by the departure of the density from a uniform

value: in other words, we find what we have previously called ΔS. It may be written in the form

$$\Delta S = - k\int d^3r \left[\rho(r)\ \ell n \left[\frac{\rho(r)}{\rho}\right] + (\rho^*-\rho)\ \ell n \left[\frac{\rho^*-\rho(r)}{\rho^*-\rho}\right]\right] \qquad (24)$$

Notice the symmetry of this equation under the transformations $\rho(r) \to \rho^* - \rho(r)$ and $\rho \to \rho^* - \rho$; this reflects the equivalence, in the lattice model, of placing N particles in K cells and placing K - N vacancies in K cells. Later we shall see this equivalence in a coexistence curve that is perfectly symmetric about the critical point.

The interaction energy is also easy to find. This energy is just the number of nearest-neighbor pairs multiplied by $-u_o$. Consider any one of the N atoms of the gas. Surrounding it are γ nearest neighbor sites. The probability that one of these sites is occupied is just N/K, since short range order is ignored. Thus the probable number of nearest neighbors for our atom is just $\gamma N/K$, and since there are N atoms just like the one at which we have been looking, the total number of nearest-neighbor pairs is just $\gamma N^2/2K$, where the factor of one-half corrects for double counting. The interaction energy, U, of the gas is then $-\gamma u_o N^2/2K$, or since $N = \rho V$ and $K = \rho^* V$

$$U = - \frac{1}{2} V\gamma u_o \rho^2/\rho^* \qquad (25)$$

If the density of the helium is not uniform, we write instead

$$U = -\frac{1}{2}\frac{\gamma u_o}{\rho^*}\int d^3r\ \rho^2(r) \tag{26}$$

If we subtract Equation (25) from Equation (26), we obtain the change in interaction energy arising from the non-uniformity of the gas,

$$U = -\frac{1}{2}\frac{\gamma u_o}{\rho^*}\int d^3r\ [\rho^2(r) - \rho^2] \tag{27}$$

Equations (24) and (25) give the free energy change of the gas, $\Delta F = \Delta U - T\Delta S$:

$$\Delta F = kT\int d^3r \left[\rho(r)\ \ell n\ \frac{\rho(r)}{\rho} + (\rho^* - \rho(r))\ \ell n \left(\frac{\rho^* - \rho(r)}{\rho^* - \rho}\right)\right.$$

$$\left. - \frac{1}{2}\frac{\gamma u_o}{\rho^*}\int d^3r\ [\rho^2(r) - \rho^2]\right. \tag{28}$$

Before finding the connections between the parameters of this model and the critical data, as we did for the Van der Waals equation, let us find the equation of state corresponding to this lattice gas free energy. For a uniform system, Equations (22) and (23) give us

$$F = -kT\ \rho V\left[\ell n\left(\frac{\rho^* - \rho}{\rho}\right) - \frac{\rho^*}{\rho}\ \ell n\left(\frac{\rho^* - \rho}{\rho}\right)\right] - \frac{1}{2}V\ \gamma u_o \rho^2/\rho^* \tag{29}$$

and using $P = -\partial F/\partial V$ we find

$$\left(P + \frac{1}{2}\gamma u_o \rho^2/\rho^*\right) \frac{1}{\rho^* \ell n \left(\frac{\rho^*}{\rho^* - \rho}\right)} = kT \qquad (30)$$

Now if we assume that the density, ρ, is small compared to ρ^*, we may expand the logarithm. Doing this and letting the specific volume $v = 1/\rho$, we find for very low densities that

$$\left(P + \frac{\gamma u_o/2\rho^*}{v^2}\right)\left(v - \frac{1}{2\rho^*}\right) = kT \qquad (31)$$

This equation has precisely the form of Van der Waals' equation, with a replaced by $\gamma u_o/2\rho^*$ and with b replaced by $1/2\rho^*$. The lattice gas reduces to a Van der Waals gas for low densities.

Of course, when treating the Van der Waals equation, we had defined a jamming density $\rho^* = 1/b$, so for low densities the Van der Waals jamming density appears to be twice the lattice gas jamming density. We will not see this ratio elsewhere: when the lattice gas is fit to critical temperature and pressure, we shall find the lattice gas jamming density to be 65 percent, not 50 percent, of the corresponding Van der Waals value, and when we fit the lattice gas to critical temperature and density, we shall find that the jamming density we must use is 67 percent of the corresponding Van der Waals value. In general, requiring the lattice gas and the Van der Waals gas to agree under different conditions requires different relationships between their jamming densities.

Now we will find the connections between the lattice gas parameters and the critical data. Again dividing the total volume V into two subvolumes, V_1 where the density is ρ_1, and V_2 where the density is ρ_2, so that $V_1 << V_2$, and introducing the variables y_1 and y^* just as we did before, we find that the expression for the free energy change becomes

$$\Delta F = kTV_1\rho\left[y_1 \ln y_1 + (y^*-y_1)\ln\left(\frac{y^*-y_1}{y^*-1}\right)\right]$$

$$- V_1 \frac{\gamma\rho u_o}{2y^*}(y_1-1)^2 \qquad (32)$$

With the requirement, $\partial(\Delta F)/\partial V_1 = 0$, Equation (32) yields

$$kT\left[y_1 \ln y_1 + (y^*-y_1)\ln\left(\frac{y^*-y_1}{y^*-1}\right)\right] - \frac{\gamma\rho u_o}{2y^*}(y_1-1)^2 = 0 \qquad (33)$$

and with the requirement, $\partial(\Delta F)/\partial y_1 = 0$, it gives

$$\frac{\gamma u_o(y_1-1)}{y^* kT} = \ln\left[\frac{y_1(y^*-1)}{y^*-y_1}\right] \qquad (34)$$

Again, we let y_1 be close to one and substitute $y_1 = 1 + \Delta y$ into Equation (34). We obtain

$$\frac{\gamma u_o}{y^* kT}\Delta y = \Delta y \frac{y^*}{y^*-1} \qquad (35)$$

so

$$T = \frac{\gamma u_o}{\rho^{*2}} \rho^2 \left(\frac{\rho^*}{\rho} - K \right) \tag{36}$$

And since at the critical point $\partial T/\partial \rho = 0$, we have

$$\rho^* - 2\rho_c = 0 \tag{37}$$

so that the critical density and the jamming density must be related by

$$\rho_c = \rho^*/2 \tag{38}$$

Substituting Equation (38) back into Equation (36) gives

$$T_c = \gamma u_o/4k \tag{39}$$

If we wish to fit the lattice gas parameters to the critical density and temperature, Equations (38) and (39) give

$$\rho^* = 2\rho_c \tag{40}$$

and

$$\gamma u_o = 4kT_c \tag{41}$$

If we wish to fit the parameters to the critical pressure and temperature, Equations (31) and (39) give

$$\rho^* = \frac{2P_c/kT_c}{2\ell n(2) - 1} \tag{42}$$

and

$$\gamma u_o = 4kT_c \tag{43}$$

If we wish, we may use Equation (33) and (34) to find the coexistence curve for the lattice gas by treating these equations just as we did Equations (7) and (8) for the Van der Waals gas. That is we may eliminate the temperature between Equations (33) and (34), and solve the resulting equation for y given y^*, and then use this value of y_1 in either Equation (33) or (34) to determine the corresponding temperature. However, for the lattice gas, this solution is easy to find. Because of the invariance of the lattice gas free energy under the transformations $\rho \to \rho^* - \rho$, $\rho(r) \to \rho^* - \rho(r)$, if ρ_1 is a solution to the minimization problem, then so is $\rho_2 = \rho^* - \rho_1$. Since $y_1 = \rho_1/\rho = 1$ is always a solution to the equation we must solve for y, this means that $y_1 = y^* - 1$ is also a solution. Using this expression for y_1 in Equation (34) gives the equation

$$T = \frac{2T_c(1 - 2\rho/\rho^*)}{\ell n\left(\frac{\rho^*}{\rho} - 1\right)} \tag{44}$$

so that, given the jamming density, ρ^*, the temperature at which ρ can be the density of one of two coexisting phases can be simply calculated. The results for both the fit to critical density and

temperature and the fit to critical pressure and temperature are shown in Figure 5.

Comparison of Figure 5 and Figure 4 shows that the lattice gas, fit to critical pressure, is perhaps the worst of all quantitatively, although it has better qualitative behavior than the Van der Waals curves. The lattice gas, fit to critical density is quite good, although the jamming density for it seems to be somewhat too low. If we want this lattice gas curve to correspond more closely to the high density side of the experimental coexistence curve, we shall need to increase to jamming density somewhat. For positron self-trapping in helium, we shall obtain a good fit using $\rho^* = 23 \times 10^{21}$ atoms/cm^3. Nonetheless, we shall use the critical density fit throughout the rest of this thesis, except when making a final comparison with experiment, or a prediction on the outcome of an experiment, when we shall use $\rho^* = 23 \times 10^{21}$ atoms/cm^3.

For future reference, let us write down the lattice gas free energy, with γu_0 replaced by $4kT_c$:

$$\Delta F = kT \int d^3r \left[\rho(r) \ln \frac{\rho(r)}{\rho} + (\rho^* - \rho(r)) \ln \frac{\rho^* - \rho(r)}{\rho^* - \rho} \right]$$

$$- 2 \frac{kT_c}{\rho^*} \int d^3r [\rho^2(r) - \rho^2] \qquad (45)$$

or, adapting this equation to the bubble model,

$$\Delta F = kTv_0\rho \left[y \ln y + (y^* - y) \ln \left(\frac{y^* - y}{y^* - 1} \right) \right] - \frac{2v_0 kT_c}{y^*} (y-1)^2 \qquad (46)$$

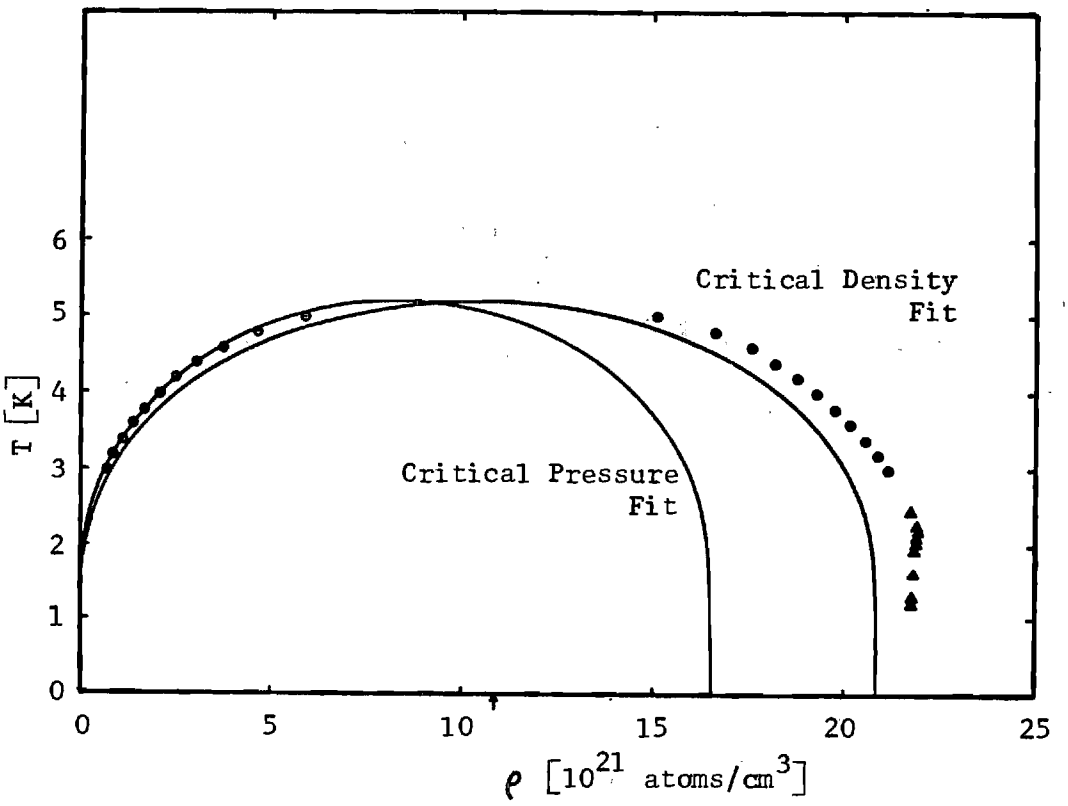

Figure 5. Lattice Gas Coexistence Curves.

The circles are experimental points from (National Bureau of Standards [1962]).

The trianges are experimental points from (Keesom [1942]).

The small arrow on the horizontal axis marks the experimental critical density.

where $y = \rho_i/\rho$, and ρ_i is the density inside the well, where $y^* = \rho^*/\rho$, and where v_o is the volume of the well, presumed to be small compared to V. Equation (46) should be compared with Equation (32). Equations (45) and (46) are the expressions for the free energy of the helium that we shall use with our variational model. The choice of the lattice gas model over the Van der Waals model is well justified by the coexistence curves, and will be justified by hindsight when we apply both models to positron self-trapping in helium. Now we must turn to the question of the surface energy of the bubble, and decide how we shall treat it.

The Surface Energy

The surface energy may be defined as the free energy of the surface per unit volume, and has an internal energy part and an entropy part. The internal energy part arises from the attractive interactions between the atoms of the system. Consider, for example, a liquid in equilibrium with a vapor above it. The atoms at the surface of the liquid do not have as many nearest neighbors as their counterparts in the bulk of the liquid, so that their energy is lowered less by the attractive forces between the atoms. Therefore, if one uses a bulk free energy for the surface layer as well as for the bulk of the liquid, one underestimates the energy of the system. The internal energy of the surface is the energy that must be added to the bulk free energy to correct for this. This energy is virtually independent of the temperature; the temperature dependence of the surface energy resides in its entropy part.

We shall calculate the surface energy of a system using linear response theory; the other workers with whose work we are acquainted use an equivalent quantum mechanical perturbation calculation (Hohenberg and Kohn [1964], Ebner and Saam [1975]). The central physical assumption in both methods is that the system's response to a perturbation is proportional to the strength of the perturbation. This is an assumption which can well be questioned for a theory which will be applied to the electron bubble or the positron droplet. For a self-trapped state, the density can deviate greatly from its average value and it is easy to imagine that for such large amplitude responses, a linear theory may be inadequate. We shall use the linear response theory anyway, because it is much easier to apply than a non-linear theory, because we have not worked out the non-linear theory to the extent that it can be applied to the problems of interest, and because, by hindsight, it will turn out to work quite well, so that the objections to it may not be too strongly grounded.

In Appendix A, we show using linear response theory that the free energy of a non-uniform system is

$$F = F_o + \frac{1}{2}\int d^3r \int d^3r' \left(\int \frac{d^3q}{(2\pi)^3} \frac{e^{-iq\cdot(r'-r)}}{\chi_q} \right) \Delta\rho(r)\Delta\rho(r') \quad (47)$$

where F_o is the free energy of the uniform system and where $\Delta\rho(r) = \Delta\rho(r) - \rho$. Here χ_q is the linear response function for the helium gas.

This equation must be approximated before we can usefully apply it. We shall use a density gradient expansion of $\Delta\rho(r')$ about the point r to help to rewrite Equation (47). This procedure is questionable, just as the use of linear response theory is. The gradient expansion requires the density $\rho(r)$ to be slowly varying compared to the interatomic spacing. We shall use this expansion anyway, for reasons similar to those we put forward for the use of a linear theory: it is easier to use than a higher order theory and, after the fact, we shall see that it seems to work well. In Appendix B, we carry out the expansion and find for the change in the free energy owing to the departure of the density from a uniform value

$$\Delta F = \int d^3r\, \Delta f(\rho(r)) + \frac{1}{2}\int d^3r\ \ \hat{g}|\nabla\rho\ (r\ |^2 \qquad (48)$$

where $\Delta f(\rho(r))$ is the local density of the free energy change (Equation (28) gives this quantity for the lattice gas) and where $\hat{g}$ is the q^2-coefficient of a small-q expansion of χ_q^{-1}. To approximate $\hat{g}$ we perform a high-temperature expansion (to be subsequently justified) of an equation relating χ_q to the generalized pair correlation function of Van Hove [1954] and use well-known sum rules to evaluate the resulting expression. This calculation is also carried out in Appendix B. The result is

$$\hat{g} = \frac{1}{6\rho kT}\left[\frac{\partial p}{\partial \rho}\right]^2_{V,T}\left[\rho\int d^3r r^2(g(r)-1) + 3\,\frac{h^2}{2M_{He}kT}\right] \qquad (49)$$

Here P is the local pressure of the gas, M_{He} is the mass of a helium atom, and g(r) is the ordinary pair correlation function. Equations (48) and (49) are those employed by Stott [1977][1] to treat the problem of positron self-trapping in helium. Of course, before Equation (49) can be put to use, the integral appearing in it must be evaluated in some way. Following Stott [1977], we estimate the value of this integral by using the low-density expression for g(r),

$$g(r) = e^{-\phi(r)/kT} \tag{50}$$

where $\phi(r)$ is the interaction between helium atoms, here taken to be represented with sufficient accuracy by a Lennard-Jones 6-12 potential,

$$\phi(r) = \frac{a}{r^{12}} - \frac{b}{r^6} \tag{51}$$

where (deBoer and Michels [1939])

$$a = 4.47 \times 10^{-10} \text{ erg-A}^{12} \qquad b = 1.59 \times 10^{-12} \text{ erg-A}^6 \tag{52}$$

Stott [1977] has performed several explicit Percus-Yevick calculations (Percus and Yevick [1958]) for temperatures above the critical point at densities of interest and found that the integral in question is insensitive to this low-density approximation. We have evaluated this integral using Equation (50) with the Lennard-Jones interaction of

[1] Actually, in (Stott [1977]), the term correspond to the last term in Equation (49) lacks the overall factor of three we have. We attribute this to a typographical error.

Equations (51) and (52) and found through curve fitting that it may be adequately approximated for 15 K < T < 120 K (suitable for the electron problem) by

$$\int d^3r r^2(g(r) - 1) = \frac{9.2462 \times 10^4 \text{Å}^5}{(T/^oK)^{1.226}} \tag{53}$$

and for 5 K < T < 15 K (suitable for the positron problem) by

$$\int d^3r r^2(g(r) - 1) = \frac{1.094 \times 10^5 \text{Å}^5}{(T/^oK)^{4/3}} \tag{54}$$

so that Equation (49) may be written

$$\hat{g} = \frac{1}{6kT} \left(\frac{\partial P}{\partial \rho}\right)^2_{V,T} H(T) \tag{55}$$

where

$$H(T) = \frac{9.2462 \times 10^4 \text{°Å}^5}{(T/°K)^{1.226}} + \frac{1.81801 \times 10^{25} \text{°Å}^5}{(\rho/cm^{-3})(T/°K)} \tag{56}$$

for the electron problem, and where

$$H(T) = \frac{1.094 \times 10^5 \text{°Å}^5}{(T/°K)^{4/3}} + \frac{1.81801 \times 10^{25} \text{°Å}^5}{(\rho/cm^{-3})(T/°K)} \tag{57}$$

for the positron problem. Here P is the local pressure at r. The ρ

in the last term of Equations (56) or (57) should properly be $\rho(r)$, but this mistake introduces only a small error in $\hat{g}$. The second term of Equations (56) or (57), which is a quantum correction term for the helium, turns out, for the densities and temperatures of interest, to be about 20 percent of the other term at the worst; more usually the quantum correction term is much smaller still. The larger term comes from the first order of the high temperature expansion performed in Appendix B, while the smaller term comes from the next higher order; we may hope that the third order term is proportionately smaller as well. If it is, the neglect of such higher order terms will introduce an error of around five percent or less at the temperatures at which we shall confidently apply our equations ($T > 5$ K).

As an exercise, we have applied Equations (48), (55) and (57) to a system consisting of two phases of helium separated by a free plane surface. The density is assumed to be constant throughout the bulk of both phases and to have a constant gradient in the interface between these phases, that is the density gradient is zero everywhere except in the interface, where it has a uniform value. This model should overestimate the surface energy, since it overestimates the density gradient at both the low-density and the high-density ends of the interface. We characterized the helium with the lattice gas model fit to the critical density.

We called the cross-sectional area of the system A, the depth of the vapor phase X_1 (so that its volume is AX_1) the depth of the liquid phase X_2 and the thickness of the interface δ. Making the

physically non-restrictive assumption that $\delta << X_1 << X_2$, which should be compared to the similar assumption preceding Equation (3) of this chapter, and minimizing the free energy with respect to variations in the densities, we found that the conditions for equilibrium on these densities are unaffected by the presence of the surface energy term, at least if the volume of the surface region is very small compared to the volumes of both phases. Thus choosing a temperature of 4.6 K, we read off of Figure 5 the values of the two densities that can coexist at that temperature for the lattice gas fit to critical density: $\rho_1 = 4.5 \times 10^{21}$ atoms/cm^3 and $\rho_2 = 16.35 \times 10^{21}$ atoms/cm^3. Minimizing the free energy with respect to variations in δ then gave δ to be 13.36 A, a reasonable number.[1] Reinserting this value for δ into the surface energy term then gave a surface energy proportional to A, the area of the surface. The proportionality constant is just the surface tension σ: we found $\sigma = 0.216$ dynes/cm. As expected, this value is indeed too high, compared with the experimental result (Allen and Misener [1938]) of .07 dynes/cm. Part of the fault is that the lattice gas generally overestimates $\partial P/\partial \rho$. For other jamming densities in the lattice gas, it can be shown to a good approximation $\sigma \propto \rho^{*3/2}$. For the fit to critical pressure, this corresponds to $\sigma = .15$ dynes/cm.

Equations (48) and (49) are useable expressions for incorporating surface effects into a self-trapping problem, as Stott [1977] proved by example. They do not, however, from the most useful expressions

---

[1] It may be compared with the results of Padmore and Cole [1974] for He^4 at T = 0 K: the "width" of their smooth density profile is about eight or nine Angstroms.

for the problems we want to study. We may combine Equations (48) and (55) to write

$$\Delta F = \int d^3r\, \Delta f(\rho(r)) + \frac{H(T)}{12kT} \int d^3r |\nabla P|^2 \tag{58}$$

and find a useful form for ∇P by using a force-balance relation involving it. We shall first obtain this force-balance relation incorrectly, and later see what corrections to it we must make.

Consider a thin spherical shell of helium atoms near the electron (or positron). This shell is in equilibrium with all the forces acting on it, so those forces must cancel. The electron repels a single particle in this shell with the force $-g\nabla\, \chi^2(r)$, so the force per unit volume acting on the shell is

$$F_{el} = -g\rho(r)\nabla\chi^2(r) \tag{59}$$

Opposing this force is the pressure gradient in the helium, which is the negative of the force per unit volume acting on the element on account of the changing density around it. Since the total force on this element must be zero, we write

$$\nabla P = -g\rho(r)\nabla\chi^2(r) \tag{60}$$

which is the equation we will use for ∇P in Equation (58).

The error in this argument is the neglect of surface forces, which also act on the element. We shall return to the role and size of the surface forces later, when we perform a correct calculation of the force-balance relation. In general, we shall find that the neglect of these forces in the force-balance equation does not constitute a significant error for the densities and temperatures in which we are

interested.

In practice we shall use Equation (60) with the right hand side evaluated using the square well density profile and overlapping wave function of our variational model. For the electron in helium, this will underestimate the surface energy, since in Equation (60) it causes the density to be too low in a region where $\nabla\chi^2$ is high, but causes the density to be too low in a region where the contribution to Equation (58) turns out to be small in any case. Similarly, the square-well functions will cause the surface energy to be overestimated for the positron in helium. In Appendix C, we approximately evaluate the integral of Equation (58) using these functions and find there that

$$\Delta F_{surf} = 4.0682 \times 10^{14} \frac{H(T)}{(T/^\circ K)} g^2 \frac{i^2}{R_o^5} \qquad (61)$$

Note that the surface tension in this expression (it is the surface energy term divided by $4\pi R_o^2$) goes like $1/R_o^7$,[1] and is thus not independent of R_o but depends strongly on it.

For the variational model, the first term of Equation (58) is just Equation (46), which, if written in terms of the variables s and y of the previous chapter, is

$$\rho g G s^3 \left(T \left[y \ln y + (y^*-y) \ln \left[\frac{y^*-y}{y^*-1} \right] \right] - \frac{2T_c(y-1)^2}{y^*} \right) \qquad (62)$$

[1] This dependence is actually only superficial: it would be strictly true if y were fixed. Since y and R_o are coupled through the minimization of F, the true dependence of F_{surf} on R_o is obscured.

where $G = 4\pi^4 kh^3/(3(2m\rho)^{3/2}g^{5/2})$ as it did in Chapter II. The electron kinetic energy and potential energy are the same as they were in the variational treatment of the last chapter

$$\frac{E}{\rho g} = \frac{z}{\pi s}^2 \pm y \tag{63}$$

where the upper sign is for the electron and the lower sign is for the positron, which attracts helium atoms. Combining Equations (61), (62), and (63) we may write the total free energy change for the variational model.

$$\frac{\Delta F}{\rho g} = \frac{z}{\pi s}^2 \pm y + Gs^3 \left(T \left[y \ell n y + (y^*-y) \ell n \left(\frac{y^*-y}{y^*-1} \right) \right] - \frac{2T_c(y-1)^2}{y^*} \right)$$

$$+ \tilde{H}(T)(\rho g)^{7/2} y^2/s^5 \tag{64}$$

where

$$\tilde{H}(T) = \frac{1.335 \times 10^{-53}}{(T/°K)^{2.226}} + \frac{2.625 \times 10^{-33}}{(\rho/cm^{-3})(T/°K)^2} \tag{65}$$

for the electron problem, and where

$$\tilde{H}(T) = \frac{1.580 \times 10^{-53}}{(T/°K)^{7/3}} + \frac{2.625 \times 10^{-33}}{(\rho\ cm^{-3})(T/°K)^2} \tag{66}$$

for the positron problem.

Equation (64) is still a complex function of s and y, on both

of which z implicitly depends. The problem of finding its minimum at any density and temperature is just the problem of finding the minimum of a (complicated) real function of two real variables. This calculation is, however, considerably simpler than the one of Manninen and Hautojärvi [1978] who, for every density and temperature of interest, interatively solve two coupled non-linear differential equations (and this for the self-trapping problem with surface energy omitted). Our calculation is also much simpler than Stott's [1977] who must solve, for each density and temperature, two non-linear coupled equations with numerous values of the variational parameter in his wave function and then find the value of this paramter which minimizes the energy of his system.

Now let us return to the question of the force-balance equation, and derive a correct version of it which includes the contribution of surface forces. First we write down the free energy change for the combined system of electron (or positron) and helium, not Equation (64) but the more general form

$$\Delta F = \frac{\hbar^2}{2m}\int d^3r\ |\nabla\chi|^2 + g\int d^3r\ \chi^2(r)\rho(r) + \int d^3r\ \Delta f(\rho(r)) + \frac{H(T)}{12kT}\int d^3r\ \left[\frac{\partial P}{\partial \rho}\right]^2_{V,T} |\nabla\rho|^2 \qquad (67)$$

Now we perform the variation of this ΔF with respect to $\rho(r)$, subject to the constraint $\int d^3r\ \rho(r) = N$. We obtain

$$g_\chi^2(r) + \frac{\partial \Delta f(\rho(r))}{\partial(\rho(r))} - \frac{H(T)}{12kT}\left[|\nabla\rho|^2 \frac{\partial}{\partial\rho}\left(\frac{\partial P}{\partial\rho}\right)^2_{V,T} + 2\left(\frac{\partial P}{\partial\rho}\right)^2_{V,T} \nabla^2\rho\right] + \lambda = 0 \quad (68)$$

where λ is an undetermined Lagrange multiplier whose value need not concern us here. Thus if one more particle is added to the volume element at the point r, the first term in Equation (68) is the corresponding change in the free energy due to the presence of the electron, the second term is the change due to the increased bulk free energy of the gas in the element $\partial(\Delta f(\rho(r))/\partial\rho(r)$ is the chemical potential at r), and the last term is the change in the surface energy. Since $\Delta f(\rho(r))/\rho(r)$ is the free energy change per particle in the element, we have

$$\frac{\partial}{\partial\rho}\left(\rho \frac{f(\rho)}{\rho}\right) = \frac{f(\rho)}{\rho} + \frac{P}{\rho} \quad (69)$$

where P is the local pressure in the element. If we take the gradient of Equation (68) then we shall find an expression for ∇P, but since Equation (68) is zero everywhere, its gradient must vanish. Taking the gradient of Equation (68) and using Equation (69) gives

$$\nabla P = -\rho g\, \nabla\chi^2(r) + \frac{H(T)\rho}{12kT} \nabla\left[|\nabla\rho|^2 \frac{\partial}{\partial P}\left(\frac{\partial P}{\partial\rho}\right)^2_{V,T} + 2\left(\frac{\partial P}{\partial\rho}\right)^2_{V,T} \nabla^2\rho\right] \quad (70)$$

where $\nabla(\partial P/\partial\rho) = \nabla\rho\ \partial(\partial P/\partial\rho)/\partial\rho$ can be used to help in this expression's evaluation.

If no electron or positron is present, then for a surface whose

thickness is small compared with the radius, R, of the bubble it encloses, there is a simple formula relating the pressure difference across the surface, ΔP, and the surface tension σ, namely

$$\Delta P = 2\sigma/R \tag{71}$$

No such simple relation is available within the surface: the simplicity of Equation (71) is a global property of the surface and not a local, microscopic one. Equation (70) contains this simplicity in the absence of the electron of positron only when integrated over the surface. If we take the surface term from Equation (67)

$$\Delta F_{surf} = \frac{H(T)}{12kT} \int d^3r \left(\frac{\partial P}{\partial \rho}\right)^2_{V,T} |\nabla \rho|^2 \tag{72}$$

and integrate it over all space for such a bubble as described in the previous paragraph, the result may be written

$$\Delta F_{surf} = 4\pi R^2 \frac{H(T)}{12kT} \int dr \left(\frac{\partial P}{\partial \rho}\right)^2_{V,T} |\nabla \rho|^2 \tag{73}$$

since the integrand only contributes over a small range of the radius. Defining the surface tension, σ, of the surface to be the surface energy divided by the surface area, we find

$$\sigma = \frac{H(T)}{12kT} \int dr \left(\frac{\partial P}{\partial \rho}\right)^2_{V,T} |\nabla \rho|^2 \tag{74}$$

If we now integrate Equation (70) without the wave function term over a volume containing the bubble, we shall obtain, after considerable manipulation and cancellation

$$\Delta P = 2\sigma/R \tag{75}$$

where σ is defined as in Equation (74). This equation is just the same as Equation (71), as it should be. Carrying out this delicate integration and seeing repeated cancellations between components of the integral may be persuasive of the fact that the simple relation between pressure difference and surface tension on a global level does not imply similar simplicity within the surface itself. The interior of a surface is a complex, subtle thing.

Fortunately, the only time we shall have to evaluate the last term of Equation (70) is when we want to check the asusmption that we can neglect it, and not when we are actually finding the density profile itself. After minimizing Equation (64), we shall take the resulting wave function and find the smoothly changing density profile that corresponds to it (we shall see how to do this later). Given this profile we can calculate the values of the terms in Equation (70) at any point around the self-trapped particle and compare the sizes of those terms. If the term we have neglected is generally much smaller than the one we have included, then our method of procedure is justified.

The simplification of neglecting the last term of Equation (70) cannot always be done. In the electron self-trapping problem, for

example, if the temperature is sufficiently low, then almost all of the helium atoms are excluded from the neighborhood of the electron. This situation forces the first term of Equation (70) to be very small, so that the dominate term is the last one.[1] Under these conditions, the electron behaves like a hard sphere immersed in the liquid helium, and the surface tension is found to be just that appropriate to such a hard sphere; in particular, the surface tension is found to be almost independent of the bubble radius (Padmore and Cole [1974]). At the higher temperatures in which we are interested, the density profile is driven by the forces produced by the electron (or positron) and the surface tension varies strongly with the radius, as we have seen (Equation (61)). In the next two chapters we shall see some explicit examples of this phenomenon.

This has been a long chapter, especially with its appendices, but this is unsurprising since a large part of the work for this thesis went into it. The essence of the problem with which we were faced was to find useable, approximate formulas capturing the effects of the helium-helium interactions, but formulas which retained sufficient accuracy to provide reasonable agreement with experimental values for the stable limit lines for electron and positron self-trapping in dense helium gas. Now we are ready to apply the results of this chapter to these self-trapping problems.

---

[1] In this case, of course, it is best not to use the force-balance relation at all.

CHAPTER IV

THE ELECTRON IN HELIUM GAS

Previous attempts to include helium-helium interactions when studying electron self-trapping in a gas have generally stopped at the second-virial coefficient for the gas. This approximation is not unreasonable since at moderately low temperatures and densities the effects of these interactions are small. We shall include helium-helium interactions through a lattice-gas equation of state for helium and find that at high helium densities the departure from the ideal gas result is no longer small, as it is in the second-virial-coefficient approximation. We shall also see what effect surface energy has on the stable limit line in this problem.

First we shall leave out the surface energy and the attractive helium-helium interactions as well. In this way, when we include these interactions we can immediately see their degree of importance for the limit line. We write down for our variational model Equation (64) of the previous chapter, leaving out the surface energy, and the term which arises from attractive helium-helium interactions.

$$\frac{\Delta F}{\rho g} = \left[\frac{z}{\pi s}\right]^2 + y + GTs^3 \left[y \ln y + (y^*-y)\ln\left(\frac{y^*-y}{y^*-1}\right)\right] \qquad (1)$$

This equation may be compared with the corresponding equation for an electron in an ideal gas, Equation (49) of Chapter II. In Equation (1), z is related to y and s as it was in Chapter II,

$$\frac{\sin(z)}{z} = \frac{1}{\pi s\sqrt{1-y}} \tag{2}$$

and G is given by Equation (32) of Chapter II:

$$G = \frac{4\pi^4 kh^3}{3(2m\rho)^{3/2} g^{5/2}} \tag{3}$$

It is convenient to let

$$\sigma(y) = y \ln y + (y^*-y) \ln\left(\frac{y^*-y}{y^*-1}\right) \tag{4}$$

so that Equation (1) becomes

$$\frac{\Delta F}{\rho g} = \left(\frac{z}{\pi s}\right)^2 + y + GTs^3\sigma(y) \tag{5}$$

We want to find the stable limit line for a system described by such a free energy change. We can proceed exactly as we did in Chapter II for the ideal gas case. Once again defining

$$b(z) = \frac{\sin(z)}{z} \tag{6}$$

and remembering that z is implicitly a function of s and y:

$$\frac{\partial z}{\partial s} = -\frac{1}{s}\frac{b(z)}{b'(z)} \qquad \text{and} \qquad \frac{\partial z}{\partial y} = \frac{1}{2(1-y)}\frac{b(z)}{b'(z)} \tag{7}$$

we find that the condition that $\partial(\Delta F/\rho g)/\partial s = 0$ gives

$$- 2z\left(z + \frac{b}{b'}\right)/\pi^2 s^3 + 3\ GTs^2\sigma(y) = 0 \qquad (8)$$

and the condition that $\partial(\Delta F/\rho g)/\partial y = 0$ gives

$$z\ \frac{b^3}{b'} + 1 + GTs^3\sigma'(y) = 0 \qquad (9)$$

where $\sigma'(y)$ is the derivative of $\sigma(y)$ with respect to y. As before, we set the $\Delta F/\rho g$ of Equation (5) equal to one and multiply the resulting equation by $\pi^2 s^2$, yielding

$$z^2 + \pi^2 GTs^5\ \sigma(y) = \pi^2 s^2(1-y) = \frac{1}{b^2(z)} \qquad (10)$$

and rewrite Equation (8) as

$$- 2z\left(z + \frac{b}{b'}\right)/3 + \pi^2 GTs^5\sigma(y) = 0 \qquad (11)$$

Eliminating the common term between these two equations gives

$$- 1 + 5\ \sin^2(z)/3 + 2\ \sin^3(z)/3(z\ \cos\ z - \sin\ z) = 0 \qquad (12)$$

This equation is exactly the same as Equation (57) of Chapter II and has the same solution, z = 2.121558. Dividing the last term of Equation (8) by the last term of Equation (9) gives

$$s^2\sigma(y)/\sigma'(y) = \frac{-2z\left(z + \frac{b}{b'}\right)/3\pi^2}{1 + z\ \frac{b^3}{b'}} \qquad (13)$$

and them eliminating s through Equation (2) and using the known value

of z on the stable limit line gives

$$\frac{\sigma(y)}{\sigma'(y)} = - .40000 \tag{14}$$

or

$$\frac{y \ln y + (y^*-y) \ln \left(\frac{y^*-y}{y^*-1}\right)}{(1-y) \ln \left[y\left(\frac{y^*-1}{y^*-y}\right)\right]} = - .40000 \tag{15}$$

Thus, unlike the situation of Chapter II, where for the ideal gas y is constant everywhere on the stable limit line, here y changes when y^* changes. Thus we must solve Equation (15) for every value of $y^* = \rho^*/\rho$ of interest. This requirement does not mean that we have to solve Equation (15) over again whenever we change the jamming density, ρ^*. For any ρ^* and ρ we calculate y^* and use the solutions of Equation (15) that we have already found.

The roots of Equation (15) are not difficult to obtain numerically unless y is extremely close to zero or one. In the latter case, the logarithms in Equation (15) may be expanded to obtain, in that limit, an equation that is easier to use. In practice, this expansion is unnecessary.

Once the value of y has been found for a given y, we may use Equation (2) and the known value of z to determine s, completing the determination of the extremum state on the stable limit line at the chosen density, ρ. We still do not know the temperature at which this

state occurs. If we solve Equation (9) for T

$$T = - \frac{1 + zb^3/b'}{Gs^3\sigma'(y)} \tag{16}$$

and we use the values of s, y, and z that we have found, we can determine this temperature. If we repeat this process for a number of different values of ρ, we may plot the stable limit line, and we have done so in the dashed curve in Figure 6 for the critical density fit to the lattice gas parameters.[1]

The striking feature of this curve in comparison with the ideal gas curve in the same figure is the difference between them that develops as the helium density becomes very high. With repulsive forces between helium atoms included, it becomes much more difficult to form the self-trapped state when the density of the helium is close to its jamming density. In terms of a mobility experiment, this suggests that, if the density is taken to a high enough value while the temperature is held fixed, the self-trapped state will cease to be energetically favorable, so that the electrons in the gas will return to free particle behavior and will consequently have the higher mobilities expected of free particles. When the density reaches this

[1] We use for g a constant value calculated for an s-wave scattering length of .62 A, corrected for high densities using a Wegner Seitz approximation. In the Wigner-Seitz calculation we somewhat arbitrarily chose to use a "typical" density of 7×10^{21} atoms/cm^3, giving an interaction strength of $g = 7.00 \times 10^{-35}$ erg-cm^3.

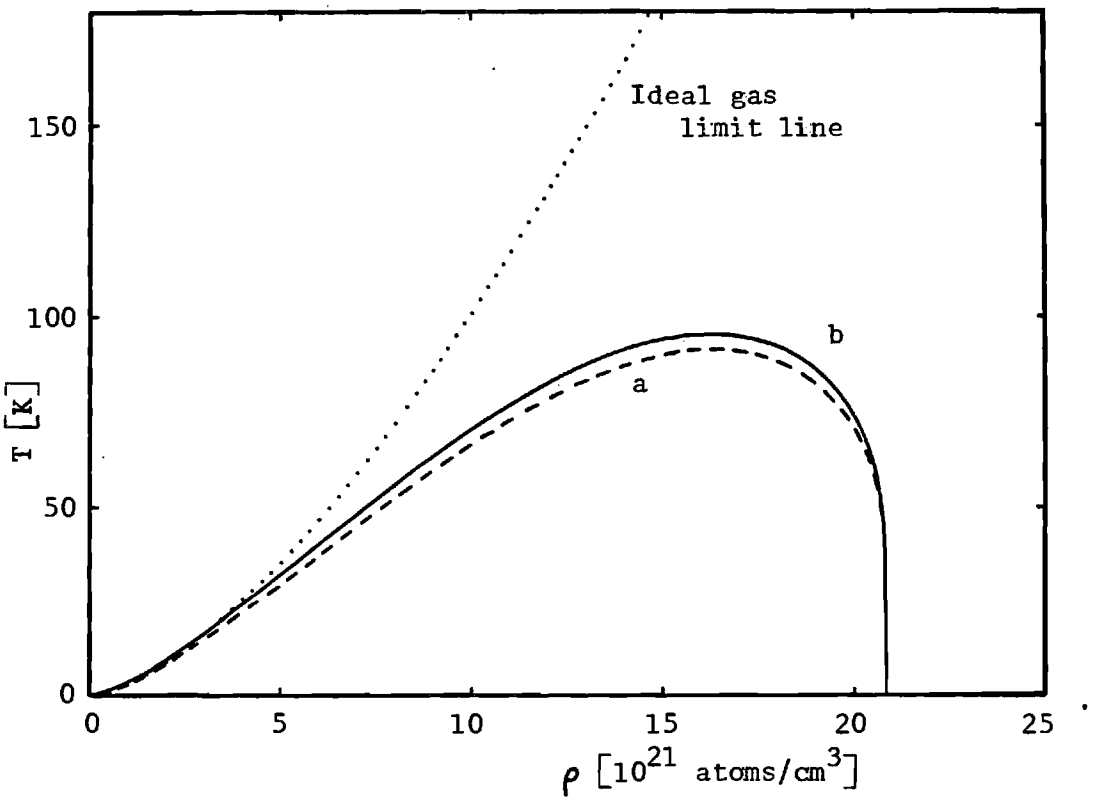

Figure 6. Variational Model Limit Lines for the Electron in Helium without Surface Energy.

Curve a is the limit line which results from neglecting attractive helium-helium interactions.

Curve b is the limit line with these attractive helium-helium interactions included. Further inclusion of the surface energy does not affect this curve, at least to graphical accuracy.

threshold value, the mobility should stop decreasing, if it has not already done so, and begin to increase rapidly toward the free particle value. We call this transition point the second mobility edge. To our knowledge, no one has seen this effect, or for that matter, even looked for it. Later in this chapter, we shall estimate experimental conditions for which this second mobility edge should occur, as well as estimate the change in mobility that can be expected when this jump occurs. First, we shall include the effects of the attractive helium-helium interactions and of the surface energy.

If we include the attractive helium-helium interactions, but still omit the surface energy term, Equation (64) of Chapter III becomes

$$\frac{\Delta F}{\rho g} = \left(\frac{z}{\pi s}\right)^2 + y + Gs^3[T\sigma(y) - u(y)] \tag{17}$$

where we have used the same $\sigma(y)$ defined in Equation (4) and also introduced the notation

$$u(y) = \frac{2T_c}{y^*}(y-1)^2 \tag{18}$$

Now the condition $\partial(\Delta F/\rho g)/\partial s = 0$ gives

$$-2z \quad z + \frac{b}{b'}/\pi^2 s^2 + 3Gs^2[T\sigma(y) - u(y)] = 0 \tag{19}$$

and the condition $\partial(\Delta F/\rho g)/\partial y = 0$ gives

$$z\frac{b^3}{b'} + 1 + Gs^3\,[T\sigma'(y) - u'(y)] = 0 \tag{20}$$

To find the stable limit line, we set the $\Delta F/\rho g$ of Equation (17) equal to one and multiply the resulting equation by $\pi^2 s^2$ to obtain

$$z^2 + \pi^2 Gs^5[T\sigma(y) - u(y)] = \frac{1}{b^2(z)} \tag{21}$$

Equation (19) may be written as

$$-2z\left[z + \frac{b}{b'}\right]/3 + 3\pi^2 Gs^5[T\sigma(y) - u(y)] = 0 \tag{22}$$

and eliminating the common term between Equations (21) and (22) again gives Equation (12) so that we again have $z = 2.121558$. Still proceeding as before, we divide the last term of Equation (19) by that of Equation (20) and eliminate s using Equation (2). This time, however, we write the result as

$$T = \frac{u(y) + \pi^2 h(z) b^2 (1-y) u'(y)}{\sigma(y) + \pi^2 h(z) b^2 (1-y)\sigma'(y)} \tag{23}$$

where

$$h(z) = \frac{2z\left[z + \frac{b}{b'}\right]/3\pi^2}{1 + z\frac{b^3}{b'}} \tag{24}$$

If we explicitly use the expression for u(y) in Equation (18) and the

known value of z, we may write this as

$$T = \frac{.2u(y)}{\sigma(y) + 4(1-y)\sigma'(y)} \tag{25}$$

Thus, given some value of y^* calculated form specified values of ρ and ρ^*, we may calculate the temperature, T, at which $y = \rho_i/\rho$ corresponds to an extremum of the system. Taking this pair of values, y and T, and substituting them into Equation (20) gives a value for G, or from Equation (3) which defines G, a calculated value of ρ, called ρ_{cal}. To find a solution to the minimization problem, we must vary y in Equation (23) until the calculated value of ρ equals the value of ρ originally input to calculate y. In other words, we must find a zero of

$$\rho_{cal}(y) - \rho = 0 \tag{26}$$

Note that although the calculation of the function whose zero we must find has grown more complex, we still have to find only a single zero of a real function of a single variable. This zero can be found numerically without much trouble.[1] Given the value of y and the already known value of z, we may calculate s from Equation (2), and knowing these three variables, as well as T, obtained from Equation (25), we have solved the minimization problem.[2] A graph of the

---

[1] It is useful to evaluate the second derivatives of $\Delta F/\rho g$ at the extremum, to be sure that a minimum has been found.

[2] In Appendix D, a method for the case $\Delta F/\rho g \neq 1$ is given.

resulting stable limit line for the fit to critical density is shown in the solid curve in Figure 6. As the reader can see, the introduction of the attractive helium-helium interactions has had no great impact. This result is not surprising: at the temperatures with this figure is predominately concerned, the repulsive forces between helium atoms are much more important than the attractive forces -- at high temperatures, the relatively weak attractive potential is too small compared to an atom's thermal energy to influence the atom very much.

If the attractive forces are relatively ineffective at the temperatures of interest in the electron problem, then we may expect the surface energy to be relatively unimportant too. In particular, we might expect the result for the limit line we shall obtain on including surface forces to fall between the two stable limit lines that we have calculated so far in this chapter.

With the surface term finally included, Equation (64) of Chapter III may be written

$$\frac{\Delta F}{\rho g} = \left(\frac{z}{\pi s}\right)^2 + y + Gs^3[T\sigma(y) - u(y)] + \tilde{H}(T)(\rho g)^{7/2}\, y^2 s^5 \qquad (27)$$

where $\sigma(y)$ and $u(y)$ are defined as before, and $\tilde{H}(T)$ is given by Equation (65) of Chapter III.

If a method of minimization similar to the ones we have used so far is employed, it results in <u>two</u> equations for which we must find simultaneous zeroes. While such a procedure is numerically feasible,

we have chosen a more direct method.[1] Given ρ, T, and g, we seek the minimum of Equation (27) by search, using a modification of Newton's method for finding the zeroes of a real function of one variable. First, we regard s and y as two cartesian coordinates and make an initial guess as to the values of s and y at the extremum, find z from these values,[2] and calculate the gradient of the $\Delta F/\rho g$ of Equation (27) at that point. The gradient roughly points away from the direction in which the minimum lies, so we shall correct our guess by moving in the direction opposite to the gradient. Taking the second derivatives of $\Delta F/\rho g$, that is, finding $\partial^2(\Delta F/\rho g)/\partial s^2$, $\partial^2(\Delta F/\rho g)/\partial y^2$ and $\partial^2(\Delta F/\rho g)/\partial s \partial y$, we can calculate the rate at which the magnitude of the gradient is changing as we move in the direction opposite the gradient. To be specific, the change per unit "length" in the magnitude of the gradient as we move in this direction is given in matrix notation by

$$|\nabla f|' = \frac{1}{2}\left(\frac{\partial f}{\partial s} \quad \frac{\partial f}{\partial y}\right)\begin{pmatrix} \frac{\partial^2 f}{\partial s^2} & \frac{\partial^2 f}{\partial s \partial y} \\ \frac{\partial^2 f}{\partial s \partial y} & \frac{\partial^2 f}{\partial y^2} \end{pmatrix}\begin{pmatrix} \frac{\partial f}{\partial s} \\ \frac{\partial f}{\partial y} \end{pmatrix}\left[\left(\frac{\partial f}{\partial s}\right)^2 + \left(\frac{\partial f}{\partial y}\right)^2\right]^{-1} \qquad (28)$$

---

[1] For the electron in helium gas, the surface term may be treated successfully with perturbation theory. A suitable perturbation theory is developed in Appendix E.

[2] This requires finding a zero of Equation (2). If either s or y is replaced as an independent variable by z, Equation (2) can be simply solved for the third variable. We have chosen to use s and y as independent variables anyway, because we mentally picture the state of the system in terms of bubble radius and depth.

Now Newton's method for finding the zeroes of a real function of a single variable gives this prescription: to find a new guess, move a distance from the old guess equal to the value of the function at the old guess divided by the slope of the function there. Of course, if the function is a straight line, this method at once yields the correct root. If the function is not linear, Newton's method converges more slowly, and, in fact, may not converge at all. The analogous method we shall use is to move in the direction opposite the gradient of $\partial F/\rho g$ a distance equal to the magnitude of the gradient divided by Equation (26), the rate of change of the magnitude of the gradient. Then, if the gradient is still not satisfactorily small at the new guess, we repeat the process again. Since we have no guarantee that Newton's method converges to a root even for the problem of finding the zero of a function of one variable, we have no such guarantee in our more general problme. In fact, we find that if the average helium density is very high or very low, the initial guess must be made with some care. If the helium density is intermediate in value, however, the method converges over a wide range of initial guesses, and if one works his way out from the intermediate densities to the extreme ones, the difficulty of finding adequate initial guesses in these more sensitive regions is not significant. Of course, this method is geometrically equivalent to finding two simultaneous zeroes to two equations, such as would arise if we tried to proceed as we did in our previous minimizations.

Carrying out this minimization for a given ρ and T (and g), we find the values of s and y and z corresponding to the extremum. We

may then calculate $\Delta F/\rho g$ from Equation (27). If it is less than one, we increase T; if it is greater than one, we decrease T. After the next minimization, we recompute $\Delta F/\rho g$, adjust T again if necessary, and so forth. Ten or twelve minimizations of $\Delta F/\rho g$ are usually adequate to determine T for the given ρ the within graphical accuracy. While the entire procedure could have been programmed onto a computer, leaving us nothing to do but plot points, we found it instructive to do the calculation for each value of ρ separately, making the initial guesses of s and y ourselves and adjusting T ourselves, and watching the way varying the input affected the results. Proceeding in this way, it took between one and one-and-one-half hours to obtain each of the limit lines that we found for the elctron system or the positron system with surface energy. For the electron in helium, the limit line with surface energy obtained in this way was too close to the limit line without surface energy but with attractive forces to plot both in Figure 6. The maximum difference between these two limit lines occurred at about $\rho = 11 \times 10^{21}$ atoms/cm^3 and was about one-half degree Kelvin. Of course, the limit line with surface energy corresponded to a slightly lower temperature for each density than the limit line without surface energy. Owing to the approximate nature of our calculations, there is little reason to distinguish between these two limit lines: when calculating the stable limit line in the electron problem, we may as well stick to the simpler calculation without surface energy. Graphs of R_o and ρ_i for the solutions along the stable limit line both with and without surface energy are shown in Figure 7. The value of R_o

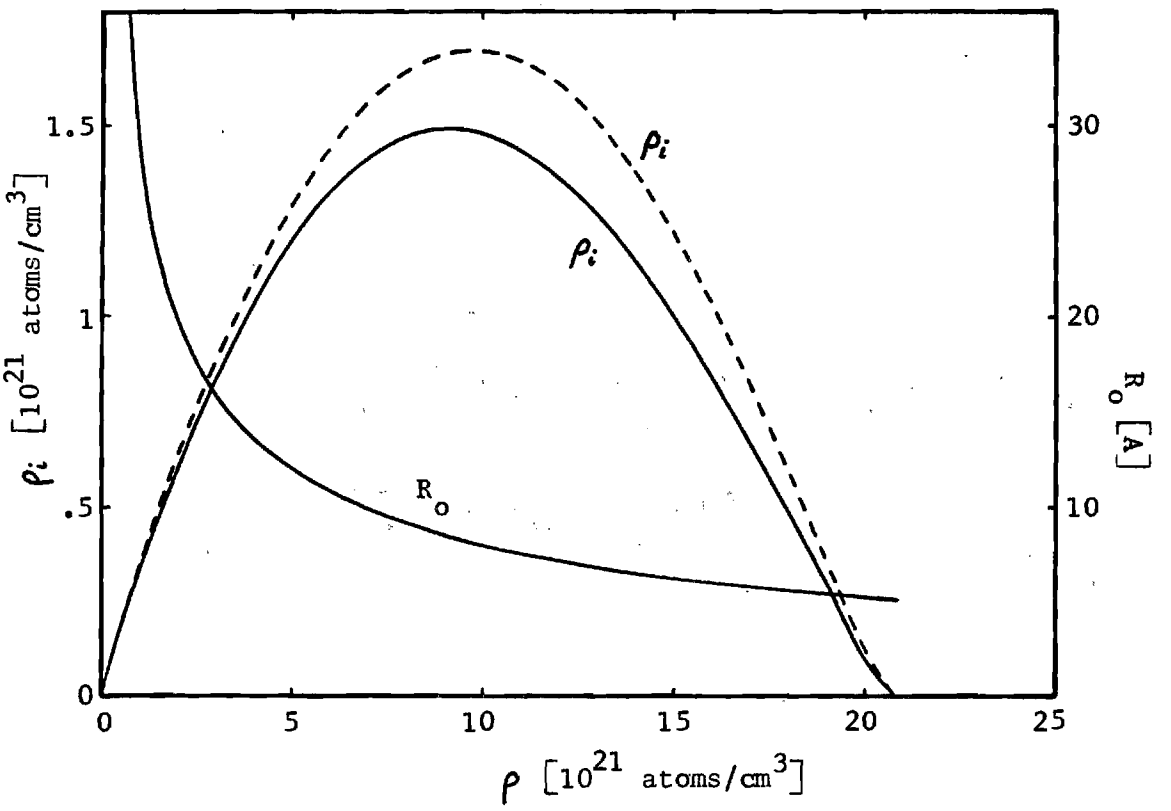

Figure 7. Variational Model Parameters on the Stable Limit Line for the Electron in Helium.

Dashed curves correspond to the limit line with surface energy neglected. Solid curves correspond to the limit line with surface energy included. To graphical accuracy, the two curves for R_o coincide.

with surface energy is actually slightly smaller than without surface energy. Considering the form of the surface term in Equation (27), it is unsurprising that the value of y decreases when the surface term is introduced, but the decrease in R_0 may initially seem strange since the surface term would evidently like R_0 to increase. In fact, the simple interpretation that the surface term of Equation (27) tends to increase R_0 holds unambiguously only if y is held fixed. Actually, y and R_0 are coupled through the minimization problem. We may see that the surface term does tend to increase R_0 by picking an average density, say $\rho = 9 \times 10^{21}$ atoms/cm^3, fixing the value of y at the value it has when surface energy is included (y = .16594 in our example) and minimizing the free energy of the system without surface energy term, with the value of y held fixed. When we do this we find a bubble radius of about 7.0 A, so that the value of 8.53 A found when surface effects are included does represent an increase in the radius at a fixed density.

We have investigated the validity of the approximate force-balance equation that we have used, Equation (60) of Chapter III, by comparing the size of the two terms of the full force-balance relation, Equation (70) of the same chapter:

$$\nabla P = - \rho(r) g \nabla \chi^2(r) + \frac{H(T)\rho(r)}{12kT} \nabla \left[|\nabla \rho|^2 \frac{\partial}{\partial \rho} \left(\frac{\partial P}{\partial \rho} \right)^2_{V,T} + 2 \left(\frac{\partial P}{\partial \rho} \right)^2_{V,T} \nabla^2 \rho \right] \qquad (29)$$

In order to calculate these terms at various points around a self-trapped particle, we need expressions for $\rho(r)$, and its first, second, and third derivatives with respect to r. We shall calculate what these quantities would be if the last term of Equation (29) can be neglected. Using these values, we shall calculate the numerical values of the two terms of Equation (27) and compare their sizes. If the second term is generally less than an order of magnitude less than the first, we shall conclude that the neglect of the second term in the force-balance relation is self-consistent.

Equation (67) of Chapter III can be written

$$\Delta F = \frac{h^2}{2m} \int d^3r |\nabla\chi|^2 + g \int d^3r\, \chi^2(r)\rho(r) + \int d^3r\, \Delta f(\rho(r)$$

$$+ \frac{H(T)}{12kT} \int d^3r\, |\nabla P|^2 \qquad (30)$$

and using the approximate force-balance relation

$$\nabla P = - g\rho(r)\chi^2(r) \qquad (31)$$

we perform the minimization of the free energy of Equation (30, with respect to variations in $\rho(r)$, subject to the constraint $\int d^3r\rho(r) = N$; we obtain

$$g\chi^2(r) + kT\, \ell n \left[\frac{\rho(r)(\rho^* - \rho)}{\rho^* - \rho(r)}\right] - \frac{4kT_c}{\rho^*}\, \rho(r)$$

$$+ \frac{H(T)g^2}{6kT}\, \rho(r)\, \nabla^2\chi(r) + \lambda = 0 \qquad (32)$$

The Lagrange undetermined multiplier can be determined through the requirement that the density far from the electron return to its average value.[1] Equation (32) can then be written in the form

$$\rho(r) = \left[\frac{\rho^* - \rho}{\rho^*} \exp\left\{ -4T_c(\rho(r)-1)/T_\rho^* + \frac{H(T)g^2}{6(kT)^2}\rho(r)\nabla^2\chi(r) + g\,\psi^2(r)/kT \right\} + \frac{\rho}{\rho^*} \right]^{-1} \tag{33}$$

The wave function $\chi(r)$ is explicitly given by

$$\chi(r) = \begin{cases} \dfrac{1}{\alpha R_o^{3/2}} \dfrac{\sin\left(\frac{zr}{R_o}\right)}{\frac{r}{R_o}} & r < R_o \\ \dfrac{\sin z}{\alpha R_o^{3/2}} \exp\left[z \cot z \left(\dfrac{r}{R_o} - 1 \right) \right] \Big/ \left(\dfrac{r}{R_o} \right) & r > R_o \end{cases} \tag{34}$$

where

$$\alpha^2 = \pi(2 - \sin(2z)/z - 2\sin^2 z \tan z/z) \tag{35}$$

where we use the values of R_o and z determined by the minimization procedure with approximate surface term. Thus $\chi(r)$ and all its derivatives can be calculated at any point of interest. Choosing some radius, r, at which we wish to check the force-balance relation,

[1] Determining λ in this way, instead of using the condition $\int d^3r\ \rho(r) = N$, introduces a negligible error in the thermodynamic limit.

we calculate the corresponding value of $\chi(r)$ and place it in Equation (33). Placing the square-well value of the density at r into the right-hand side of Equation (33), we calculate a first iterate for $\rho(r)$. Placing this value into the right-hand side, we calculate the second iterate. We continue the interations until the values of the iterates stops changing appreciably. This iterative procedure converges surprisingly rapidly, and the covergence is almost independent of the initial guess used for $\rho(r)$. Taking the first, second and third derivatives of Equation (33) gives a set of equations each of which can be evaluated once the lower order equations have been. In this way, all the derivatives in Equation (29) can be found at any point, and the two terms of this equation can be compared.

For the electron in helium at points along the stable limit line, we examined the values of these two terms for radii between one Angstrom and two or three times the bubble radius, R_o. We did this for average Helium densities of 4×10^{21} atoms/cm^3, 10×10^{21} atoms/cm^3, 15×10^{21} atoms/cm^3, and 20×10^{21} atoms/cm^3. Only for the density of 20×10^{21} atoms/cm^3 was our criterion for neglecting surface forces in the force balance equation exceeded. There, where the radius of the square well was 5.2 A, the surface tension contribution to the force-balance relation for radii less than 4.5 A was greater that ten percent of the term we have kept; at a radius of 2.5 A the surface term is 26 percent of the term we have kept. Thus in this extremely high region of density, the approximation to the force-balance relation that we have used is questionable. However, we find it hard to believe that an

increases in the gradient of the pressure by 25 percent, or even 500 percent, will modify the limit line of Figure 6 very much for such densities. With the approximate force-balance equation, the change in temperature at this point that occurs when the surface term is first included is eight-thousandths of a degree.

We desired to apply these equations at a point well below the stable limit line, to see the surface tension term of the force-balance relation assume the dominant role, as it is expected to do at very low temperatures. Unfortunately, our method of calculating the minimum of the free energy breaks down at very low temperatures. The essential reason for this breakdown follows. At very low temperatures, the density in the well is very nearly zero. In an attempt to find this small value, the minimization by search may (and usually does) overshoot the true value of the density. If the density in the well is not too small, no harm is done: later iterations will increase the density toward the correct value. If the density is very small, however, the new guess for the density in the well may be negative, a physically preposterous situation and a calculational disaster. If the density in the well is very low, the initial guesses for R_0 and y must be made with extreme care. If such care is taken, our calculational procedure still works, but the difficulties outlined here make it much more difficult to use, and we have not pursued the minimum of the free energy into this difficult region.

At a density of 19×10^{21} atoms/cm^3, for example, our procedure becomes very difficult at temperatures below 20 K, when the density in

the well is about .003 x 10^{21} atoms/cm^3. As the temperature is lowered to this value, the surface-tension contribution to the force-balance equation becomes relatively more and more important until, at 20 K, this contribution is greater at all radii than the term we have kept, although not by as much as an order of magnitude. It is necessary to go to still lower temperatures before the surface tension becomes truly dominant in the electron self-trapping problem. This behavior invites further research.

Finally, let us crudely estimate experimental conditions at which the second mobility edge can occur. Let us refer to the solid curve of Figure 6, and imagine that we are conducting an experiment at a fixed temperature of 85 K. We suppose that when we have increased the density to a value of 19 x 10^{21} atoms/cm^3 at this temperature, the electrons are making the transition to free states, so that the mobility is rising to a free-particle value. Using this temperature and density, an empirical equation of state (National Bureau of Standards [1962]) gives a pressure of 353 atmospheres. At a temperature of 74 K, the stable limit line falls at a density of 20 x 10^{21} atoms/cm^3, which corresponds to a pressure of 331 atmospheres. Whie these pressures are high, they are attainable.

To calculate the mobility jump that occurs at the second mobility edge is more difficult, because no reliable formulas are available for the mobility of the self-trapped state near the limit line. On the free particle side of the limit line, we may estimate the mobility using the kinetic theory formula (Levine and Sanders [1966])

$$\mu = \frac{4}{3} \frac{e}{\rho\sigma(2\pi mkT)^{1/2}} \tag{36}$$

Here μ is the mobility, σ is the total cross section for electrons scattering off of helium (which we correct for high densities using a Wigner-Seitz approximation), m is the electron's mass and e is its charge in esu. At a density of 20×10^{21} atoms/cm^3 and a temperature of 74 K, this gives a free-particle mobility of about 2500 cm/volt-sec. Inside the region where self-trapping dominates, the mobilities observed so far are well less than 10 cm^2/volt-sec. While these numbers should not be taken too seriously in our application, the large difference between them indicates than a mobility increase should occur at very high densities that is large enough to be seen experimentally.

With this conclusion we leave the electron in helium. It is hoped that we have shown that the problem of finding the extremum states is tractable when treated in the simplified way that we have employed. Unfortunately, the problem of electron self-trapping is not a sensitive test of the lattice gas model or of the surface term, largely because of a lack of relevant experimental data. In the next chapter, we shall consider the problem of positron self-trapping, where experimental data are available to enable us to judge the adequacy of our techniques more directly.

CHAPTER V

THE POSITRON IN HELIUM GAS

The differences between electron and positron self-trapping are minor formally but major in physical effect. To adapt any of the equations of the last chapter to the positron problem, we have merely to note that the interaction strength g is negative for the positron-helium interaction, whereas it is positive for the electron-helium interaction. Actually, in our notation, we wish to use g to denote the magnitude of the interaction strength, so this difference amounts to replacing g by -g everywhere it occurs in the equations we have developed for electron self-trapping.

The physical consequences of this replacement are wide-ranging. In particular, in the electron case, when the density outside the bubble is low, the density inside the bubble is low as well, permitting the use of an ideal-gas approximation or a second-virial-coefficient approximation for helium at these low densities. For the positron, where the interaction between the positron and the helium is attractive, there are no self-trapped states for which the density inside the "droplet" around the positron does not contain helium at essentially liquid densities. Thus, in the positron problem, we must characterize the helium much more carefully than in the electron problem: there is no region of densities for which a simple second-virial-coefficient approximation can be adequate for positron

self-trapping in helium. It was in this context that the theory of Chapter III was developed; its application to the electron problem was incidental to our research into the positron problem.

We shall also find that the effects of surface energy, which are almost negligible for electron self-trapping, are quite significant for positron self-trapping. For the high densities surrounding a positron, $(\partial P/\partial \rho)_{V,T}$ is quite large, resulting in a significantly larger surface energy (see Equation (67) of Chapter III) than in the electron problem.

As the reader may have surmised, we intend to use a Fermi pseudopotential for the positron-helium interaction, so a few words are in order about the nature of this interaction. Just like the electron-helium interaction, the positron-helium interaction has two parts: a repulsive core and an attractive tail. The attractive tail has the same physical origin in both cases -- it arises from forces induced by the polarization of helium atoms by a charged particle in their vicinity. There is no notable difference between the attractive polarization tails for the two particles: in particular, both are long-ranged. For the electron, the repulsive core arising from the Fermi exclusion principle dominates the interaction, and we have used this face in partial justification for the use of a Fermi pseudopotential in that problem. The repulsive core for the positron is different. It arises from the Coulomb repulsion felt by the positron when it gets close to an atom's nucleus. Since the positron must penetrate the screening electrons around the nucleus before it can

feel this repulsion, this repulsion has extremely short range and is much weaker than the repulsive core for an electron in helium. In the positron-helium interaction, it is the polarization tail that dominates.

Even though the positron wavelength in the self-trapped state is larger ($\gtrsim$ 20 A) than the corresponding wavelength in the electron problem, replacing an essentially long-range potential by an extremely short-range one, such as a Fermi pseudopotential, seems hard to justify. We are helped somewhat by the weakness of the positron-helium interaction, but basically we simply make the assumption that such a replacement will lead to no serious errors in our approximate calculations, hoping that subsequent comparison with experiment will support, rather than deny, the validity of this assumption.[1]

The principal experimental information about positron self-trapping in helium comes from positron annihilation rate experiments, such as the one described in the Introduction. In Figure 8, annihilation rate is plotted versus average density for two temperatures, 5.7 K and 7.2 K. These curves were obtained by Manninen and Hautojärvi [1978]. The departure of the annihilation rate from the naively expected linearity is striking. By performing many experiments at various temperatures, it is possible, by noting at each temperature the range of densities for which abnormal annihilation rates occur, to map out the region of the (ρ,T)-plane in which

[1] It is worth doing the calculation in this way in any case. Regardless of the outcome, we shall have learned something important about the effects of the range of the positron-helium interaction on the limit line.

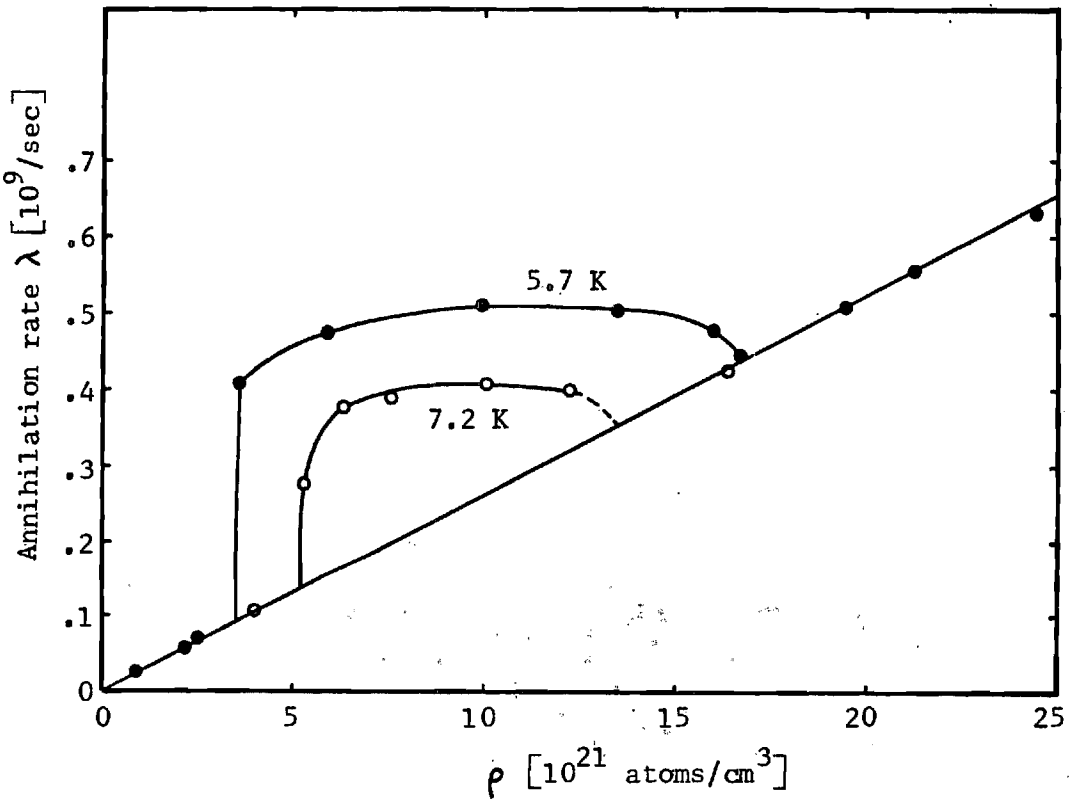

Figure 8. Experimental Positron Annihilation Rates.

These annihilation rates were measured by Manninen and Hautojärvi [1978]. The solid dots are experimental points for T = 5.7 K, while the hollow dots are experimental points for T - 7.2 K. The curves are those provided by the experimenters, and have no theoretical significance.

self-trapped states occur. The perimeter of this region is the stable limit line. The crosses in Figure 9 denote points on this limit line as determined by Manninen and Hautojärvi [1967] from their experiments. One notable feature of these experimental points is that they peak very nearly at the critical density of helium. This suggests that the positron merely acts as a nucleation kernel for the condensation of helium. We shall see that this simple picture is inadequate. The central goal of this chapter is the reproduction of Manninen and Hautojärvi's limit line, using our simple variational model.

Manninen and Hautojärvi [1978] have their own theory of self-trapped positrons. They essentially minimize a functional which is the Gibbs free energy change which occurs when the helium is permitted to depart from a uniform density:[1]

$$\Delta\Omega[\rho(r)] = \frac{h^2}{2m}\int d^3r|\nabla\chi(r))|^2 - g\ \ d^3r\ \chi^2(r)\rho(r) + F[\rho(r)]$$
$$-\mu\int d^3r\rho(r) - (-\rho g + F[\rho] - \mu\int d^3r\rho) \qquad (1)$$

where $F[\rho(r)]$ is the Helmholtz free energy functional for the gas when its density is given by $\rho(r)$ and is taken to be a Van der Waals free energy[2] such as we discussed in Chapter III. In Equation (1),

[1] Here g is given by Equation (4) of Chapter II, where the s-wave scattering length, a, is taken as .27 A, so that $g = 2.07 \times 10^{-35}$ erg-cm^3. We shall also use this value of g, which is not corrected for high densities.

[2] Using the critical pressure, critical temperature fit.

ρ is the density far from the positron and μ is the chemical potential there. This equation may be written

$$\Delta\Omega = \frac{h^2}{2m}\int d^3r|\bar{v}\chi(r)|^2 - g\int d^3r\ \chi^2(r)(\rho(r) - \rho) + F[\rho(r)] - F[\rho] - \mu\int d^3r(\rho(r)-\rho) \tag{2}$$

where

$$F[\rho(r)] - F[\rho] = kT\int d^3r \left\{ \rho(r)\ \ell n\left[\frac{\rho(r)}{\rho}\right] + (r)\ \ell n\left(\frac{1-\rho b}{1-\rho(r)b}\right) - \frac{\rho(r)-\rho}{1-\rho b} - (\rho(r)-\rho)^2\ \frac{a}{kT}\right\} \tag{3}$$

It is worth noting that if Equation (3) is applied to a system with density ρ_1 in subvolume V_1, and ρ_2 in subvolume V_2, it reduces to Equation (6) of Chapter III, where we were discussing the Van der Waals free energy change.[1] The Helmholtz free energy used by Manninen and Hautojärvi is the same as the Van der Waals free energy that we have previously discussed. Minimizing Equation (2) with respect to variations in the wave function, subject to the usual normalization constraint, gives

[1] In obtaining Equation (6) of Chapter III, we assumed that the volume V_1 was much smaller than V_2. The reason why no similar assumption has been made here, has to do with the difference between the canonical ensemble which we use, and the grand canonical ensemble that Manninen and Hautojärvi use. The assumption that they make instead is that it is possible to go far enough away from the positron to find the density unaffected by the positron's existence.

$$-\frac{h^2}{2m}\nabla^2\chi - g\chi^2(r)[\rho(r)-\rho] = E\chi(r) \qquad (4)$$

while minimization of Equation (2), using Equation (3), with respect to $\rho(r)$, subject to the condition that $\rho(r)\to\rho$ as $r\to\infty$, gives

$$-g\chi^2(r) + kT\left\{\ell n\left[\frac{\rho(r)}{\rho}\right] + \ell n\left[\frac{1-\rho b}{1-\rho(r)b}\right] + \frac{1}{1-\rho(r)b} - \frac{1}{1-\rho b}\right\}$$

$$+ 2a(\rho(r)-\rho) = 0 \qquad (5)$$

Manninen and Hautojärvi report that they have self-consistently solved Equations (4) and (5) by a numerical iteration without parameterizing the wave function or the density profile although they give no prescription. It may be noted that Equation (5) can be solved for $\chi^2(r)$, the square root of which can be taken to be $\chi(r)$, since the ground-state wave function can be expected to be of uniform sign. This expression for $\chi(r)$ can then be substituted into Equation (4), resulting in a differential equation for $\rho(r)$ of rather formidable complexity. In principle, one may solve this differential equation by numerical integration, as we have solved a non-linear Schrödinger equation (Moore, Cleveland, and Gersch [1978]). This, however, is presumably not the method chosen by Manninen and Hautojärvi, if one may judge by their choice of words.

The results which these researchers obtain for the stable limit line are shown as the solid curve in Figure 9.[1] As Manninen and Hautojärvi [1978] themselves note, the value they obtain for the maximum temperature at which self-trapped states occur is quite close to the

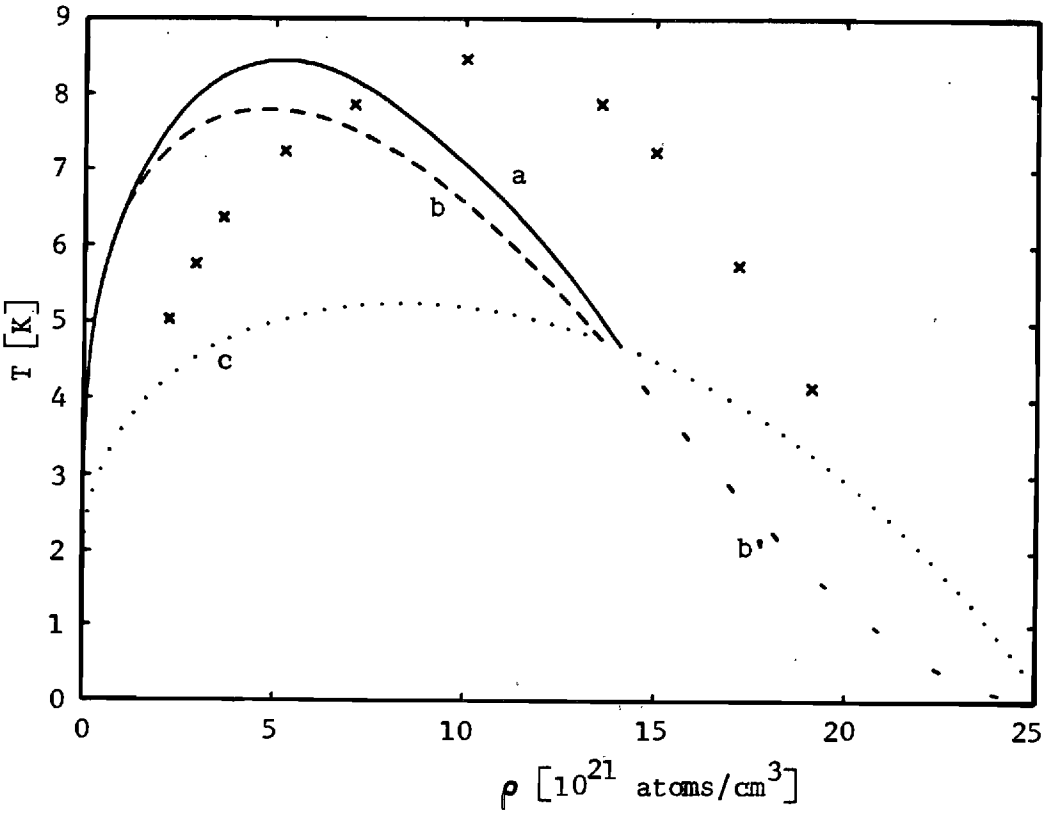

Figure 9. Limit Lines for the Van der Waals Equation of State with Critical Pressure Fit.

Curve a is that calculated by Manninen and Hautojärvi [1978] through the exact numerical minimization of a free energy functional.

Curve b is the result from our new variational model, using the same description of helium as Manninen and Hautojärvi. Surface energy is omitted in both calculations.

Curve b' is an artificial continuation of the limit line, b (see text).

Curve c is the Van der Waals coexistence curve for the critical pressure fit.

The crosses are experimental points obtained by Manninen and Hautojärvi [1978].

experimental result. However, as they also point out, the stable limit line is shifted too far toward low densities, a defect that they seem to regard as unimportant. We shall see later than the omission of surface energy, which these researchers leave out as being too small to significantly affect their results, is at fault here. If surface energy is included, the good value they have for the maximum temperature at which self-trapping occurs will be lost.

Nonetheless, their having performed an exact minimization of the free energy with a Van der Waals description of helium permits us to judge the adequacy of our variational model for position self-trapping without surface energy. In this model, the Helmholtz free energy change which occurs when the interaction is turned on is

$$\frac{\Delta F}{\rho g} = \left(\frac{z}{\pi s}\right)^2 - y + Gs^3 \left[T\sigma(y) - u(y)\right] \tag{6}$$

where s, y, and z are defined as in previous chapters and where we use the Van der Waals expressions for $\sigma(y)$ and $u(y)$,[1]

$$\sigma(y) = u\, \ell n y - y\, \ell n \left(\frac{y^* - y}{y^* - 1}\right) - \frac{y^*(y-1)}{y^* - 1} \tag{7}$$

and

$$u(y) = \frac{27\ kT_c}{8y^*}\ (y-1)^2 \tag{8}$$

[1] Here $y^* = \rho^*/\rho$, and $\rho^* = 1/b$, as in Chapter III.

These equations should be compared with Equation (17) of Chapter IV, and with Equation (6) of Chapter III. The procedure that we use to find the stable limit line is identical to the procedure we used to find the stable limit line for the electron problem with attractive helium-helium interactions but without surface energy, except that we must set $\Delta F/\rho g$ equal to -1 to locate the stable limit line, instead of setting it to +1, and that now $\sin(z)/z = 1 \pm \sqrt{y-1}$, as can be easily seen by replacing g by -g in Equation (47) of Chapter II. We shall not repeat the procedure here, but will note that the value of z on the stable limit line turns out, once more, to be 2.121558. The resulting limit line is shown as the dashed curve in Figure 9. The error in temperature which has occurred because we have only approximately minimized the free energy is only about ten percent: apparently our variational method can take the place of an exact minimization without much loss in accuracy.

In an attempt to locate the source of the difficulty in these curves, we investigated the effect of changing the description of the bulk properties of helium, that is, we altered the equation of state of the gas. For fits to critical density and temperature, we calculated the stable limit line with our variational model, for the lattice gas, and for the Van der Waals gas. These are shown in Figure 10: the solid curve corresponds to the lattice gas and the dashed curve to the Van der Waals gas. Comparing the variational model results for the Van der Waals gas, fit to critical pressure, in Figure 9 with the results for the same equation of state, fit to critical density, in Figure 10,

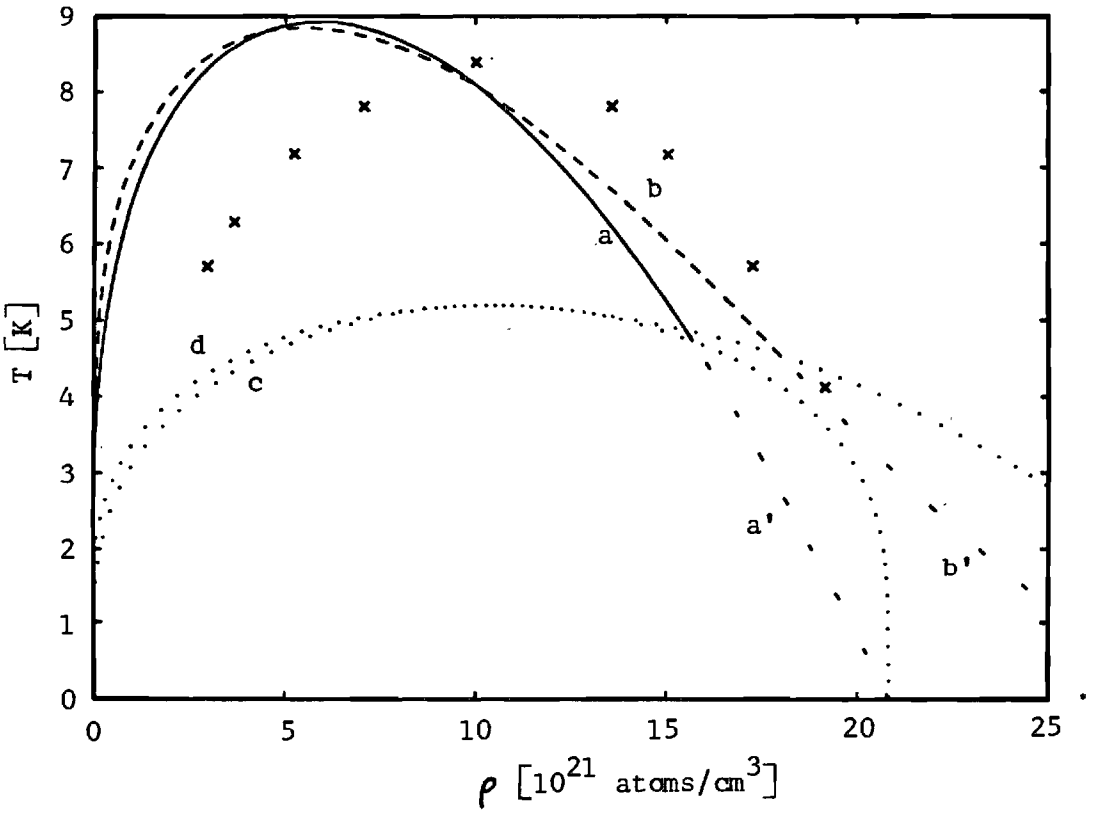

Figure 10. Limit Lines for Van der Waals and Lattice-Gas Equations of State with Critical Density Fit.

Curve a is the lattice gas limit line.

Curve a' is an artificial continuation of the limit line, a.

Curve b is the Van der Waals limit line.

Curve b' is an artificial continuation of the limit line, b.

Curve c is the lattice gas coexistence curve for the critical density fit.

Curve d is the Van der Waals coexistence curve for the critical density fit.

The crosses are experimental points obtained by Manninen and Hautojärvi [1978].

we find that the critical density curve peaks at both a higher temperature and higher density and, on the average, agrees better with the experimental points. For this critical density fit, the qualitative behavior of the curve begins to fail at high densities, where the tail of the curve starts to curve upward. This upward curvature is a necessary feature of the Van der Waals model of the self-trapped state. It is not hard to show that the slope of the limit line[1] for this equation of state goes to zero at the jamming density. Comparing the limit lines for the critical density fits for the lattice gas and the Van der Waals gas (Figure 10) we find that the lattice gas curve peaks at a slightly higher temperature and density than the Van der Waals curve. More importantly, the high density behavior of the lattice gas curve is better. Although the limit line is too low for high densities, it parallels the experimental points and goes to zero with finite slope. We see that adjusting the jamming density to a higher value may permit fairly good agreement with the experimental points in this range of densities, whereas adjusting the jamming density for the Van der Waals theory will not similarly be helpful. This observation led us to abandon the Van der Waals gas in favor of the lattice gas.

---

[1] Extended through the coexistence curve by pretending that the helium remains a uniform gas whose density is the average density, ρ. Actually, of course, the density outside the droplet will not be this average value, but instead will be one of the two densities that can coexist at the temperature of the system.

It is also worth noting the similarities between the curves of Figure 9 and Figure 10. All of these curves are deficient in the same way in spite of considerable variations in the equations of state that they represent. They all peak at densities which are much too low. This similarity suggests that the deficiencies in these curves do not arise from the equations of state which are used, but from some other factor, such as the use of a Fermi pseudopotential for the positron-helium interaction or the neglect of surface energy or the neglect of the dependence of the interaction strength, g, on the density.

Let us turn to a more successful theory, that of Stott and Zaremba [1977]. They minimize a Gibbs free energy and treat the positron-helium interaction with a pseudopotential, just as Manninen and Hautojärvi [1978] do. In addition, they include a surface energy term. The free energy that they use is

$$\Omega = -\frac{h^2}{2m}\int d^3r\, \chi^*(r)\, \nabla^2\chi(r) + \int d^3r E_0(\rho(r))\,|\psi(r)|^2 + \int d^3r f(\rho(r)) - \mu(\rho)\int d^3r\, \rho(r) + \frac{1}{2}\int d^3r\, \hat{g}(\rho(r))|\nabla\rho(r)|^2 \qquad (9)$$

where

$$\hat{g}(\rho) = \frac{1}{6\rho kT}\left(\frac{\partial P}{\partial \rho}\right)^2_{V,T}\left[\rho\int d^3r r^2(g(r) - 1) + \frac{h^2}{2kTM_{HE}}\right] \qquad (10)$$

In Equation (9), $E_0(\rho(r))$ is the potential energy at point r for the positron, $\mu(\rho)$ is the chemical potential in the absence of a positron, and $f(\rho(r))$ is the Helmholtz free energy density of the gas. The

term of Equation (9) involving $\hat{g}$ is the surface energy term. It is identical with the surface energy term obtained in Appendices A and B except for a missing factor of three in the last term of Equation (10), which we attribute to a typographical error. Stott and Zaremba use an empirical equation of state for $f(\rho(r))$ and for the determination of $(\partial P/\partial \rho)_{V,T}$ and they evaluate the integral in Equation (10) by the method given in Chapter III, obtaining a function of the temperature. Minimizing Ω with respect to variations in $\rho(r)$, they obtain

$$|\chi(r)|^2 dE_o d\rho(r) = [\mu(\rho(r))-\mu(\rho)] + \hat{g}(\rho(r))\nabla^2\rho(r) + \frac{1}{2}\hat{g}'(\rho(r))|\nabla\rho(r)|^2 \tag{11}$$

where $\mu(\rho(r))$ is the local chemical potential of the gas and is given by

$$\mu(\rho(r)) = \frac{\partial(f(\rho(r))/\rho(r))}{\partial\rho(r)} \tag{12}$$

Minimizing Ω with respect to variations in $\chi(r)$, subject to the usual normalization constraint, they find

$$-\frac{h^2}{2m}\nabla^2\chi(r) + E_o\rho(r)\chi(r) = \varepsilon\chi(r) \tag{13}$$

Before proceeding further, the positron potential energy $E_o(\rho(r))$ must be evaluated. To find the strength of the pseudopotential that they will use, these researchers start with a realistic positron-helium

interaction, with the polarization part taken from Reeh [1960] and the repulsive core taken from Kestner, et al., [1965], and then scale the potential so that the consequent s-wave scattering length was equal to -.277 A, which they regard as the best theoretical estimate (Houston and Drachman [1971]). Applying to this potential an adaption of the positron pseudopotential method which Stott had developed with Kubica for positrons in metals (Kubica and Stott [1969]) and which is a modification of a Wigner-Seitz calculation, they estimate the pseudopotential interaction to be

$$E_0(\rho(r)) = -\ 132.4\ \text{meV} \left[\frac{\rho(r)}{10^{22}/\text{cm}^3}\right] - E_2 \left[\frac{\rho(r)}{10^{22}/\text{cm}^3}\right]^2 \qquad (14)$$

where E_2 varies from 14.08 meV to 3.22 meV as the temperature increases from 5 K to 10 K. In terms of the interaction strength g, this corresponds to

$$g = -\ 2.121 \times 10^{-35}\ \text{erg}\cdot\text{cm}^3 - \varepsilon_2\rho \qquad (15)$$

where ε_2 varies from 2.256×10^{-58} erg-cm^6 to 5.159×10^{-59} erg-cm^6 as the temperature increases from 5 K to 10 K. This interaction strength may be compared with the value $g = 2.070 \times 10^{-35}$ erg-cm^3, which Manninen and Hautojärvi [1978] use, and which we use also.

At this point, after obtaining Equations (11), (12), and (13) and with all of the functions in them other than $\rho(r)$ and $\chi(r)$ carefully determined, it would seem that the next step is to solve

these equations exactly, which would befit the use of an empirical equation of state and the inclusion of the small density dependence of the positron-helium interaction strength. However, these researchers decline to do this, as do we. Just the same, it is worth pointing out that the solution of these equations can be attempted by the same method that we suggested for Manninen and Hautojärvi's [1978] equations: solve Equation (11) for $\chi^2(r)$ and use the square root of this expression in Equation (13) to obtain a differential equation for $\rho(r)$, a solution for which can be sought numerically.

Instead of solving these equations, Stott and Zaremba choose a variational model for the wave function,

$$\chi(r) + \left(\frac{3}{4\pi\sigma r^3}\right)^{1/2} \exp\left[-\frac{1}{2}\left(\frac{r}{\sigma}\right)^3\right] \qquad (16)$$

which only involves one adjustable parameter, σ. Given this wave function, they can numerically determine the corresponding density at any point r, through Equations (10) and (11) and their empirical equation of state, if they omit the surface energy term. If they now numerically calculate the first derivative of $\rho(r)$ with respect to r, they have evaluated all of the expressions involved in Equation (9). Numerically integrating this equation, they find the value of Ω that corresponds to the particular choice of σ made. Varying σ, they seek the minimum value of Ω that they can obtain with their variational model. They must repeat this procedure for many densities and temperatures as they seek points on the stable limit line. Their resulting limit line is

shown as the dashed curve in Figure 11.

Although the value that they find for the maximum temperature is too high, the density at which this peak occurs is not far from the experimental value, unlike the results previously reported in this chapter. They attribute their high values for temperatures to uncertainty in the positron-helium interaction strength, saying that a ten percent reduction in its magnitude would lead to the correct value for the maximum temperature. Since their calculation seems to have incorporated the features necessary to correct the deficiencies of the models previously discussed in this chapter, it is important to us to know just which of the refinements that Stott and Zaremba have made are responsible for the improvement, and which are inessential.

In an effort to determine whether the inclusion of surface energy is the essential refinement, we shall minimize Equation (64) of Chapter III

$$\frac{\Delta F}{\rho g} = \left(\frac{z}{\pi s}\right)^2 - y + Gs^3\left(T\left[y\ \ell n y + (y^*-y)\ \ell n\left(\frac{y^*-y}{y^*-1}\right)\right] - \frac{2T_c(y-1)^2}{y^*}\right)$$

$$+ \tilde{H}(T)(\rho g)^{7/2}\ y^2/s^5 \qquad (17)$$

where H(T) is given by Equation (66) of Chapter III. Equation (17) incorporates the surface energy through our approximate force-balance relation,

$$\nabla P = \rho(r)\ \ g\nabla\chi^2(r) \qquad (18)$$

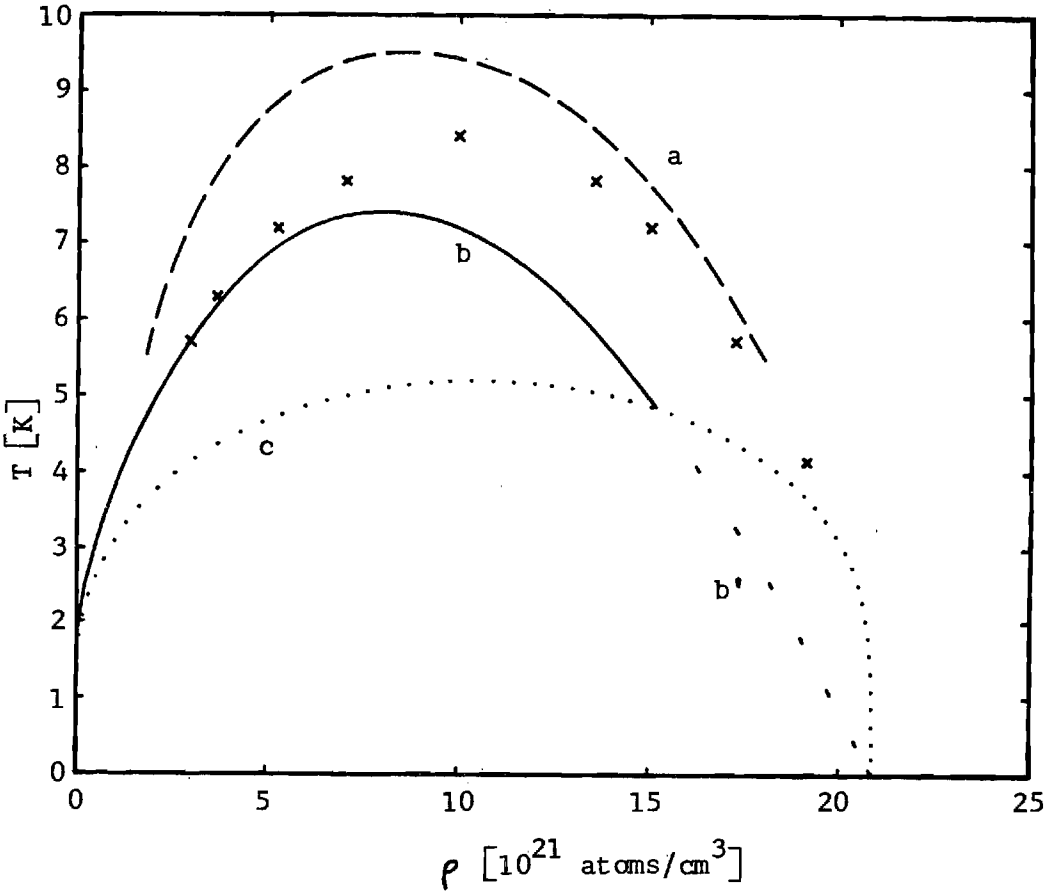

Figure 11. The Limit Line of Stott and Zaremba [1977] and that of the Lattice Gas Fit to Critical Density, Surface Energy Included.

Curve a is the limit line of Stott and Zaremba.

Curve b is the lattice gas limit line.

Curve b' is an artificial continuation of the limit line, b.

Curve c is the lattice gas coexistence curve for the critical density fit.

The crosses are experimental points obtained by Manninen and Hautojärvi [1978].

We shall perform the minimization by search, just as we did in Chapter IV for the electron problem with surface energy.[1] This method will not be described again here. The resulting stable limit line for the lattice gas, fit to critical density and temperature, is shown as the solid curve in Figure 11. In Figure (12), we show, as functions of the average density, the droplet radius, R_0, and droplet density, ρ_i, along the stable limit line for our variational model both with and without surface energy.

The solid curve of Figure 11 represents a significant improvement over the solid curve of Figure 10. These two curves differ only in whether or not surface energy has been included. The poor qualitative behavior of the limit line of Figure 10 for low densities has been removed; for average densities lower than about 6×10^{21} atoms/cm^3, even the quantitative agreement is quite good. There is no such improvement for high average densities, on the other hand, and none could be expected: since the surface energy is always positive in this problem, it can only lower the limit line and cannot improve it in a region where it is already too low. Indeed, so long as the jamming density has its current value (20.85×10^{21} atoms/cm^3), very little can be done to improve the high density side of this limit line, since the limit line must drop to zero Kelvin at the jamming density, while the experimental points seem to be tending to a higher limiting value of the density. Figure 13 shows the effect on the stable limit line of

[1] We attempted to treat the surface energy perturbatively, but failed. The perturbation theory we used is developed in Appendix E.

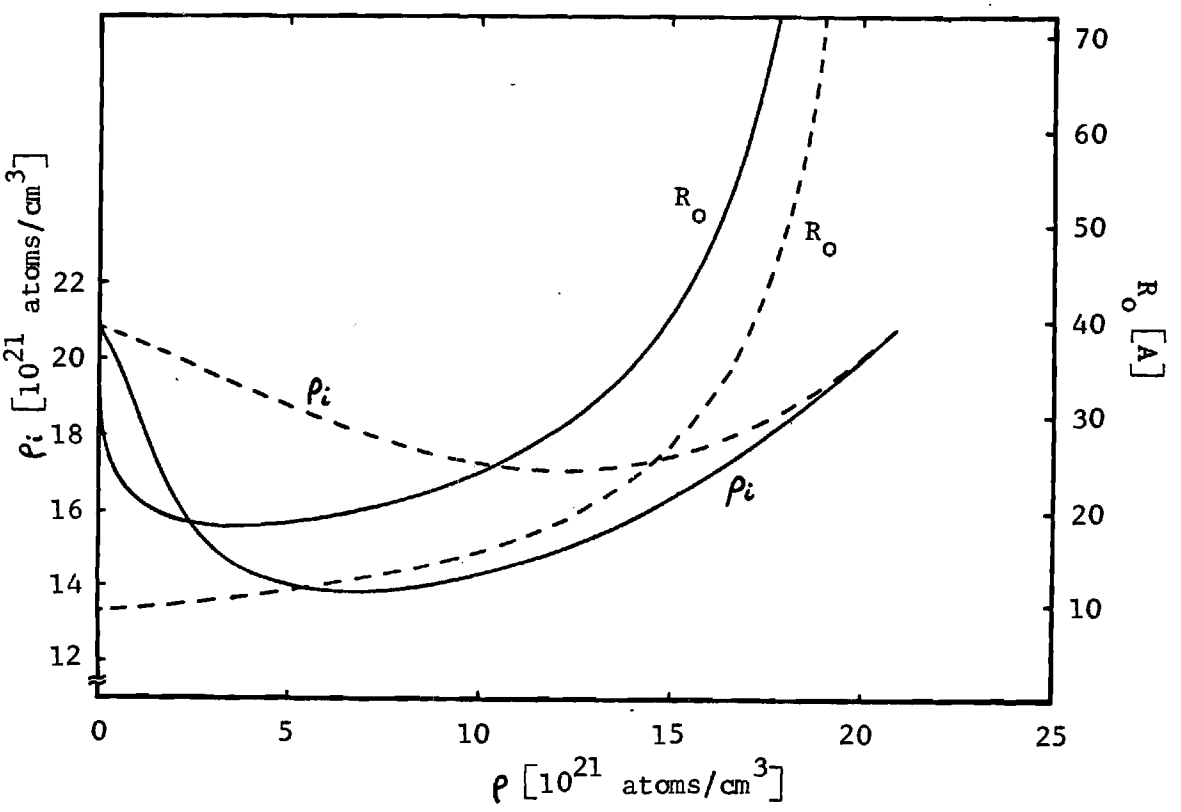

Figure 12. Variational Model Parameters on the Stable Limit Line for the Positron in Helium.

Dashed curves correspond to the limit line with surface energy neglected. Solid curves correspond to the limit line with surface energy included.

increasing the jamming density from the value of 20.85×10^{21} atoms/cm^3, obtained from the critical density fit, to 22×10^{21} atoms/cm^3, and finally to 23×10^{21} atoms/cm^3. As is easily seen, the peak of these curves shifts toward higher densities and temperatures as the jamming density is increased, while the agreement between theory and experiment is significantly improved in the high density region. Less noticeable is the drop in temperature at a specified temperature which simultaneously occurs in the low density region. Actually, the points in this region are not so much shifted down, as to the right, as the jamming density is increased; at a fixed density, this shift to the right looks like a decrease in temperature at low densities.

The limit line corresponding to $\rho = 23 \times 10^{21}$ atoms/cm^3 appears to be about as good a limit line as our simple variational model can produce. As it stands, this line is about as good as Stott and Zaremba's, although they are not guilty of curve fitting, as we are. We could alter the positron-helium interaction strength in an attempt to improve the fit still further, but increasing this strength by ten percent only shifts the curve up by .4 K at its peak. This change is small because the surface energy term of Equation (17) also increases when the positron-helium interaction strength in increased, and this effect partially counteracts the large increase in temperature on the stable limit line that would occur otherwise. The larger effect which Stott and Zaremba [1977] attribute to changes in this interaction strength is not noticeable in our model. It may be that they found

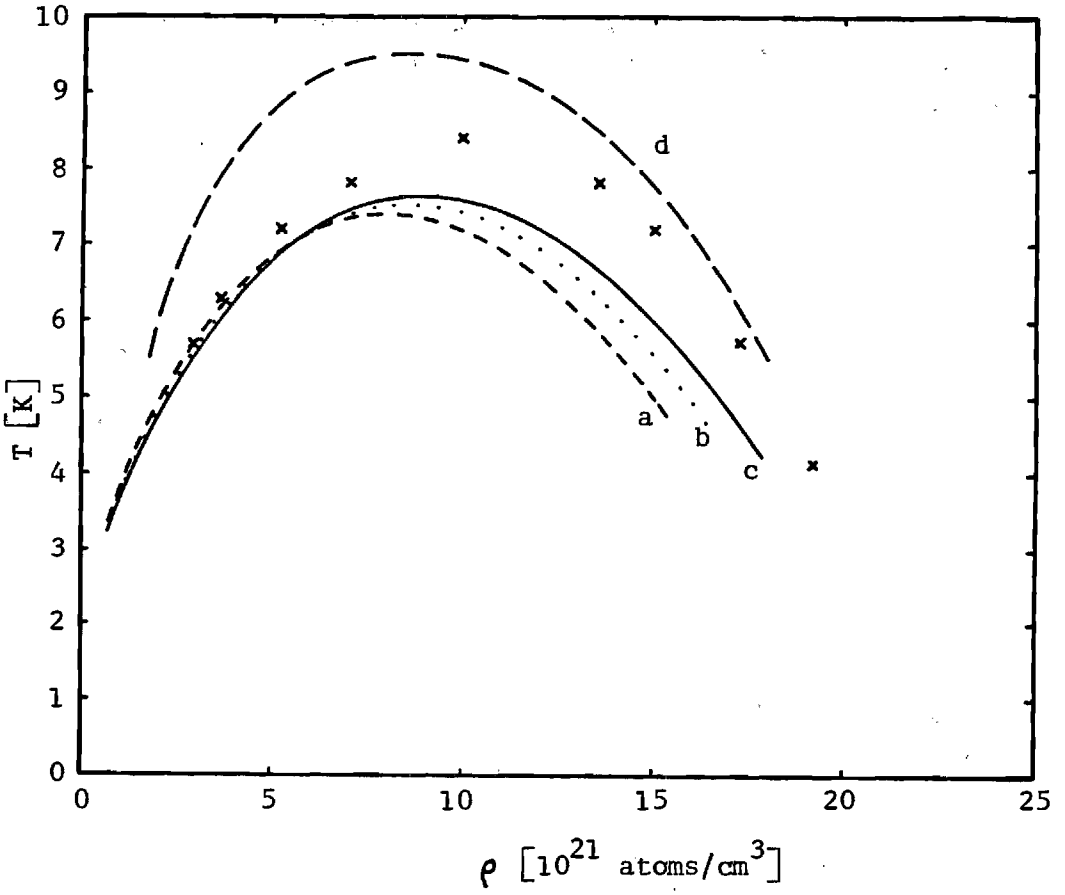

Figure 13. Limit Lines with Surface Term for the Lattice Gas Fit to Various Jamming Densities.

Curve a corresponds to the critical density fit: $\rho^* = 20.85 \times 10^{21}$ atoms/cm^3.

Curve b corresponds to $\rho^* = 22 \times 10^{21}$ atoms/cm^3.

Curve c corresponds to $\rho^* = 23 \times 10^{21}$ atoms/cm^3.

Curve d is the limit line of Stott and Zaremba [1977].

The crosses are experimental points obtained by Manninen and Hautojärvi [1978].

the metastable limit line, which would help to account for their curve's being too high. The metastable limit line in our variatonal model does turn out to be more sensitive to changes in the interaction strength, but only by about 40 percent, so that even this increased sensitivity seems insufficient to account for Stott and Zaremba's result. Unfortunately, to explore this question properly, we would need to repeat their calculation, and we are unwilling to do this.

We have checked the validity of the approximate force-balance relation in just the same way that we did for the electron problem in the last chapter. We examined the relative sizes of the two terms of the full force-balance relation. Equation (70) of Chapter III, at various distances from the center of the droplet for self-trapped states on the stable limit line. We examined the states for average densities of 4×10^{21} atoms/cm^3, 6×10^{21} atoms/cm^3, 10×10^{21} atoms/cm^3, and 15×10^{21} atoms/cm^3. The critierion that the term we have neglected by at least ten times smaller than the term we have kept was well met, except for a small region in the droplet for an average density of 4×10^{21} atoms/cm^3. There, where the size of the variational-model droplet is 18.5 A, the criterion was not met for radii less than five Angstroms, and at one Angstrom the neglected term is nearly 40 percent of the term we have kept. Thus the limit line at this point is probably slightly too high, and for still lower average densities is probably considerably too high. If we do not place much confidence

in our results below 5 K in any case,[1] then in the range of average densities where we do have confidence in our predictions, the inclusion of surface forces in the force-balance relation would only affect the limit line for ρ between about 2×10^{21} atoms/cm^3 and 4×10^{21} atoms/cm^3.

Finally, we have calculated theoretical annihilation rate curves to be compared with the experimental curves of Figure 8. We use the formula of Manninen and Hautojärvi [1978],

$$\lambda = \pi r_o^2 \, c \, Z_{eff} \int d^3r \, \rho(r) \, \chi^2(r) \tag{19}$$

where λ is the annihilation rate, r_o is the classical electron radius, c is the speed of light, and Z_{eff} is the effective number of electrons per atom seen by the positron. Manninen and Hautojärvi state that Z_{eff} depends in helium only very weakly on the density (Hautojärvi, et al., [1976], Fox, et al., [1977]) and assign it the value of 3.5, which we adopt here. Using the square-well density profile and wave function from our variational model, the integral of Equation (35) may be evaluated, so that Equation (35) becomes

$$\lambda = 2.619 \times 10^{-14} \frac{\text{cm}^3}{\text{sec}} \left[\frac{\rho_i(1-\sin(2z)/2z) + \rho(-\sin^2 z \tan(z)/z)}{1-\sin(2z)/2z-\sin^2 z\tan(z)/z} \right] \tag{20}$$

[1] Because of the high temperature expansion that we used in deriving our expression for the surface energy, and because we use a classical equation of state for helium.

Using values for ρ_i and z obtained from the minimization by search method that we employed for our model with surface energy and with $\rho^* = 23 \times 10^{21}$ atoms/cm^3, we evaluated Equation (36) for the annihilation rate as a function of density for temperatures of 5.7 K and 7.2 K. To find the effective annihilation rate, we took it to be a weighted average of the annihilation rate just found and the free particle annihilation rate; the weight factors were the relative probabilities that each type of state occurs, as calculated from their known free energies. In the case of the 5.7 K annihilation rate, the self-trapped state was overwhelmingly probable once the stable limit line was crossed. In the case of the 7.2 K annihilation rate, the self-trapped state in our model never gets very far below the limit line and the free-particle annihilation rate makes a contribution almost everywhere. The resulting curves are shown in Figure 14. The qualitative behavior of both curves is good; in particular, the relative constancy of the annihilation rate once the self-trapped states come into play is evident, and the estimations of the onset of the self-trapped state are fairly good. The increase to self-trapped values for the 5.7 K curve is too rapid, and is reminiscent of similar results obtained in electron mobility calculations. In the Introduction, we attributed to the neglect of fluctuations near the limit line the failure of the bubble model to account for the gradual drop in mobility to self-trapped values that is experimentally observed. We may attempt to account for the overly rapid increase in annihilation rate for 5.7 K in the same way. This neglect of fluctuations may also account for

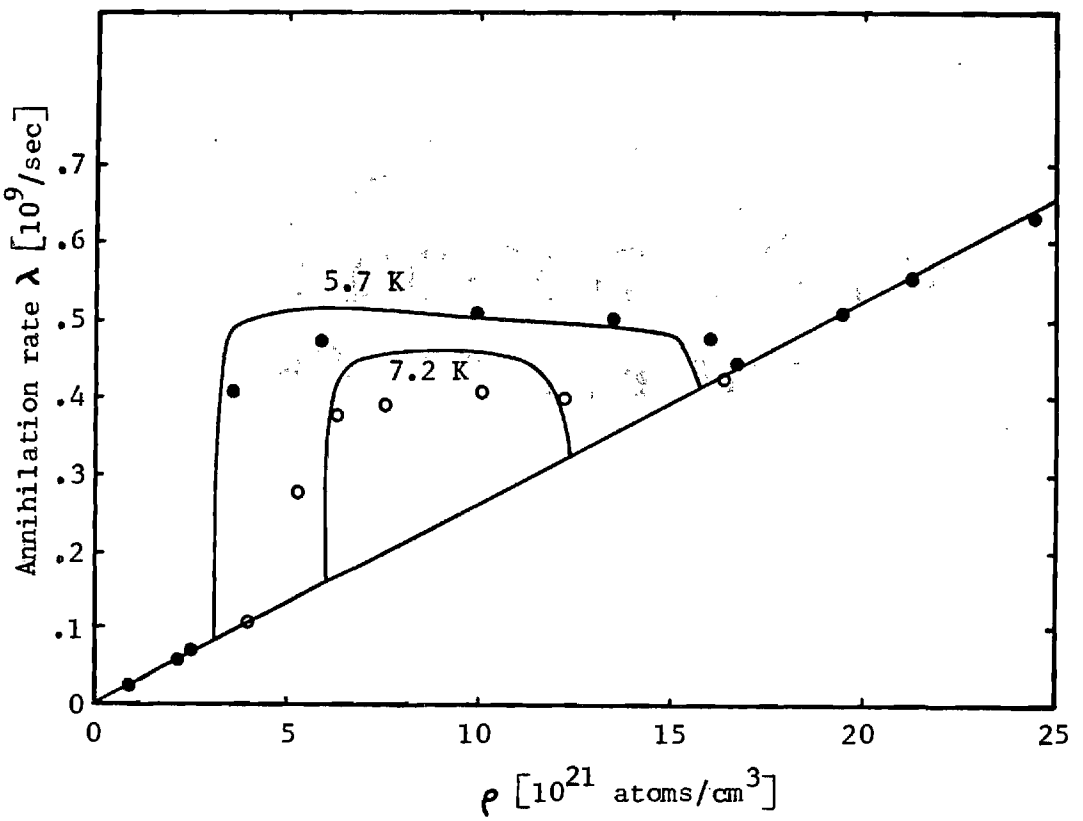

Figure 14. Calculated Annihilation Rate

The dots are experimental points obtained by Manninen and Hautojärvi [1978]. The solid dots are experimental points for T = 5.7 K, while the hollow dots are experimental points for T = 7.2 K.

the poor quantitative agreement for the 7.2 K annihilation rate curve, since in our variational model, the 7.2 K curve is everywhere close to the limit line. Of course, some error has been introduced in our use of variational model expression for $\rho(r)$; we could have calculated the $\rho(r)$ that corresponds to our given wave function, as we had to do when checking the force-balance relation, and used this function for $\rho(r)$ instead, numerically integrating Equation (35). Such a calculation is contrary to the spirit of this thesis, however. We prefer to use the variational model functions unless it is necessary to do otherwise.

With this calculation, we leave the self-trapped positron. In the next chapter, we shall review what we have found in the thesis and make some recommendations for further work.

CHAPTER VI

CONCLUSIONS AND RECOMMENDATIONS

Conclusions

In this section we shall review what we have done. At first, we shall make a few comments which are not specific to either the electron self-trapping problem or the positron self-trapping problem. Subsequently, we shall have some specific remarks to make about each of these problems.

We have invented a simple variational model which can be applied to both electron and positron self-trapping in helium gas. This model seems to compare well with exact minimizations of the free energy in those versions of these self-trapping problems where exact minimizations have been performed. A major virtue of this variational model is its ability to accommodate a fluid which is described by a full equation of state without becoming difficult to use. This permits us, for the electron problem, to go beyond the second-virial-coefficient approximation with which previous researchers have stopped. In the positron problem, a full description of the bulk interactions of helium is essential, so that this feature of the variational model is essential if it is to be applied to positron self-trapping. So long as the free energy change per unit volume of the gas can be written as a function of the local gas density, our methods can be applied. In particular, an empirical equation of state may be employed, if the researcher so desires. We have chosen instead to use an approximate

equation of state, the so-called lattice gas equation of state, and have found that this equation of state is quite adequate for reproducing the qualitative features of the stable limit line in positron self-trapping in helium and, with a little adjustment in the parameters of this equation of state, the quantitative features as well. We presume that it consequently works well for electron self-trapping as well, although the experimental information required to check this assumption is currently lacking. The superiority for helium of the lattice gas equation of state over the Van der Waals equation seems to have been generally overlooked and deserves to be pointed out.

We have developed an approximate expression for the surface energy of a bubble or droplet involving the gradient of the pressure inside the surface. Stott and Zaremba [1977] have previously developed an essentially identical form. We have simplified the application of this surface energy term by using an approximate force-balance relation, whose validity we have subsequently checked self-consistently. The use of such an approximate force-balance relation is apparently novel, but cannot be applied at very low temperatures, since at such temperatures, this approximate force-balance relation loses its validity.

In the specific case of electron self-trapping, the surface energy seems to play no significant role in the determination of the stable limit line, although it does noticeably affect the character of the state which occurs on that line. Much more important in this problme are the bulk helium-helium interactions, particularly the repulsive interactions between helium atoms. Inclusion of these

interactions through the lattice gas equation of state results in dramatically different behavior for the limit line at high average densities than occurs when an ideal-gas or second-virial coefficient approximation to the equation of state of the helium is used. Thus we are enabled to make the novel prediction of a second mobility edge, other than the one which has previously been observed, and have estimated experimental conditions at which this second mobility edge can be found, along with the mobility change that should occur there.

In the positron self-trapping problem, on the other hand, the surface energy is important, even though it generally is less than ten percent of the remainder of the free energy of the system. This importance is not generally recognized by researchers in this field and deserves to be pointed out. Respectable agreement with the experimental limit line for positron self-trapping cannot be obtained unless this term is included; with such an inclusion, our variational model gives agreement with experiment as good as any other theory put forward to date, with considerably less computational effort that these other theories require.

Recommendations

The remarks in this section will not generally be specific to either of the two problems we have considered. When restricting ourselves to a particular one of these problems, we shall give the reader appropriate warning.

An improvement on the theory of this thesis can be immediately made with little effort. The approximate equation of state which we

have used may be replaced with an empirical one. This may be of some utility in the positron self-trapping problem. By eliminating inaccuracy in the equation of state, other deficiencies in our theory are brought into sharper focus. In particular, the role of the positron-helium interaction strength can be investigated, and the sensitivity of the stable limit line to changes in this interaction strength can be explored: after introducing an empirical equation of state, we may see whether or not the dependence of this interaction strength on density is of importance. In the electron problem, the use of an empirical equation of state has a more practical application. Our estimate of experimental conditions at which the second mobility occurs is necessarily crude, because we cannot tell, a priori, just what choice of the parameters in the lattice gas equation of state is appropriate for this problem; we have arbitrarily used the critical density, critical pressure fit. With an empirical equation of state, this uncertainity can be eliminated, and an accurate estimation of these conditions can be made.

One class of applications of this theory will probably already have occurred to the reader. This theory may be applied to electron or positron self-trapping in host materials other than helium gas, and it may be applied to the self-trapping of quantum mechanical particles other than electrons and positrons. In the latter area, the self-trapping of positronium in liquid helium comes to mind. The interaction between positronium and helium arises principally from the Fermi exclusion forces between the electron in the positronium and the electrons in the helium atoms, just as was the case for a simple

electron in helium; there is thus great similarity between these two problems. Of course, the equation of state that we have used will have to be replaced by one adequate for the description of a quantum mechanical fluid, but this replacement presents no difficulty for our methods. More significant is the expected failure of our approximate force-balance relation, which will probably be useless. Our surface energy term in general, involving the gradient of the pressure, is questionable below the critical temperature and should be replaced by another expression appropriate to the low temperatures of liquid helium. The nature of the surface energy is an area of study in its own right, and will be mentioned later as an area of study suggested by the work of this thesis.

If self-trapping of electrons and positrons in host materials other than helium gas is of interest, an application or our variational model may be attempted. All of the concerns that have arisen in this thesis will be important for these other host materials, so that many interesting questions present themselves. For the host material of interest, is the Fermi pseudopotential an adequate approximation for the interaction between the host atoms and the introduing particle? Since the polarizability of almost all atoms is greater than that of helium, the answer to this question may not be yes. Can the lattice-gas equation of state, or the Van der Waals equation be used, or must another description of the bulk interactions of the host atoms be employed? Is the variational model itself adequate? With host atoms of high polarizability, the electron bubble will in principle be

surrounded by a region of excess density, since host atoms will be drawn in toward the electron by long-range polarization forces. Such an excess density "lip" around the electron bubble is not represented in our variational model. Can another tractable variational model be found which includes such a lip? Does the inclusion of such a lip noticeably affect the limit line for a very polarizable host material? Even if we assume that the approximate form that we have for the surface energy, involving the gradient of the pressure, is adequate, we have still to worry about the use of the approximate force-balance relation for each new host material. If it is not adequate, can the complicated full force-balance relation be simplified to give a useful approximation that is adequate? Can a way be found which includes the surface energy in the form involving the gradient of the pressure without invoking the force-balance relation at all, but which still only requires relatively simple calculations? These seem to us to be interesting questions.

As noted in the Introduction, electron mobilities have been measured in neon, nitrogen, hydrogen, argon, and krypton. We may attempt to apply our theory to any of these and discover whether or not it predicts a second mobility edge for electrons in any of these gases. If it does, we may estimate experimental conditions at which this mobility edge occurs, or if we prefer, attempt to experimentally observe such a mobility edge in any of these gases.

Positron annihilation rate experiments have been carried out in He^3, neon, and argon, as noted in the Introduction. Application

of our theory to He^3 is especially attractive, since the experimental coexistence curve for He^3 is even more symmetrical than that of ordinary helium, indicating that the lattice gas may work extremely well for He^3. Many of the questions that we have to answer when applying our theory to a new host material have, for He^3, already been answered in our treatment of ordinary helium, so that our theory should be straightforwardly applicable to this new situation. Manninen and Hautojärvi [1978] have applied their theory to positron self-trapping in He^3, and their resulting limit line suffers the same general deficiency as the one they obtained for ordinary helium. The inclusion of surface energy by our methods should provide significant improvement. For positrons in neon, Canter and Roellig [1978] observe no evidence of self-trapping. Would our model predict this? In argon, these same experimentalists found that self-trapped states form below 170 K at a density about one-sixth the critical density of argon. If the peak in the limit line falls near the critical density (we see no compelling reason why it should) the maximum temperature at which self-trapped states may be found may be as high as the 400 K that Manninen and Hautojärvi [1978] predict. What would our sort of calculation give? Can positrons self-trap in argon at room temperature? Since the surface tension of argon in equilibrium with its vapor is about 100 times as large as the surface tension of helium in equilibrium with its vapor, we might expect that the surface energy, which Manninen and Haurtojärvi neglect, will play an even more important role for argon than it does for helium. We must carry out the calculation to know for sure.

We have two experimental recommendations to make. One of them,

of course, is the location of the second mobility edge for electrons in helium, if this mobility edge in fact exists. The other experiment is for positrons in helium gas. By examining the correlation between gamma rays emitted when the positron annihilates, direct information may be obtained about the momentum distribution of the positron at the time of its annihilation. This information is available because of the conservation of momentum: the total momentum of the gammas produced in the annihilation event must equal the sum of the momenta of the electron and the positron which annihilated. Such an experiment has already been carried out for positronium bubbles in liquid helium (Hautojärvi, et al., [1976a]) and the consequent momentum distribution of the positronium in its self-trapped state calculated. Such an experiment is far superior to an annihilaton rate experiment for ascertaining the success of a variational model. The annihilation rate experiment primarily gives information about the conditions under which the self-trapped state forms. These conditions depend basically on the free energy of the self-trapped state. As is well known, the energy of a state, found by a variational calculation, is relatively insensitive to changes in the state function; it is precisely for this reason that crude variational calculations are useful for finding ground state energies. The gamma-gamma coincidence experiment that we suggest, on the other hand, provides direct information about the state itself, and thus provides a much more sensitive check on our extremum state than the annihilation rate experiments that have already been carried out.

Finally, we would like to note several areas of our theory which require further basic work, all of which relate to the surface energy. In deriving our basic surface energy term, involving the gradient of the pressure, we have used a linear theory to describe the response of the gas to an external perturbation. In principle, this use of a linear theory is wrong. For example, if the density in the bubble surrounding a self-trapped electron is already essentially zero, no increase in the perturbing force can reduce it further, while a reduction in this force can permit the density in the bubble to increase. For the positron, a similar situation exists near the jamming density of the gas, where it is much easier to reduce the density than to increase it. A linear theory cannot cope with such behavior. What is needed is a non-linear theory which can treat such situations, while remaining tractable in some useful approximation. Such a strictly set problem may have no solution; but its investigation could prove to be a rewarding project. In any case, it seems that the determination of the conditions under which our linear theory is valid will have to wait on some treatment of the non-linear aspects that we have neglected.

A more straightforward improvement of our treatment of surface energy has to do with the density gradient expansion, of which we have kept only the lowest order terms. To improve this approximation we need to include higher order terms. It appears that doing this will introduce higher order terms in the q^2-expansion of χ_q^{-1}, for which terms useful expressions must be found, and will also introduce

higher order derivatives of the density. If these corrections can be incorporated in a way that leaves the minimization of the free energy tractable, then it would be possible to directly gauge the importance of these higher order terms to self-trapping problems, and to determine the conditions under which our low order approximation is adequate.

As for ourselves, the brief study of the full force-balance relation which has been necessary in this thesis invites the most interesting line of inquiry. While accomplishing the goals which we set for ourselves, we have not had to truly come to grips with the nature of the surface of a bubble or a droplet, or with the play of forces inside such a surface. This play is both subtle and complex: the force per unit volume which the surface effects induce depends on derivatives of the density as high as the third order. We do not understand at all the elementary physical processes which give rise to such dependencies. At the radius of the droplet, where the wave function in our variational model has discontinuities in its derivatives of higher than first order, the surface tension force[1] in our model not only changes dramatically, it changes sign. Outside this radius the surface force is toward the center of the droplet, inside this radius the force is away from the center. If the density profile in our variational model were smoothly varying, so that all the derivatives of the wave function would be continuous (the physical situation), would a sign change not occur? or must the presence of the intruding

---

[1] By this force, we mean the force that is exerted on a volume element of the fluid within the surface, and that arises from the non-uniformity of the fluid within the surface.

particle necessarily force the density profile into a form that causes the surface to change sign as the distance from the particle is increased? Does the surface force on a volume element in a free surface change sign from one point to another? Why, in terms of basic physics, does the surface force change sign at all? We expect much time in the future exploring these and relating questions, and enthusiastically recommend that others do likewise.

APPENDIX A

A LITTLE LINEAR RESPONSE THEORY

In linear response theory, the density fluctuations produced by a perturbing force are simply related to that force. If the perturbing Hamiltonian is

$$H^{\rho} = \int d^3r \; \rho(\vec{r})V(\vec{r}) \tag{1}$$

and the $\rho(\vec{r})$ are thought of as generalized coordinates describing the fluid, then

$$F^{\rho}(\vec{r}') = - \frac{\delta H^{\rho}}{\delta \rho(\vec{r}')} = - V(\vec{r}') \tag{2}$$

is the generalized force, corresponding to the coordinate $\rho(\vec{r})$, produced by the perturbation. The connection between $\Delta\rho(\vec{r}) = \rho(\vec{r}) - \rho$ and $F\rho(\vec{r})$ is given in linear response theory by

$$\Delta\rho(\vec{r}) = \int d^3r' \; \chi(\vec{r}-\vec{r}')F^{\rho}(\vec{r}') \tag{3}$$

This equation assumes a simpler form if its Fourier transform is taken. One finds

$$\Delta\rho_{\vec{q}} = \chi_{\vec{q}} F^{\rho}_{\vec{q}} \tag{4}$$

where

$$\Delta\rho_{\vec{q}} = \int d^3r e^{-i\vec{q}\cdot\vec{r}}\, \Delta\rho(\vec{r}) \tag{5}$$

and

$$F^{\rho}(\vec{r}) = \int \frac{d^3q}{(2\pi)^3}\, e^{i\vec{q}\cdot\vec{r}}\, F^{\rho}_{\vec{q}} \tag{6}$$

and

$$\chi(\vec{r}-\vec{r}') - \int \frac{d^3q}{(2\pi)^3}\, e^{i\vec{q}\cdot(\vec{r}-\vec{r}')}\, \chi_{\vec{q}} \tag{7}$$

If we presume that $\chi(\vec{r}-\vec{r}')$ only depends on the distance between $\vec{r}$ and $\vec{r}'$, Equation (4) may be written as

$$\Delta\rho_{\vec{q}} = \chi_q\, F^{\rho}_{\vec{q}} \tag{8}$$

The linear response theory will be presumed to be valid for all components of $\Delta\rho_{\vec{q}}$ and $F^{\rho}_{\vec{q}}$ except the $\vec{q} = 0$ component. This restriction is necessary because of the normalization condition $\int d^3r \Delta\rho(r) = 0$:

$$\int d^3r \Delta\rho(\vec{r}) = \int d^3r \int \frac{d^3q}{(2\pi)^3}\, e^{i\vec{q}\cdot\vec{r}}\, \Delta\rho_{\vec{q}} = \Delta\rho_{\vec{q}=0} = 0 \tag{9}$$

Although any $\vec{q} \neq 0$ component can be arbitrarily varied without disturbing the normalization condition and linear response may be

presumed to hold for that component, the $\vec{q} = 0$ component cannot be varied. When the time comes to find the work done by the external force, $F^{\rho}(\vec{r})$, we shall recall that its $\vec{q} = 0$ component does no work.

Equation (8) has a simple physical interpretation. If $F^{\rho}(\vec{r})$ is a sinusoidal function of wavenumber $\vec{q}$, then Equation (8) says that the resulting $\Delta\rho(\vec{r})$ is also a sinusoidal function with the same spatial dependence and the amplitude of $\Delta\rho(r)$ equals the amplitude of $F^{\rho}(\vec{r})$ times χ_q. We want to find the work done by each of the sinusoidal components of $F^{\rho}(\vec{r})$ as the interaction is turned on; the sum of these will be the total work done by $F^{\rho}(\vec{r})$ and will, by the conservation of energy, be the change in the energy of the system due to the distortion which $F^{\rho}(\vec{r})$ produces.

If we want to find the work done when the generalized coordinate $\rho_{\vec{q}}$ increases from zero to its final value as the interaction is turned on, we need to find the generalized force $\tilde{F}^{\rho}_{\vec{q}}$ that corresponds to $\rho_{\vec{q}}$:

$$\tilde{F}^{\rho}_{\vec{q}} = -\frac{\delta H^{\rho}}{\delta \rho_{\vec{q}}} = -\frac{\delta}{\delta \rho_{\vec{q}}} \int d^3r\, \rho(\vec{r}) V(\vec{r}) \tag{10}$$

which gives, since $V(\vec{r}) = -F^{\rho}(\vec{r})$,

$$\tilde{F}^{\rho}_{\vec{q}} = F^{\rho}_{-\vec{q}'}/(2\pi)^3 \tag{11}$$

The work done for the coordinate $\rho_{\vec{q}}$ $(\vec{q} \neq 0)$ is just

$$W_{\vec{q}} = \int_0^{\rho_{\vec{q}}} \tilde{F}_{\vec{q}}\, d\rho_{\vec{q}} = \int_0^{\Delta\rho_{\vec{q}}} \tilde{F}_{\vec{q}}\, d(\Delta\rho'_{\vec{q}}) \tag{12}$$

Equation (11) gives

$$W_{\vec{q}} = \frac{1}{(2\pi)^3} \int_0^{\Delta\rho_{\vec{q}}} F^{\rho}_{-q}\, d(\Delta\rho'_{\vec{q}}) \tag{13}$$

and the use of Equation (8) yields

$$W_{\vec{q}} = \frac{1}{(2\pi)^3} \int_0^{\Delta\rho_{\vec{q}}} \frac{\Delta\rho'_{-q}}{\chi_q}\, d(\Delta\rho'_q) \tag{14}$$

or

$$W_{\vec{q}} = \frac{1}{2} \frac{1}{(2\pi)^3} \frac{\Delta\rho_{\vec{q}}\, \Delta\rho_{-\vec{q}}}{\chi_q} \tag{15}$$

for the work done by the generalized force $\tilde{F}^{\rho}_{\vec{q}}$ ($\vec{q} \neq 0$).

The Fourier components are independent, so the work done by the corresponding generalized forces add to give the total work done:

$$W = \frac{1}{2} \int' \frac{d^3q}{(2\pi)^3} \frac{\Delta\rho_{\vec{q}}\, \Delta\rho_{-\vec{q}}}{\chi_{\vec{q}}} \tag{16}$$

Here the ' on the integral means that the $\vec{q} = 0$ component "term" is omitted. This prime may be safely dropped, since the integrand for $\vec{q} = 0$ is finite even if $\Delta\rho_{\vec{q}=0} \neq 0$ and since the point $\vec{q} = 0$ is of measure zero. Dropping the prime and taking the inverse Fourier transforms of $\Delta\rho_{q}$ and $\Delta\rho_{-q}$ gives

$$W = \frac{1}{2} \int d^3r \int d^3r' \left(\int \frac{d^3q}{(2\pi)^3} \frac{e^{-i\vec{q}\cdot(\vec{r}'-\vec{r})}}{\chi_q} \right) \Delta\rho(\vec{r})\Delta\rho(\vec{r}') \quad (17)$$

This expression gives the change in the free energy of the system which occurs when the distortion $\Delta\rho(r)$ is quasistatically induced in it. If the free energy of the system before the distortion was induced was $F_o(\rho)$, then the free energy of the system after the distortion is

$$F = F_o + \frac{1}{2} \int d^3r \int d^3r' \left(\int \frac{d^3q}{(2\pi)^3} \frac{e^{-i\vec{q}\cdot(\vec{r}'-\vec{r})}}{\chi_q} \right) \Delta\rho(\vec{r})\Delta\rho(\vec{r}') \quad (18)$$

This equation is identical to Equation (2.7) of (Ebner and Saam [1975]).

APPENDIX B

DENSITY GRADIENT EXPANSION OF THE SURFACE ENERGY

We need to reduce Equation (18) of Appendix A to a useful form. In order to do this, we perform a density gradient expansion of $\Delta\rho(r')$ about the point r. We write

$$\Delta\rho(r') = \Delta\rho(r) + \nabla(\Delta\rho(r)) \cdot \vec{R} + \frac{1}{2} \sum_{i,j} R_i R_j \frac{\partial^2}{\partial r_i \partial r_j} \Delta\rho(r) \quad (1)$$

where $R = r' - r$. Inserting Equation (1) into Equation (18) of Appendix A, and letting

$$\chi^{-1}(R) = \int \frac{d^3q}{(2\pi)^3} e^{i\vec{q}\cdot(\vec{r}-\vec{r}')} \chi_q^{-1} \quad (2)$$

we find

$$\begin{aligned} F = F_o &+ \frac{1}{2}\int d^3r\, \chi^{-1}_{q=o} [\Delta\rho(r)]^2 \\ &+ \frac{1}{2} \int d^3r \int d^3R\, \chi^{-1}(R)\, \Delta\rho(\vec{r})[\nabla(\Delta\rho(r)\cdot\vec{R}] \\ &+ \frac{1}{4} \sum_{i,j} \int d^3r \int d^3R\, \chi^{-1}(R)\, \Delta\rho(r) R_i R_j \frac{\partial^2}{\partial r_i \partial r_j} \Delta\rho(r) \end{aligned} \quad (3)$$

The second term vanishes from symmetry. In any application to which

we intend to apply this equation, $\Delta\rho(r)$ will always either have spherical symmetry or vary in one dimension only, so Equation (3) equals

$$F = F_o + \frac{1}{2}\int d^3r\ \chi^{-1}_{q=o}\ [\Delta\rho(r)]^2$$

$$+ \frac{1}{4}\sum_i\ d^3R\ \chi^{-1}(R)R_i^2\int d^3r\ \Delta\rho(r)\ \frac{\partial^2}{\partial r_i^2}\ \Delta\rho(r) \qquad (4)$$

In the spherical problem, we may convert the last term of Equation (4) to

$$\frac{1}{4}\int d^3R\ \chi^{-1}(R)R^2\int d^3r\ \Delta\rho(r)\ \frac{\partial^2}{\partial r^2}\Delta\rho(r) \qquad (5)$$

or

$$-\frac{1}{4}\int d^3R\ \chi^{-1}(R)R^2\int d^3r|\nabla\rho(R)|^2 \qquad (6)$$

where we have used $\nabla(\nabla\rho(r)) = \nabla(r)$ and the spherical symmetry of $\rho(r)$. Now from Equation (2) we may write

$$\int d^3R\ \chi^{-1}(R)R^2 = -\int d^3R\int\frac{d^3q}{(2\pi)^3}\chi_q^{-1}\frac{\partial^2}{\partial q^2}e^{i\vec{q}\cdot\vec{R}} \qquad (7)$$

or

$$\int d^3R\chi^{-1}(R)R^2 = -\int d^3q\chi_q^{-1}\frac{\partial^2}{\partial q^2}\int\frac{d^3R}{(2\pi)^3}e^{i\vec{q}\cdot\vec{R}} \qquad (8)$$

Integration by parts gives

$$\int d^3R\chi^{-1}(R)R^2 = - \left. \frac{\partial^2 \chi_q^{-1}}{\partial q^2} \right|_{q=o} \tag{9}$$

Using the definition $\hat{g} = (\partial^2 \chi_q^{-1}/\partial q)/2$, the q^2-coefficient of a small-q expansion of χ_q^{-1}, we may combine Equations (4), (6), and (9) to write

$$F = F_o + \frac{1}{2}\int d^3r\ \chi^{-1}_{q=o}\ [\Delta\rho(r)]^2 + \frac{1}{2}\int d^3r\ \hat{g}\ |\nabla\rho(r)|^2 \tag{10}$$

If we define a free energy density $f(\rho) = F/V$ then we may use the compressibility sum rule (Pines and Nozieres [1966]),

$$\chi^{-1}_{q=o} = \left. \frac{\partial^2 f}{\partial \rho'^2} \right|_{\rho'=\rho} \tag{11}$$

to write

$$F = \int d^3r\ f(\rho) + \frac{1}{2}\int d^3r\ \left. \frac{\partial^2 f}{\partial \rho'^2} \right|_{\rho'=\rho} [\Delta\rho(r)]^2 + \frac{1}{2}\int d^3r\ \hat{g}\ |\nabla\rho(r)|^2 \tag{12}$$

Now the first two terms of Equation (12) are just the first two non-vanishing terms of the expansion

$$F = \int d^r 3f(\rho(r)) = \int d^3r \left[f(\rho) + \left.\frac{\partial f(\rho')}{\partial \rho'}\right|_{\rho'=\rho} \Delta\rho(r) \right.$$

$$\left. + \frac{1}{2} \left.\frac{\partial^2 f(\rho')}{\partial \rho'^2}\right|_{\rho'=\rho} [\Delta\rho(r)]^2 + \cdots \right] \tag{13}$$

Since we shall consider large density variations in the self-trapped state, we need to replace the low order terms in this expansion present in Equation (12) by the entire series. We write

$$F = \int d^3r f(\rho(r)) + \frac{1}{2} \int d^3r \; \hat{g} \; |\nabla\rho(r)|^2 \tag{14}$$

Equation (14) is identical to an expression used by Stott [1977] for positron self-trapping in helium. We intend to work with the free energy change that occurs when the system departs from a uniform density, so let us subtract from Equation (14) the value it has for a uniform density.

$$\Delta F = \int d^3r [f(\rho(r)) - f(\rho)] + \frac{1}{2} \int d^3r \; \hat{g} \; |\nabla\rho(r)|^2 \tag{15}$$

or

$$\Delta F = \int d^3r \; \Delta f(\rho(r)) + \frac{1}{2} \int d^3r \; \hat{g} \; |\nabla\rho(r)|^2 \tag{16}$$

Before we can use Equation (16) we must reduce it to a useable form by obtaining an approximate expression for $\hat{g}$, which in general will depend on the density, temperature, and equation of state of the gas.

We loosely follow the procedure of Stott [1977].

Let us begin[1] by writing down a more general version of Equation (3) of Appendix A.

$$\Delta\rho(\vec{r},t) = \int d^3r' \int d^3t' \; \chi\,(r-r',t-t')F^P(r',t) \tag{17}$$

If the applied force in this expression is not time-dependent, but instead is constant, Equation (17) reduces to

$$\Delta\rho(\vec{r}) = \int d^3r' \; \chi(r-r',\omega = 0)F^P(r') \tag{18}$$

where $\chi(r-r'\omega) = \int d\tau \; e^{i\omega\tau} \; \chi(r-r',\tau)$, so we see that the χ_q of Appendix A is $\chi(q, \omega=0)$ in the more general context of this appendix.

Since, physically, the system cannot response until a perturbing force has been applied, the $\chi(r-r',t-t')$ of Equation (1) must be zero whenever $t < t'$. The reader may recognize this χ as the retarded Green's function for the system. As is well known (Fetter and Walecka [1971]), the retarded Green's function may be written as

$$\chi\,(r-r',\; t-t') = \frac{i}{k}\,\theta\,(t-t')\;\left\langle\left[\hat{\rho}(r,t),\hat{\rho}(r',t)\right]\right\rangle \tag{19}$$

where $\theta(t-t')$ is the Heavyside step function, the $\hat{\rho}$'s are second

---

[1] The reader may usefully refer to (Martin [1968]) in this section, but must be careful: we have followed Van Hove [1954] in defining quantities that we shall use (except for normalizing the dynamic structure factor in a more standard way). Martin uses different definitions.

quantization density operators which evolve according to the unperturbed Hamiltonian of the system, and where $\langle A \rangle$ means trace $\{\exp(-H/kT)A\}$ where H is the unperturbed Hamiltonian.

Because the Fourier transform

$$\chi(r-r',\omega) = \int d\tau e^{i\omega\tau} \chi(r-r',\tau) \tag{20}$$

is analytic in the upper half of the complex plane, it follows that

$$\chi(r-r',\omega) = \lim_{\varepsilon\to 0} \int \frac{d\omega'}{\pi} \frac{\chi''(r-r',\omega)}{\omega'-\omega-i\varepsilon} \tag{21}$$

where $\chi''(r-r',\omega)$ is the imaginary part of $\chi(r,r',\omega)$. $\chi''(r-r')$ is the Fourier transform of

$$\chi''(r-r',t-t') = \frac{1}{2\hbar} \left\langle [\hat{\rho}(r,t),\hat{\rho}(r',t')] \right\rangle \tag{22}$$

Now we are prepared to relate $\chi''(r-r',t-t')$ to $G(r,r',t,t')$, the generalized pair correlation function of Van Hove [1954], which is defined by

$$G(r,r',t,t') = \frac{1}{\rho} \left\langle \hat{\rho}(r,t)\hat{\rho}(r',t') \right\rangle \tag{23}$$

for a system with translational invariance. Comparing Equations (21) and (22) we write

$$\chi''(r-r',t-t') = \frac{\rho}{2\hbar} [G(r,r',t,t') - G(r',r,t',t)] \tag{24}$$

so that Equation (20) becomes

$$\chi(r,r',\omega) = \lim_{\varepsilon\to 0} \frac{\rho}{2\hbar} \int \frac{d\omega'}{\pi} \frac{G(r,r',\omega') - G(r',r,-\omega')}{\omega'-\omega-i\varepsilon} \tag{25}$$

Since $G(r,r',\omega)$ satisfies the Fluctuation-dissipation theorem (Pines and Nozieres [1966])

$$G(r',r,-\omega') = e^{h\omega/kT}\, G(r,r',\omega) \tag{26}$$

we write

$$\chi(r-r',\omega=0) = \lim_{\varepsilon\to 0} \frac{\rho}{2\hbar} \int \frac{d\omega'}{2\pi} \frac{(1-e^{-h\omega'/kT})G(r,r',\omega)}{\omega'-i\varepsilon} \tag{27}$$

The next step is to make a high temperature expansion of the exponential in Equation (26). This may seem odd, since the theory we are developing will be applied to helium at temperatures as low as 5 K, but arguments are made in Chapter III to support this approximation. Expanding the exponential and keeping only terms of up to the second order in 1/kT, we find

$$\chi(r-r',\omega=0) = \frac{\rho}{2\pi\hbar} \int d\omega' \left[\frac{\hbar}{kT}\, G(r,r',\omega) - \frac{h^2}{2(kT)^2}\, \omega' G(r,r',\omega) \right] \tag{28}$$

or

$$\chi(r-r',\omega=0) = \frac{\rho}{kT} G(r,r',t=0) - \frac{\rho h}{2(kT)^2} \int \frac{d\omega'}{2\pi} \omega' G(r,r',\omega') \quad (29)$$

Since $G(r,r',t=0)$ equals $\langle\rho(r)\rho(r')\rangle/\rho$, it is related to the pair correlation function, $g(\vec{r})$. Given that there is an atom at some point, $g(\vec{r})$ is the probability of finding another atom a displacement $\vec{r}$ from that atom. Van Hove [1954] shows easily that

$$G(\vec{r},\vec{r}',t=0) - \delta^3(r-r') + \rho g(\vec{r}-\vec{r}') \quad (30)$$

So letting $\vec{R} = \vec{r}'-\vec{r}$, and taking the spatial Fourier transform of Equation (28),[1] we may write

$$\chi(q,\omega=0) = \frac{\rho}{kT}\int d^3R e^{-i\vec{q}\cdot\vec{R}}(\delta(R) + \rho[g(\vec{R})-1] + \rho)$$
$$- \frac{\rho h}{2(kT)^2} \int \frac{d\omega'}{2\pi} \omega' S(\vec{q},\omega) \quad (31)$$

Now we use the sum rule (Marshall and Lovesey [1971])

$$\int \frac{d\omega'}{2\pi} \omega' S(\vec{q},\omega) = \frac{hq^2}{2M_{He}} \quad (32)$$

---

[1] Conventionally, the spatial Fourier transform of $G(\vec{r},\vec{r}')$ is denoted by $S(\vec{q})$ instead of $G(\vec{q})$. $S(\vec{q},\omega)$ is called the dynamic structure factor.

where M_{He} is the mass of a helium atom. This term will turn out to be a small quantum correction. It arises from the partial localization of helium atoms due to a density variation that is periodic with wavenumber $\vec{q}$. In the first term in Equation (30), we expand the exponential. Since our desire is to find the q^2-coefficient of χ_q^{-1}, we need keep no terms of higher order. We obtain

$$\chi(q,\omega=0) = \frac{\rho}{kT}\left[1 + \rho\int d^3r(g(R)-1) + \rho\delta^3(q) - \frac{\rho}{2}\int d^3R(\vec{q}\cdot\vec{R})^2(g(R)-1)\right] - \frac{\rho\hbar^2q^2}{4M_{He}(kT)^2} \tag{33}$$

The $\delta^3(q)$ term is unphysical; it can apply only in a truly infinite system and thus cannot physically contribute. All the terms but the last two form the $\vec{q} = 0$ component of $\chi(q,\omega=0) = \chi_q$. $\chi_{q=0}$ can be written in another form that is better for our purposes. It is easy to show using a force balance argument (Pines and Nozieres [1966]) that

$$\chi_{q=o} = \rho\left(\frac{\partial\rho}{\partial P}\right)_{V,T} \tag{34}$$

So we write for Equation (32)

$$\chi_q = \rho\left(\frac{\partial\rho}{\partial P}\right)_{V,T} - \frac{\rho q^2}{6}\int d^3RR^2(g(R)-1) - \frac{\rho\hbar^2q^2}{4M_{He}kT} \tag{35}$$

Then

$$\chi_q^{-1} = \frac{1}{\chi_q} =$$

$$= \frac{1}{\rho}\left(\frac{\partial P}{\partial \rho}\right)_{V,T}\left\{1 + \frac{q^2}{kT}\left(\frac{\partial P}{\partial \rho}\right)_{V,T}\left[\frac{\rho}{6}\int d^3r r^2(g(R)-1) + \frac{h^2}{4M_{He}kT}\right]\right\} \tag{36}$$

so $\hat{g} = \frac{1}{2}\,\partial^2\chi_q^{-1}/\partial q^2\big|_{q=o}$ is

$$\hat{g} = \frac{1}{6\rho kT}\left(\frac{\partial P}{\partial \rho}\right)^2_{V,T}\left[\rho \int d^3r r^2(g(r)-1) + 3\,\frac{h^2}{2M_{He}kT}\right] \tag{37}$$

Equation (14) of Appendix A and Equation (36) of this Appendix are those employed by Stott [1977][1] to treat the problem of positron self-trapping in helium.

---

[1] Actually, in (Stott [1977]), the term corresponding to the last term in Equation (37) lacks the overall factor of three we have. We attribute this to a typographical error.

APPENDIX C

EVALUATION OF SURFACE ENERGY FOR THE VARIATIONAL MODEL

Using Equations (56) and (58) of Chapter III, we write

$$\Delta F_{surf} = \frac{H(T)g^2}{12kT} \int d^3r \rho^2(r) |\nabla\chi^2(r)|^2 \tag{1}$$

or for the variational model

$$\Delta F_{surf} = \frac{H(T)g^2}{12kT} \left[4\pi\rho_i^2 \int_0^{R_o} dr r^2 |\nabla\chi^2(r)|^2 + 4\pi\rho^2 \int_{R_o}^{\infty} dr r^2 |\nabla\chi^2(r)|^2 \right] \tag{2}$$

where R_o is the radius of the square well, and where

$$\chi(r) = \begin{cases} \dfrac{1}{\alpha R_o^{3/2}} \dfrac{\sin\left(\dfrac{zr}{R_o}\right)}{\dfrac{r}{R_o}} & r < R_o \\ \dfrac{\sin z}{\alpha R_o^{3/2}} \dfrac{e^{z \cot z}\left(\dfrac{r}{R_o} - 1\right)}{\dfrac{r}{R_o}} & r > R_o \end{cases} \tag{3}$$

where

$$\alpha^2 = \pi(2 - \sin(2z)/z - 2\sin^2 z \tan(z)/z) \tag{4}$$

In this calculation we will take z to have the value it would have on the stable limit line without the surface term, namely $z = 2.121558$.[1] Of course, once the surface term is included, the value of z on the stable limit line will shift, but, in general, it will not shift so much that our estimate of the surface energy is much in error.

Using these expressions, after some manipulation Equation (2) may be written as

$$\Delta F_{surf} = \frac{H(T) g^2 z^3}{3kT\alpha^4 R_o^5} \left[\rho_i^2 \int_0^z \frac{d\eta}{\eta^2} \sin^2\eta \left(\cos\eta - \frac{\sin\eta}{\eta} \right)^2 \right.$$

$$\left. + \sin^4 z |z \cot z|^3 e^{4|z\cot z|} \rho^2 \int_0^{|z\cot z|^{-1}} d\eta (1+\eta)^2 e^{-4/\eta} \right] \quad (5)$$

These integrals may be evaluated numerically. For $z = 2.121558$, the first integral equals 0.173179 while the second equals 8.78664×10^{-4}. This second value is so small that the term in which it appears may be neglected. Using our chosen value of z and Equations (4) and (5), we may write

$$\Delta F_{surf} = 4.0682 \times 10^{14} \frac{H(T)}{(T/°K)} g^2 \frac{\rho_i^2}{R_o^5} \quad (6)$$

---

[1] This value always occurs for the stable limit line without surface energy, regardless of whether electron or positron self-trapping is being considered.

which is the desired approximation of the surface energy for our variational model.

APPENDIX D

MINIMIZATION, OFF OF THE STABLE LIMIT LINE, OF FREE ENERGY WITH ATTRACTIVE HELIUM-HELIUM FORCES INCLUDED

We wish to minimize the free energy of Equation (17) of Chapter IV:

$$\frac{\Delta F}{\rho g} = \left(\frac{z}{\pi s}\right)^2 + y + Gs^3\,[T\sigma(y) - u(y)] \tag{1}$$

This is our approximate expression for the free energy of a self-trapped electron in helium with the repulsive and attractive forces between helium atoms included, but with the surface energy omitted. The quantities $\sigma(y)$ and $u(y)$ are given by Equations (4) and (18) of Chapter IV. The quantities s, y, and z are related by Equation (2) of Chapter IV,

$$\frac{\sin(z)}{z} = \frac{1}{\pi s\sqrt{1-y}} \tag{2}$$

and as before, we shall use the definition

$$b(z) = \frac{\sin(z)}{z} \tag{3}$$

The condition $\partial(\Delta F/\rho g)/\partial s = 0$ gives

$$-2z(z + b(z)/b'(z))/\pi^2 s^3 + 3Gs^2[T\sigma(y) - y(y)] = 0 \tag{4}$$

and the condition $\partial(\Delta F/\rho g)/\partial y = 0$ gives

$$z\, b^3(z)/b'(z) + 1 + Gs^3\,[T\sigma'(y) - u'(y)] = 0 \qquad (5)$$

For the electron problem, the stable limit line occurs when $\Delta F/\rho g = 1$. Let us subtract one from both sides of Equation (1) and multiply both sides of the resulting equation by $\pi^2 s^2$. We obtain

$$\pi^2 s^2 \left\{\frac{\Delta F}{\rho g} - 1\right\} = z^2 - \pi^2 s^2 (1-y) + \pi^2 G s^5 [T\sigma(y) - u(y)] \qquad (6)$$

Using Equations (2) and (3), this may be written

$$\pi^2 s^2 \left\{\frac{\Delta F}{\rho g} - 1\right\} = z^2 - \frac{1}{b^2} + \pi^2 G s^5\,[T\sigma(y) - u(y)] \qquad (7)$$

or using Equation (4) to eliminate the term involving G, we may write this as

$$s^2 = \left[z^2 - \frac{1}{b^2} + \frac{2z(z + b/b')}{3}\right] \Big/ \pi^2 \left(\frac{\Delta F}{\rho g} - 1\right) \qquad (8)$$

Using Equations (2) and (3) again, we may write Equation (7) as

$$y = 1 - \frac{\frac{\Delta F}{\rho g} - 1}{z^2 b^2 - 1 + 2z(z + b/b')b^2/3} \qquad (9)$$

Thus, if we specify the value of $\Delta F/\rho g$ for which we want to find solutions ($\Delta F/\rho g \neq 1$) Equations (7) and (9) give s and y as

functions of z. In other words, at a specified value of $\Delta F/\rho g$, all the variables in the problem are functions of the single variable, z. Now solving Equations (4) and (5) for G and equating these two values for G, we find an equation that can be solved for T. The resulting expression for T is

$$T = \frac{u(y) + u'(y)\left(\frac{2}{3} z\left(z + \frac{b}{b'}\right) / \left(\pi^2 s^2 \left(1 + z \frac{b^3}{b'}\right)\right)\right)}{\sigma(y) + \sigma'(y)\left(\frac{2}{3} z\left(z + \frac{b}{b'}\right) / \left(\pi^2 s^2 \left(1 + z \frac{b^3}{b'}\right)\right)\right)} \qquad (10)$$

This is the same result that we obtained in Chapter IV for the case $\Delta F/\rho g = 1$. Through Equations (8) and (9), Equation (10) gives us T as a function of z. Taking the solutions of Equation (5) for G and using the definition $G = 4\pi^4 kh^3/(3(2mp)^{3/2} g^{5/2})$, we may write an equation for a calculated value of ρ, which we call ρ_{cal}:

$$\rho_{cal} = \frac{s^2}{2m}\left[\left(\frac{4\pi^4 kh^3}{3g^{5/2}}\right)\left(\frac{u'(y) - T\sigma'(y)}{1 + z\frac{b^3}{b'}}\right)\right]^{.2/3} \qquad (11)$$

The value of ρ_{cal} depends only on z, because of Equations (7), (9), and (10). Thus our prescription for finding the extremum of Equation (1) for an arbitrary free energy ($\Delta F/\rho g \neq 1$) is almost the same as the one given in Chapter IV for the case $\Delta F/\rho g = 1$. In this version, we first specify the value of the free energy that we wish to find at the extremum (Actually, we do this in the other version as well: there

the choise is always $\Delta F/\rho g = 1$). Then, given the jamming density, ρ^*, for the lattice gas, we choose the average density, ρ, for which we want to find an extremum. We may then calculate the parameter y^* which appears in (y) and u(y) and proceed with the minimization. Equation (11) gives a calculated value of ρ called ρ_{cal} which is a function of z only. We seek by varying z[1] to find a zero of

$$\rho_{cal}\,(z) - \rho = 0 \tag{12}$$

The resulting value of z must correspond to the extremum state. Given this value of z, we may calculate values of s and y through Equations (7) and (9) and the value of T through Equation (10), and have thus completed the minimization problem.

If it is desired to perform this calculation for positron self-trapping instead of electron self-trapping, only a small modification is necessary. In the positron problem, the +y term of Equation (1) is replaced by -y, the free energy on the stable limit line is -1 instead of +1, and Equation (2) is replaced by

$$\frac{\sin z}{z} = \frac{1}{\pi s\sqrt{y-1}} \tag{13}$$

---

[1] It is useful to evaluate the second derivatives of $\Delta F/\rho g$ at the extremum, so that one can be sure that a minimum has been found.

The only alteration we must make in procedure when we solve the positron problem is to subtract -1 from $\Delta F/\rho g$ when we reach the point just before Equation (6), instead of subtracting +1. Otherwise the procedure is identical.

APPENDIX E

A PERTURBATION THEORY

In this appendix, we develop a perturbation theory which can be used to include the effects of surface energy (as a perturbation) into the problem of minimizing the free energy of a self-trapped electron in helium. This perturbation theory fails for the corresponding positron problem unless carried out to very high orders. We write for the total free energy

$$\Delta F^T(s,y) = \Delta F(s,y) + \alpha V(s,y) \tag{1}$$

Here $\Delta F(s,y)$ is the free energy change in the absence of the perturbation and $V(s,y)$ is the perturbation. The quantity α represents the strength of the perturbation and we shall use α as an expansion parameter. At the extremum of Equation (1), the values of s and y depend on α, so we denote these values by s_α and y_α. The free energy at the extremum is

$$\Delta F^T(s_\alpha,y_\alpha) = \Delta F(s_\alpha,y_\alpha) + \alpha V(s_\alpha,y_\alpha) \tag{2}$$

and at the extremum, we must have

$$\frac{\partial}{\partial s} \Delta F^T(s_\alpha,y_\alpha) = 0 \quad \text{and} \quad \frac{\partial}{\partial y} \Delta F^T(s_\alpha,y_\alpha) = 0 \tag{3}$$

where

$$\frac{\partial}{\partial s}\ \Delta F^T(s_\alpha,y_\alpha) \equiv \frac{\partial}{\partial s}\ \Delta F^T(s,y)\Big|_{s_\alpha,y_\alpha}$$

$$\frac{\partial}{\partial y}\ \Delta F^T(s_\alpha,y_\alpha) \equiv \frac{\partial}{\partial y}\ \Delta F^T(s,y)\Big|_{s_\alpha,y_\alpha} \tag{4}$$

We wish to expand these extremum conditions in powers of α. We write

$$s_\alpha = s_o + \alpha s_1 + \alpha^2 s_2 + \cdots$$

$$y_\alpha = y_o + \alpha y_1 + \alpha^2 y_2 + \cdots \tag{5}$$

so that

$$\Delta F^T(s_\alpha,y_\alpha) = \Delta F^T(s_o,y_o) + \Delta F_1^T(s_o,y_o)(s_\alpha-s_o) + \Delta F_2(s_o,y_o)(y_\alpha-y_o)$$

$$+ \frac{1}{2}\Delta F_{11}^T(s_o,y_o)(s_\alpha-s_o)^2 + \Delta F_{12}^T(s_o,y_o)(s_\alpha-s_o)(y_\alpha-y_o)$$

$$+ \frac{1}{2}\Delta F_{22}^T(s_o,y_o)(y_\alpha-y_o)^2 + \cdots \tag{6}$$

where

$$\Delta F_1^T(s_o,y_o) = \frac{\partial}{\partial s}\Delta F^T(s,y)\Big|_{s_o,y_o}$$

$$\Delta F^T_{12} = \frac{\partial}{\partial s}\frac{\partial}{\partial y}\ \Delta F^T(s,y)\Big|_{s_o,y_o} \tag{7}$$

et cetera. Using Equations (2) and (5), Equation (6) can be written

$$\begin{aligned}\Delta F^T(s_\alpha,y_\alpha) = \Delta F(s_o,y_o) &+ \alpha[\Delta F_1(s_o,y_o)s_1 + \Delta F_2(s_o,y_o)y_1 + V(s_o,y_o)] \\ &+ \alpha^2[\Delta F_1(s_o,y_o)s_2 + \Delta F_2(s_o,y_o)y_2 + \tfrac{1}{2}\ \Delta F_{11}(s_o,y_o)s_1^2 \\ &+ \Delta F_{12}(s_o,y_o)s_1y_1 + \tfrac{1}{2}\Delta F_{22}(s_o,y_o)y_1^2 + V_1(s_o,y_o)s_1 \\ &+ V_2(s_o,y_o)y_1]\end{aligned} \tag{8}$$

or

$$\Delta F^T(s_\alpha,y_\alpha) = [\Delta F^T]_o + \alpha[\Delta F^T]_1 + \alpha^2[\Delta F^T]_2 + \cdots \tag{9}$$

Henceforth, we shall often use a superscript (0) to indicate that a function is to be evaluated at (s_o,y_o); for example, $\Delta F_1^{(0)} = \partial\Delta F(s_o,y_o)/\partial s$. Now we perform this expansion in Equations (5) as well and require that the coefficients of different powers of α vanish separately, since α is a small but otherwise arbitrary parameter. The resulting equations are

Zeroth Order:

$$\begin{aligned}\Delta F_1^{(0)} &= 0 \\ \Delta F_2^{(0)} &= 0\end{aligned} \tag{10}$$

First Order:

$$\Delta F_{11}^{(o)} s_1 + \Delta F_{12}^{(o)} y_1 + V_1^{(o)} = 0$$

$$\Delta F_{12}^{(o)} s_1 + \Delta F_{22}^{o} y_1 + V_2^{(o)} = 0 \qquad (11)$$

Second Order:

$$\Delta F_{11}^{(o)} s_2 + \Delta F_{12}^{(o)} y_2 + \frac{1}{2} \Delta F_{111}^{(o)} s_1^2 + \Delta F_{112}^{(o)} s_1 y_1 + \Delta F_{122}^{(o)} y_1^2$$

$$+ V_{11}^{(o)} s_1 + V_{12}^{(o)} y_1 = 0$$

$$\Delta F_{12}^{(o)} s_2 + \Delta F_{22}^{(o)} y_2 + \frac{1}{2} \Delta F_{112}^{(o)} s_1^2 + \Delta F_{122}^{(o)} s_1 y_1 + \Delta F_{222}^{(o)} y_1^2 + V_{12}^{(o)} s_1$$

$$+ V_{22}^{(o)} y_1 = 0 \qquad (12)$$

The zeroth order equations just say

$$\frac{\partial}{\partial s} \Delta F(s,y) \Big|_{s_o, y_o} = 0$$

$$\frac{\partial}{\partial y} \Delta F(s,y) \Big|_{s_o, y_o} = 0 \qquad (13)$$

so that s_o and y_o are just the extremum values of s and y in the absence of the perturbation, as they should be. The free energy at the extremum is just

$$\Delta F^{T}(s_o, y_o) = \Delta F(s_o, y_o) \qquad (14)$$

Using Equation (10) in Equation (8) gives the first order correction to the energy,

$$[\Delta F^T]_1 = V(s_o, y_o) \tag{15}$$

The first order equations can be solved for the first order corrections to s_o and y_o. We obtain

$$s_1 = \frac{-\Delta F_{22}^{(o)} V_1^{(o)} + \Delta F_{12}^{(o)} V_2^{(o)}}{\Delta F_{11}^{(o)} \Delta F_{22}^{(o)} - (\Delta F_{12}^{(o)})^2} \tag{16}$$

and

$$y_1 = \frac{-\Delta F_{11}^{(o)} V_2^{(o)} + \Delta F_{12}^{(o)} V_1^{(o)}}{\Delta F_{11}^{(o)} \Delta F_{22}^{(o)} - (\Delta F_{12}^{(o)})^2} \tag{17}$$

Using Equations (10), (16), and (17) in Equation (8) gives the second order correction to the energy

$$[\Delta F^T]_2 = \frac{1}{2} \Delta F_{11}^{(o)} s_1^2 + \Delta F_{12}^{(o)} s_1 y_1 + \frac{1}{2} \Delta F_{22}^{(o)} y_1^2 + V_1^{(o)} s_1 + V_2^{(o)} y_1 \tag{18}$$

It is worth noting that $[\Delta F^T]_2$ can be shown to always be negative if the point (s_o, y_o) corresponds to a minimum as we assume. If Equations (10) and (11) are used in the expression for $[\Delta F^T]_3$ (which we have not written down), we find

$$[\Delta F^T]_3 = \frac{1}{6} \Delta F_{111}^{(o)} s_1^3 + \Delta F_{112}^{(o)} s_1^2 y_1 + \Delta F_{221}^{(o)} s_1 y_1^2 + \frac{1}{6} \Delta F_{222}^{(o)} y_1^3 + \frac{1}{2} V_{11}^{(o)} s_1^2 + V_{12}^{(o)} s_1 y_1 + \frac{1}{2} V_{22}^{(o)} y_1^2 \tag{19}$$

Finally, we note that Equations (12), the second order conditions on the extremum, may be solved for s_2 and y_2 in terms of quantities that we now know. We have not carried this perturbation theory beyond this point.

These results can be applied toward finding the stable limit line in the presence of surface energy in the following way. We pick an average density, and find the point on the stable limit line without surface energy, along with the corresponding s_0 and y_0. We then find, through the desired order of perturbation theory, the change in the free energy which the perturbing surface energy causes. The first order change in the free energy is $V(s_0,y_0)$, for example, and is always positive. Thus with the perturbation included, the point (s_0,y_0) no longer corresponds to the stable limit line, and we must seek another point which does.

To first order, for example, the new free energy is too large, so we must choose a new state (s_0,y_0) for which $\Delta F/\rho g$ in the absence of the perturbation is less than +1 (-1 for the positron). Such a state corresponds to a lower temperature than the old state. To find such a state, we must solve the minimization problem without surface energy for $\Delta F/\rho g \neq 1$ ($\Delta F/\rho g \neq -1$ for the positron). A procedure for doing this is given in Appendix D. Given this state (s_0,y_0), we again apply the perturbation theory to find the new free energy in the presence of the surface energy. If the new $\Delta F/\rho g$ is not equal to +1 (-1 for the positron) we must repeat the process until we find a state (s_0,y_0) with its corresponding temperature T, for which the perturbed

free energy is equal to this stable limit line value. In this way we can find the stable limit line when surface forces are included.

In the electron problem, the perturbation theory converges rapidly. For the positron problem, if the average density is very high, the perturbation theory still converges rapidly, but if the average density is not so high (less than about 17×10^{21} atoms/cm^3 for the critical density fit for the lattice gas) then, through the third order in the free energy, the perturbation theory does not converge. At lower densities, such as 10×10^{21} atoms/cm^3, as we go from the first order correction to the free energy to the third order, the corrections oscillate in sign and increase by orders of magnitude. Under such conditions, the use of perturbation theory is a waste of time.

Fortunately for the positron case, we have another method which we can use, namely the minimization by search described in Chapter IV. When this method is used, we find that the oscillating terms of the perturbation expansion of the energy nearly cancel each other. At an average density of 10×10^{21} atoms/cm^3, for example, and for the temperature at the stable limit line with surface energy, the total change in the free energy when the surface effects are introduced is only about three percent of the energy without surface term. Thus the perturbation fails for the positron problem because the state without surface effects is quite different from the state with surface effects included, and not because the energy of those states is much different. Since the validity of the use of linear

response theory, which is of low order, has little to do with how much the state changes when surface effects are included, this validity is not brought into question for the positron problem by the failure of the perturbation theory of this appendix.

BIBLIOGRAPHY

Allen, J. F., and A. D. Misener [1938], Proc. Combr. Phil. Soc. 34, 299.

Atkins, K. R. [1959], Phys. Rev. 116, 1339.

Atkins, K. R. [1963], in Proceedings of the International School of Physics, Course XXI, Liquid Helium, edited by G. Careri (Academic Press, New York).

Canter, K. F., J. D. McNutt, and L. O. Roellig [1975a], Phys. Rev. A 12, 375.

Canter, K. F., and L. O. Roellig [1975b], Phys. Rev. A. 12, 386.

Careri, G., F. Scaramuzzi, and J. O. Thomson [1959], Nuovo Cimento 13, 186.

Cleveland, C. L., H. A. Gersch, and R. L. Moore [1977], Phys. Rev. B. 15, 5991.

de Boer, J., and A. Michels [1938], Physica 5, 945; [1939], Physica 6, 409.

Ebner, C., and W. F. Saam [1975], Phys. Rev. B. 12, 923.

Eggarter, Thomas P., and M. H. Cohen [1970], Phys. Rev. Lett. 25, 807.

Eggarter, Thomas P., [1972], Phys. Rev. A. 5, 2496.

Ferrell, Richard A. [1957], Phys. Rev. 108, 167.

Fox, R. A., K. F. Canter, and M. Fishbein [1977], Phys. Rev. A. 15, 1340.

Fowler, W. B., and D. L. Dexter [1968], Phys. Rev. 176, 337.

Friedberg, R., and J. M. Luttinger [1975], Phys. Rev. B. 12, 4460.

Halpern, B., J. Lekner, S. A. Rice, and R. Gomer [1967], Phys. Rev. 156, 351.

Harrison, H. R., [1971a], thesis, University of Michigan (unpublished).

Harrison, H. R., and B. E. Springett [1971b], Phys. Lett. 35, 73.

Hautojärvi, P., M. T. Loponen, and K. Rytsölä [1976a]), J. Phys. B. 9, 411.

Hautojärvi, P., K. Rytsölä, P. Tuovinen, and P. Jauho [1976b], in Proceedings of the Fourth International Conference on Positron Annihilation, Helsingør, Denmark (unpublished).

Hautojärvi, P., K. Rytsölä, P. Tuovinen, A. Vehanen, and P. Jauho [1977], Phys. Rev. Lett. 38, 842.

Hernandez, J. [1973], Phys. Rev. A. 7. 1955.

Hernandez, J. [1975], Phys. Rev. B. 11, 1289.

Hernandez, J. [1977], Phys. Rev. B. 15, 5078.

Hohenberg, P., and W. Kohn [1964], Phys. Rev. 136, B 864.

Houston, S. K., and R. J. Drachman [1971], Phys. Rev. A. 3, 1335.

Janhke, J. J., L. Meyer, and S. A. Rice [1971], Phys. Rev. A. 3, 734.

Keesom, W. H. [1942], Helium (Elsevier Press, Amsterdam).

Kestner, N. R., J. Jortner, M. H. Cohen, and S. A. Rice [1965], Phys. Rev. 140, A 56.

Kubica, P., and M. J. Stott [1974], J. Phys. F. 4, 1969.

Kuper, C. G. [1961], Phys. Rev. 122, 1007.

Kuper, C. G. [1963], in Proceedings of the International School of Physics, Course XXI, Liquid Helium, edited by G. Careri (Academic Press, New York).

Landau, L. D., and E. M. Lifshitz [1965], Quantum Mechanics: Non-Relativistic Theory, 2nd ed. (Pergamon Press, Oxford).

Levine, J. L., and T. M. Sanders [1966], Phys. Rev. 154, 138.

Lifshitz, I. M. [1965], Usp. Fiz. Nauk 83, 617 (Soviet Physics Uspekii 7, 549).

Loveland, R. J., P. G. LeComber, and W. E. Spear [1972], Phys. Lett. 39, 225.

Manninen, M., and P. Hautojärvi [1978], Phys. Rev. B. 17, 2129.

Marshall, W., and S. W. Lovesey [1971], Theory of Thermal Neutron Scattering: The Use of Neutrons for the Investigation of Condensed Matter (Clarendon Press, Oxford).

Martin, P. C. [1968], in Problème à N Corps: Many-Body Physics, edited by C. DeWitt and R. Balian (Gordon and Breach, New York).

Meyer, L., and F. Reif [1958], Phys. Rev. 110, 279.

Moore, R. L., C. L. Cleveland, and H. A. Gersch [1978a], Phys. Rev. B. (to be published).

Moore, R. L. [1978b], thesis, Georgia Institute of Technology.

National Bureau of Standards [1962], Technical Note 154.

Northby, J. A., and T. M. Sanders [1967], Phys. Rev. Lett. 18, 1184.

Padmore, T. C., and M. W. Cole [1974], Phys. Rev. A. 9, 802.

Percus, J. K., and G. J. Yevick [1958], Phys. Rev. 110, 1.

Reeh, H. [1960], Z. Naturforsch. 15a, 377.

Schnyders, H., S. A. Rice, and L. Meyer [1966], Phys. Rev. 150, 127.

Sommer, W. T. [1964], Phys. Rev. Lett. 12, 271.

Stott, M. J., and E. Zaremba [1977], Phys. Rev. Lett. 38, 1493.

Van Hove, L. [1954], Phys. Rev. 95, 249.

VITA

Charles L. Cleveland was born in Rome, Georgia, on October 11, 1948. He is the son of Claude Hugh Cleveland and Clara Lucile McCurry Cleveland.

Mr. Cleveland attended Campbell High School in Smyrna, Georgia, and graduated in 1966. He entered the Georgia Institute of Technology in this same year, and received the degree of Bachelor of Science in Physics in 1971 and the degree of Master of Science in Physics in 1975. Throughout his graduate career he was supported by a graduate teaching assistantship.

Mr. Cleveland is a member of the American Association of Physics Teachers and of the American Physical Society.